

Room-Temperature Amination of Chloroheteroarenes in Water by a Recyclable Copper(II)-Phosphaadamantium Sulfonate System

Udaysinh Parmar, Dipesh Somvanshi, Santosh Kori, Aman A. Desai, Rambabu Dandela, Dilip K. Maity, and Anant R. Kapdi*



Cite This: <https://doi.org/10.1021/acs.joc.1c00845>



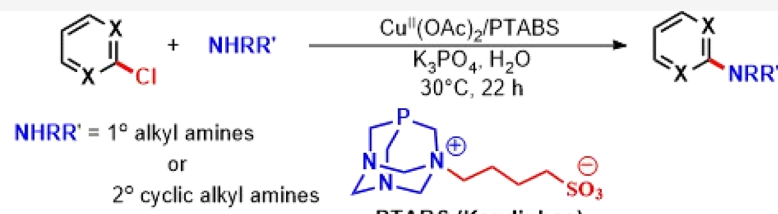
Read Online

ACCESS |

Metrics & More

Article Recommendations

Supporting Information



- ◆ Ambient temperature
- ◆ Large substrate scope
- ◆ Water as the sole solvent
- ◆ Turn Over Number: >900,000
- ◆ Excellent functional group tolerance
- ◆ Late-stage modification of antibiotic and anticancer agents
- ◆ Recyclability: 12 recycles
- ◆ DFT support

ABSTRACT: Buchwald–Hartwig amination of chloroheteroarenes has been a challenging synthetic process, with very few protocols promoting this important transformation at ambient temperature. The current report discusses about an efficient copper-based catalytic system (Cu/PTABS) for the amination of chloroheteroarenes at ambient temperature in water as the sole reaction solvent, a combination that is first to be reported. A wide variety of chloroheteroarenes could be coupled efficiently with primary and secondary amines as well as selected amino acid esters under mild reaction conditions. Catalytic efficiency of the developed protocol also promotes late-stage functionalization of active pharmaceutical ingredients (APIs) such as antibiotics (floxacins) and anticancer drugs. The catalytic system also performs efficiently at a very low concentration of 0.0001 mol % (TON = 980,000) and can be recycled 12 times without any appreciable loss in activity. Theoretical calculations reveal that the π -acceptor ability of the ligand PTABS is the main reason for the appreciably high reactivity of the catalytic system. Preliminary characterization of the catalytic species in the reaction was carried out using UV–VIS and ESR spectroscopy, providing evidence for the $\text{Cu}(\text{II})$ oxidation state.

INTRODUCTION

Catalytic amination of haloarenes¹ is one of the most well-researched topics, primarily due to the occurrence of the diarylamine structural motif in a wide variety of natural products,¹ active pharmaceutical ingredients (APIs),² and agrochemicals.¹ The meteoric rise of the metal-catalyzed aminations has been assisted largely by the introduction of activating ligands, providing greater electronic control on the metal reactivity (Pd or Cu). Such a strategy although successful for the synthesis of the functionalized diarylamines from aryl halides fails to provide satisfactory results when applied to the heteroaryl counterparts.

The significance associated with the heteroarylamine structural motifs stems from their extensive presence in active pharmaceutical ingredients such as alogliptin,³ buparlisib,⁴ alomoucine,⁵ puromycin,⁶ roscovitine,⁷ and many more (Figure 1). Transition-metal catalyzed (especially palladium-based catalytic systems) functionalization of heteroaryl chlorides with different nucleophiles (primary or secondary amines,

phenols, thiophenols, and thiols) in recent years has been extensively explored by various research groups. Palladium-catalyzed amination of heteroaryl chlorides compared to other catalytic processes has seen significant development with Buchwald,⁸ Organ et al.,⁹ and Reetz et al.¹⁰ reporting competitive yields, albeit at higher temperatures. Recently, our research group reported an improved catalytic protocol by the employment of a highly active Pd/PTABS (phosphaadamantan-1-ium-1-yl butane-1-sulfonate or Kapdiphos) catalytic system¹¹ capable of performing the synthetically useful transformation at ambient temperature.¹² Despite all these advances, several questions remain unanswered such as the possible replacement

Received: April 12, 2021

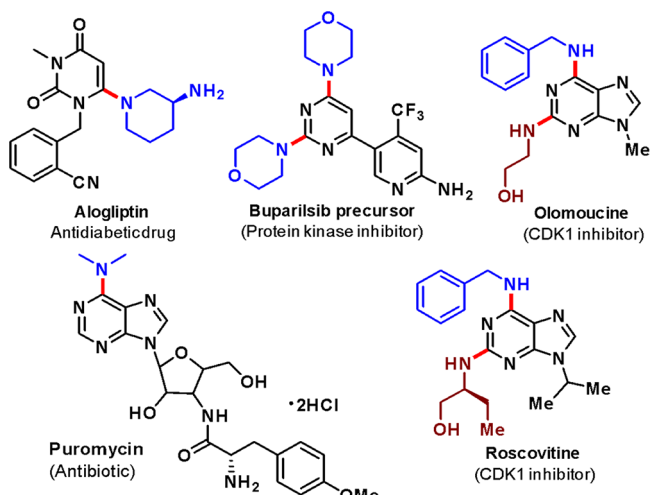


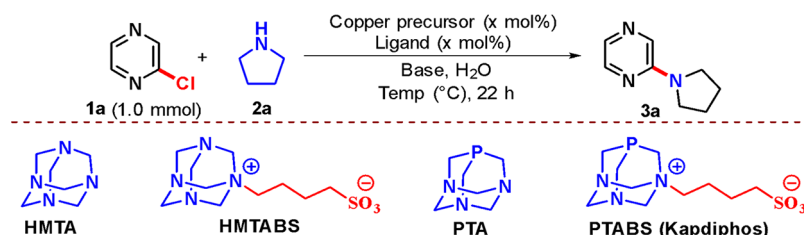
Figure 1. Heteroarylamine structural motif in active pharmaceutical ingredients.

of costly palladium with a cheaper earth-abundant 3d transition metal (such as Cu, Ni, or Co), low catalyst loading, recyclable

ability, and wide substrate scope not limited to secondary amines. Copper-based catalytic amination holds more promise than other 3d metals in solving this problem as a substantial amount of literature reports is known for haloarenes. Ullmann-type or Ullmann condensation reactions catalyzed^{13a,b} by copper catalysts have made a significant impact compared to the palladium-based coupling processes from the point of view of cost-effectiveness. The Goldberg reaction (Ullmann-type C–N coupling^{13c–e}), which was first introduced in 1906^{13f} and involving the coupling of aryl halides with amines using copper catalysts, has been looked upon as a promising alternative to the palladium-catalyzed Buchwald–Hartwig amination. However, a look into the literature suggests several limitations including higher catalyst concentration, limited substrate scope (aryl halides used as coupling partners and very few examples of heteroarene coupling), and significantly high reaction temperature.¹⁴ It is therefore pertinent to improve the reaction conditions by incorporating heteroarene coupling partners given their importance in commercially relevant molecules, thus making the protocol synthetically more attractive.

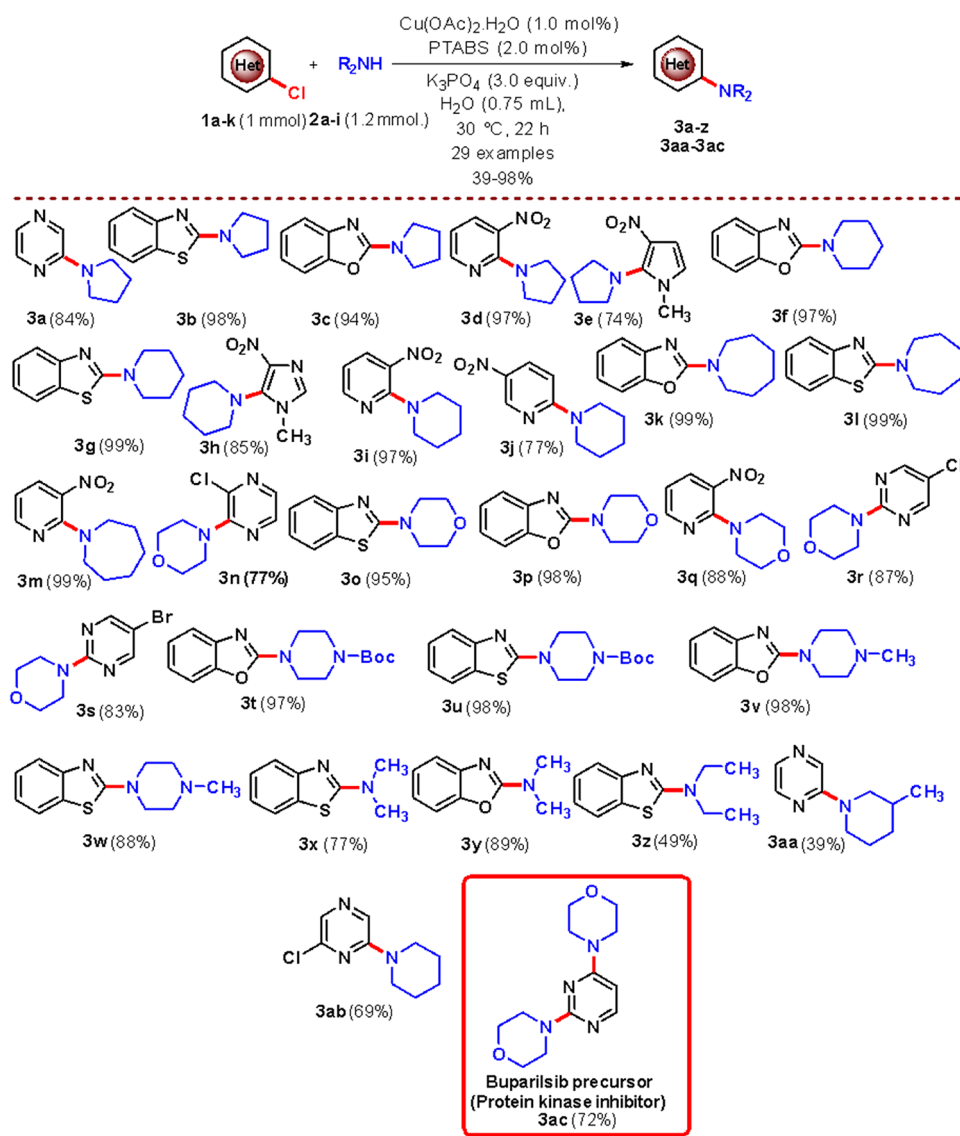
Taking into consideration all these shortcomings, we have developed a copper-based Cu/PTABS protocol for the amination of chloroheteroarenes with primary and secondary

Table 1. Screening Studies for the Amination of Chloroheteroarenes^a



no.	catalyst		ligand		solvent		reaction temp (°C)	isolated yield (%)
	precursor	mol %	name	mol %	name	volume (mL)	base	
1.					H ₂ O	3.0	K ₃ PO ₄	30
2.	Cu(OAc) ₂ ·H ₂ O	10			H ₂ O	3.0	K ₃ PO ₄	3
3.	Cu(OAc) ₂ ·H ₂ O	1.0			H ₂ O	3.0	K ₃ PO ₄	26
4.	Cu(OAc) ₂ ·H ₂ O	1.0			H ₂ O	0.75	K ₃ PO ₄	39
5.	CuI	1.0			H ₂ O	0.75	K ₃ PO ₄	11
6.	Cu(OTf) ₂	1.0			H ₂ O	0.75	K ₃ PO ₄	8
7.	Cu(OAc) ₂ ·H ₂ O	1.0	HMTABS	2.0	H ₂ O	0.75	K ₃ PO ₄	76
8.	Cu(OAc) ₂ ·H ₂ O	1.0	HMTABS	2.0	H ₂ O	0.75	K ₂ CO ₃	62
9.	Cu(OAc) ₂ ·H ₂ O	1.0	HMTABS	2.0	H ₂ O	0.75	Na ₂ CO ₃	34
10.	Cu(OAc) ₂ ·H ₂ O	1.0	HMTABS	2.0	H ₂ O	0.75	Et ₃ N	47
11.	Cu(OAc) ₂ ·H ₂ O	1.0	HMTA	2.0	H ₂ O	0.75	K ₃ PO ₄	58
12.	Cu(OAc) ₂ ·H ₂ O	1.0	pyridine	2.0	H ₂ O	0.75	K ₃ PO ₄	62
13.	Cu(OAc) ₂ ·H ₂ O	1.0	2,2'-bipyridine	2.0	H ₂ O	0.75	K ₃ PO ₄	69
14.	Cu(OAc) ₂ ·H ₂ O	1.0	1,10-phenanthroline	2.0	H ₂ O	0.75	K ₃ PO ₄	12
15.	Cu(OAc) ₂ ·H ₂ O	1.0	proline	2.0	H ₂ O	0.75	K ₃ PO ₄	65
16.	Cu(OAc) ₂ ·H ₂ O	1.0	PTA	2.0	H ₂ O	0.75	K ₃ PO ₄	61
17.	Cu(OAc) ₂ ·H ₂ O	1.0	PTABS	2.0	H ₂ O	0.75	K ₃ PO ₄	84
18.			PTABS	2.0	H ₂ O	0.75	K ₃ PO ₄	0
19.	Cu(OAc) ₂ ·H ₂ O	1.0	PPh ₃	2.0	H ₂ O	0.75	K ₃ PO ₄	15
20.	Cu(OAc) ₂ ·H ₂ O	1.0	DPEphos	2.0	H ₂ O	0.75	K ₃ PO ₄	76
21.	Cu(OAc) ₂ ·H ₂ O	1.0	DPPE	2.0	H ₂ O	0.75	K ₃ PO ₄	74
22.	Cu(OAc) ₂ ·H ₂ O	1.0	DPPB	2.0	H ₂ O	0.75	K ₃ PO ₄	70
23.	Cu(OAc) ₂ ·H ₂ O	1.0	DPBP	2.0	H ₂ O	0.75	K ₃ PO ₄	72
24.	Cu(OAc) ₂ ·H ₂ O	1.0	PCy ₃	2.0	H ₂ O	0.75	K ₃ PO ₄	45

^aReaction conditions: 1.0 mmol of 1a (2-chloropyrazine), 1.2 mmol of 2a (pyrrolidine), 1.0 mol % of catalyst, 2.0 mol % of ligand, 0.75 mL of water, 3.0 mmol of base, stirring at 30 °C temperature for 22 h. ^bWithout added ligand, 3.0 mL water. ^cWithout added ligand.

Scheme 1. Substrate Scope for the Amination of Chloroheteroarenes with Secondary Amines

^aReaction conditions: 1.0 mmol of chloroheteroarenes, 1.2 mmol of secondary amine, 1 mol % Cu(OAc)₂·H₂O, 2 mol % PTABS, 3.0 equiv of K₃PO₄, 0.75 mL of water, stirring at 30 °C temperature for 22 h. Isolated yield. For 3ac, 2.4 mmol of secondary amine, 6.0 equiv of K₃PO₄.

amines at ambient temperature under palladium-free conditions in water as the sole reaction solvent. Significant improvement in yield (isolated via the column-free protocol), reduction in catalyst loading (0.0001 mol %), and excellent recycling ability (up to 12 recycles without any significant reduction in yield) were achieved. This study has also been assisted with a thorough mechanistic understanding of the activating effect of the PTABS ligand on the catalytic activity. DFT studies performed on the ligand suggest the π -acceptor ability of PTABS playing a significant role in promoting the catalytic transformation under such competitive conditions.

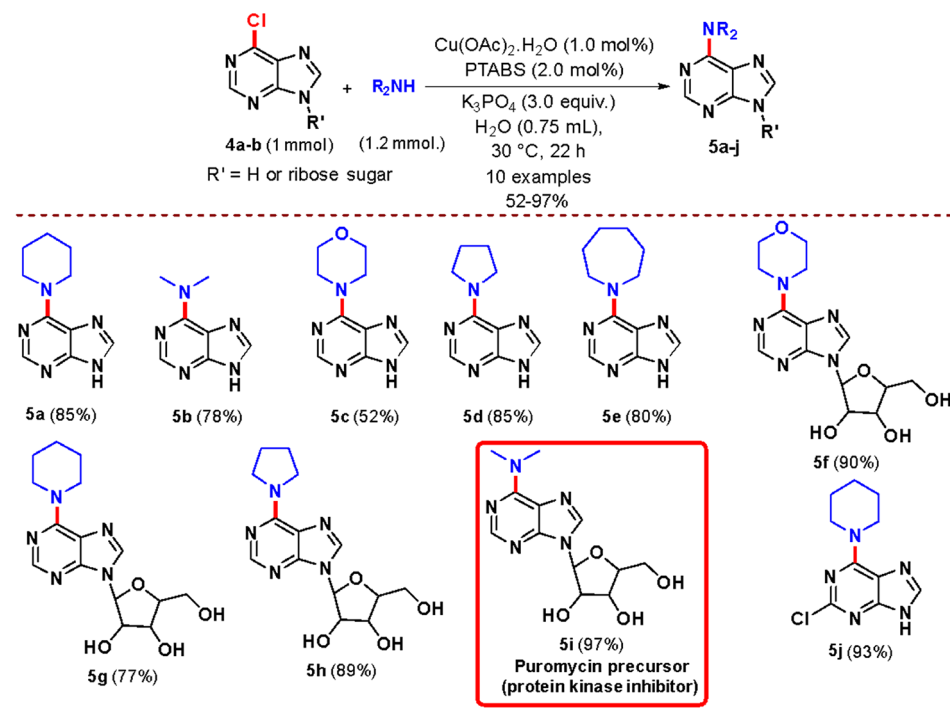
RESULTS AND DISCUSSION

The literature reports for the Buchwald–Hartwig amination of chloroheteroarenes are dominated by the employment of palladium-based catalytic systems that are expensive.^{15,16} Given the powerful nature of the C–N cross-coupling protocol and to promote their commercial exploitation for the synthesis of APIs, agrochemicals, etc., the use of cheaper alternatives in the

form of the earth-abundant 3d transition metals¹⁷ has become a necessity. However, the mere replacement of Pd would not entirely serve the purpose and a conscious effort should be made to incorporate other important aspects such as Ullmann-type coupling reactions (copper-catalyzed Goldberg reaction)^{13,14} that could prove beneficial. To overcome these deficiencies, we therefore decided to explore copper salts in combination with different ligands for the coupling of 2-chloropyrazine with pyrrolidine in water (3.0 mL) as the reaction solvent and preferably at ambient temperature (Table 1).

At the outset of our studies, a background reaction with no catalyst and only base was performed to ascertain the reactivity under catalyst-free conditions. It was observed that the reaction did not furnish any product (Entry 1, Table 1). Encouraged by this result, we employed Cu(OAc)₂ salt (10 mol %) at 30 °C without any added ligand, providing only 3% isolated yield of the desired product (Entry 2, Table 1). Isolation of the coupled product was carried out via a column-free protocol (detailed procedure provided in the Experimental Section). Lowering the

Scheme 2. Catalytic Amination of Purine and Purine Riboside with Secondary Amines



^aReaction conditions: 1.0 mmol of chloropurines and chloropurine ribosides, 1.2 mmol of secondary amine, 1 mol % $\text{Cu(OAc)}_2 \cdot \text{H}_2\text{O}$, 2.0 mol % PTABS, 3.0 equiv of K_3PO_4 , 0.75 mL of water, stirring at 30 °C temperature for 22 h. Isolated yield.

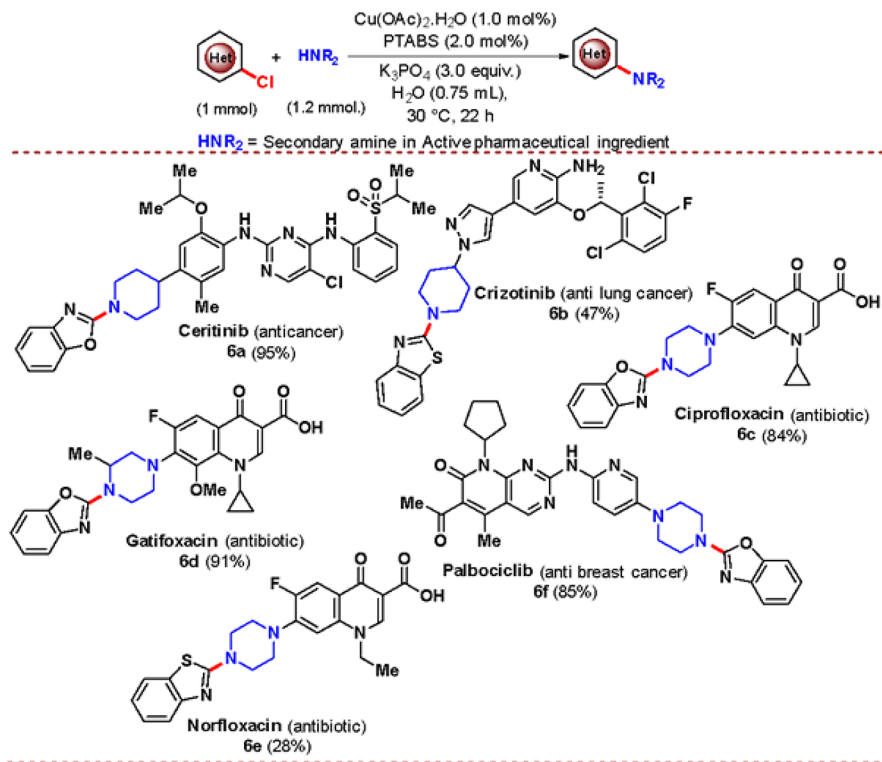
concentration of the copper salt (1.0 mol %) proved to be effective in providing up to 26% products (Entry 3, Table 1). Agglomeration at higher catalyst concentrations could be the reason for the reduced yield in Entry 2 compared to Entry 3. Reduction in the solvent concentration (0.75 mL) was also found to further promote the catalytic activity, giving 39% of the coupled product (Entry 4, Table 1). Other catalyst precursors such as CuI and Cu(OTf)_2 however proved to be less effective under the developed conditions (Entries 5 and 6, Table 1). The solubility and stability of the catalytic system in water could be a deciding factor for obtaining improved catalytic activity.

Accordingly, a water-soluble nitrogen-containing ligand (HMTABS-2.0 mol %) derived from hexamethylenetetramine (HMTA) was first employed in combination with Cu(OAc)_2 as the catalyst precursor (Entry 7, Table 1). Improvement in the product yield was immediately observed, and encouraged by this result we decided to further investigate the role of different bases as well as ligands. All the previous reactions were performed using K_3PO_4 as the base and therefore the next set of experiments were performed using bases such as K_2CO_3 , Na_2CO_3 , and Et_3N (Entries 8–10 respectively, Table 1), although their reactivity was not comparable to that obtained with K_3PO_4 . Other nitrogen-based ligands such as HMTA, pyridine, 2,2'-bipyridine, 9,10-phenanthroline, and proline were next to be investigated in an attempt to further improve the product yield (Entries 11–15, Table 1). However, the lower yield observed in all the cases suggested the superior catalytic efficiency of the water-soluble Cu(II) /HMTABS system.

In recent years, our research group has successfully demonstrated the employment of water-soluble phosphines namely, 1,3,5-triaza-7-phosphadamantane (PTA)¹⁸ and its derivative PTABS¹⁹ (Kapdiphos) for the modification of chloroheteroarenes either as preformed palladium complexes

or in combination with Pd(II) precursors. PTA under the given set of conditions did not improve the catalytic activity; however, PTABS gave 84% of the isolated coupled product (Entries 16 and 17, Table 1). To ascertain the role of the ligand in that whether it could act as a Lewis Base in catalyzing the reaction without the metal catalyst, a reaction with PTABS and no Cu source added was performed. As no product formation was observed, it clearly suggests that the ligand PTABS plays no role in promoting the transformation and a combination of Cu(II)/PTABS is therefore necessary (Entry 18, Table 1). Encouraged by the improvement in the yield, several activating phosphines such as PPh_3 , DPEphos, DPPE, DPPB, PPP, and PCy_3 were next to be tried (Entries 19–24, Table 1). Interestingly, none of these ligands were able to further enhance the reactivity, and therefore the combination of Cu(OAc)_2 with PTABS can be finalized as the one for further exploration.

We next turned our attention to the employment of the optimized reaction conditions for the catalytic amination of chloroheteroarenes with secondary amines. Efficient access to 29 derivatives using the developed catalytic protocol was made possible by the combination of 11 chloroheteroarenes with 9 secondary amines in good to excellent yields (Scheme 1). A variety of heteroarenes ranging from benzoxazole, benzothiazole, pyrazine, pyrimidine, and several others worked efficiently with secondary amines such as pyrrolidine, piperidine, hexahydro azepine, morpholine, etc. 5-Chloro-4-nitroimidazole as a substrate also performed equally well (3h, Scheme 1); however, 2-chloropyridine, when employed as a coupling partner with a secondary amine (piperidine), failed to provide the desired product (Scheme 1). The failure of the pyridine heterocycle could be attributed to the possible complexation (observed by following the reaction with ESI-MS) of the pyridine N atom with the copper complex as well as the lower

Scheme 3. Late-Stage Modification of Active Pharmaceutical Ingredients (APIs) Using the Cu(II)/PTABS System

^aReaction conditions: 0.5 mmol of chloroheteroarenes, 0.5 mmol of APIs, 1 mol % Cu(OAc)₂·H₂O, 2 mol % PTABS, 3.0 equiv of K₃PO₄, 0.38 mL of water, stirring at 30 °C temperature for 22 h. Isolated yield.

electrophilicity of the pyridine substrate. To verify such an assumption, pyridine substrates with an electron-withdrawing NO₂ group in the 3rd and 5th positions were employed. The resultant catalytic amination reaction (with piperidine nucleophile) proceeded with good yields of the coupled product (**3i,j**, Scheme 1).

The Cu(II)/PTABS catalytic system was also found to promote good regio- and chemoselectivity for substrates such as 2,5-dichloropyrimidine and 5-bromo-2-chloropyrimidine, respectively (**3r,s**, Scheme 1). Cyclic secondary amines were effective in most of the transformations, and a similar trend was observed for acyclic secondary amine, dimethylamine (**3x,y**, Scheme 1). However, the introduction of diethylamine as the coupling partner brought about a slight reduction in reactivity (**3z**, Scheme 1). Finally, the diamination of 2,6-dichloropyrazine and 2,4-dichloropyrimidine was carried out with piperidine and morpholine as the amine coupling partners, respectively (**3ab,ac**, Scheme 1). The product **3ab** however indicates the requirement of an electron-deficient heteroarene to promote the second amination, and in this case, clearly the first amination leads to the deactivation of the heteroarene ring toward the 2nd C–Cl activation. The formation of the coupling product between 2,4-dichloropyrimidine and morpholine in good yields has significance due to the occurrence of this structural motif in Buparlisib,⁴ which is an important protein kinase inhibitor (**3ac**, Scheme 1).

The successful exploitation of the developed amination protocol for the installation of the amine functionality on the various heteroarenes was further explored for privileged synthetic scaffolds such as purine and purine riboside (Scheme 2). The importance of the amine-functionalized purine or purine ribosides stems from their occurrence in a variety of

pharmaceutically active molecules such as puromycin.⁶ Accordingly, several research groups such as Koomen et al.,²⁰ Lanver and Schmalz,²¹ and Lakshman et al.,²² as well as our group have reported the amination using palladium catalysis with limited scope and reactivity.²³ Excellent reactivity of the developed Cu(II)/PTABS catalytic system could therefore serve the double purpose of improving reactivity and providing a cheaper alternative to the expensive palladium catalyst precursors.

6-Chloropurine (**4a**) was the first to be subjected to the developed catalytic conditions, providing good yields of the desired 6-amino purine products (Scheme 2). A slightly reduced result was obtained with morpholine when used as the nucleophilic coupling partner (**5c**, Scheme 2). Due to the higher solubility of the purines in water, the column-free isolation was also a bit more complex than the general heteroarenes (see the Experimental Section for a detailed procedure). 6-Chloropurine riboside was the next to be coupled with different secondary amines (**5f–i**, Scheme 2), giving in all the cases good to excellent yield of the amination product. The puromycin (an important protein kinase inhibitor) precursor (**5i**) starting from 6-chloropurine riboside was also obtained in close to quantitative yield.

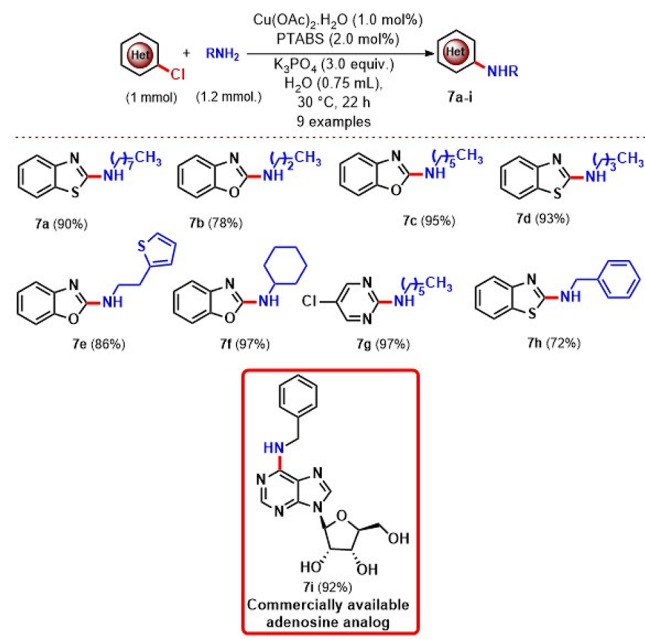
To further test the efficacy of the Cu(II)/PTABS system, we envisioned the challenging late-stage modification of the various active pharmaceutical intermediates (APIs). The APIs were selected based on the presence of a secondary amine functionality in the core structure of some commercially available anticancer agents such as Ceritinib,²⁴ Crizotinib,²⁵ and Palbociclib²⁶ as well as the well-known antibiotics such as Ciprofloxacin,²⁷ Gatifloxacin,²⁸ and Norfloxacin²⁷ that were employed as the nucleophilic coupling partners (Scheme 3). Benzoxazole and benzothiazole were accordingly coupled with

the abovementioned APIs in good yields, although the presence of the free-CO₂H functionality in the case of the floxacins complicated the isolation process as well as affected the overall catalytic activity. These results, however, demonstrate the versatile nature of the developed catalytic system.

Functionalization of chloroheteroarenes with secondary amines is relatively well-reported due to the higher nucleophilicity of the amines, while primary alkyl amines as coupling partners are still a challenging prospect. Most examples of such couplings have been reported with different palladium catalytic systems and aryl halides as coupling partners at higher reaction temperatures.²⁹ Hartwig et al.,^{30,31} Shaughnessy et al.,³¹ and a few others have reported ambient-temperature protocols for the above transformation; however, chloroheteroarenes as coupling partners have seldom performed at such low temperatures. The catalytic efficiency of the Cu(II)/PTABS system was therefore tested for a range of primary alkyl amines at ambient temperature.

Straight chain primary alkylamines such as *n*-propyl, butyl, hexyl, and octyl amines worked very well, giving good yields of the amination products with different chloroheteroarenes (7a–d, Scheme 4). This is a very encouraging result with the

Scheme 4. Primary Alkyl Amines as Coupling Partners for the Cu(II)/PTABS-Catalyzed Amination



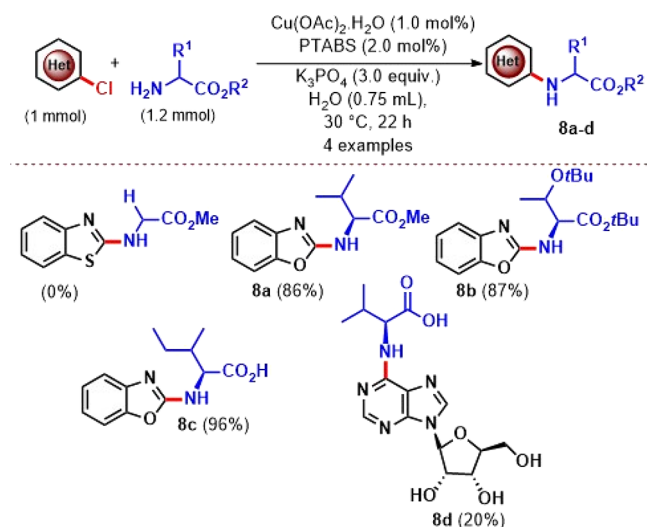
^aReaction conditions: 1.0 mmol of chloroheteroarenes, 1.2 mmol of primary alkyl amine, 1 mol % Cu(OAc)₂·H₂O, 2 mol % PTABS, 3.0 equiv of K₃PO₄, 0.75 mL of water, stirring at 30 °C temperature for 22 h. Isolated yield.

synthetically challenging primary alkyl amines that could also be coupled at ambient temperature and in water as a solvent. A few other primary alkyl amines including 1-aminocyclohexane, benzylamine, etc. were also employed.

One such reaction of benzylamine with 6-chloropurine riboside furnished a good yield of the product (7i, Scheme 4) that has been a commercially very useful adenosine³² analog. Another catalytic process that has proved challenging is the coupling with amino acids³³ or their corresponding esters. The relevance of N-substituted amino acids as useful modified

analogs for biological applications has led to the development of several synthetic protocols allowing easy access to these moieties.³⁴ However, one of the commonly associated problems is the poor reactivity of the NH₂ group to undergo functionalization and is related directly to the rate-limiting reductive elimination step of the cross-coupling pathway. This was also evident from the initial experiments performed without the Cu(II)/PTABS catalytic system for the functionalization of glycine ester with chloroheteroarene (Scheme 5). To overcome

Scheme 5. Amino Acid Functionalization Using the Cu(II)/PTABS System



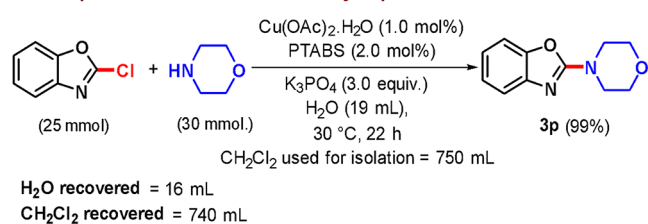
^aReaction conditions: 1.0 mmol of chloroheteroarenes, 1.2 mmol of amino acid esters, 1 mol % Cu(OAc)₂·H₂O, 2 mol % PTABS, 3.0 equiv of K₃PO₄, 0.75 mL of water, stirring at 30 °C temperature for 22 h. Isolated yield.

this problem, we envisioned the use of sterically hindered amino acid esters such as valine and *tert*-butyl amino acid ester and isoleucine. The coupling proceeded efficiently with both these amino acid esters to provide good to excellent yields of the desired products. Functionalization of amino acid esters at ambient temperature in water as the reaction solvent is the first to be reported.

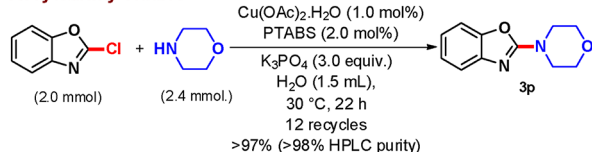
We next turned our attention to test the scalability of the developed catalytic protocol as well as develop an efficient solvent recovery procedure (for the column-free isolation of the product)^{19a,35} to promote a sustainable solution for further applicability (Scheme 6). 2-Chlorobenzoxazole coupled with morpholine using the Cu(II)/PTABS catalytic system at the 25 mmol scale in the water at ambient temperature proceeded efficiently in nearly quantitative yield (99%).

In one of our previous reports, we had successfully demonstrated the recyclability of the catalytic solution of Pd(II)/PTABS for the Suzuki–Miyaura coupling of halonucleosides promoted by the extensive water solubility of PTABS as well as the resulting catalyst.^{19b} On similar lines, it was decided to test the Cu(II)/PTABS catalytic system for recyclability for the coupling of 2-chlorobenzoxazole with morpholine (Scheme 7).

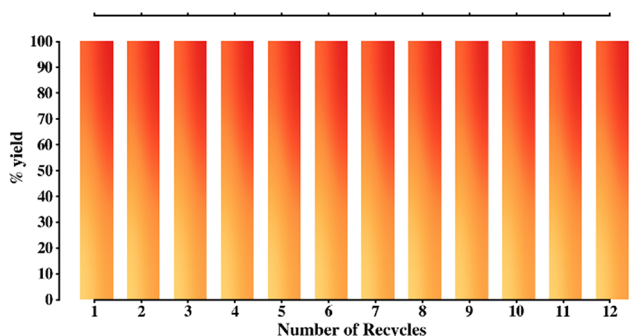
A background reaction without the addition of Cu(II)/PTABS to check the extent of SNAr occurring in the given transformation was performed at ambient temperature. It was observed that 26% of the desired product was obtained after 24

Scheme 6. Scaleup Protocol and Solvent Recovery**Scale-up reaction & solvent recovery experiment**

^aReaction conditions: 25 mmol of 2-chlorobenzoxazole, 30 mmol of morpholine, 1.0 mol % $\text{Cu}(\text{OAc})_2 \cdot \text{H}_2\text{O}$, 2.0 mol % PTABS, 3.0 equiv of K_3PO_4 , 19 mL of water, stirring at 30 °C temperature for 22 h. Isolated yield.

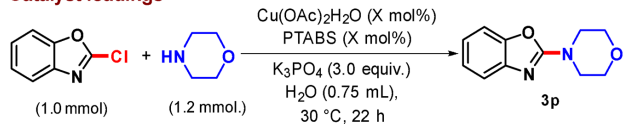
Scheme 7. Recyclability Studies for Cu(II)/PTABS**Recyclability studies**

Reaction conditions: 2.0 mmol of 2-chlorobenzoxazole, 2.4 mmol of morpholine, 1 mol % of $\text{Cu}(\text{OAc})_2 \cdot \text{H}_2\text{O}$, 2 mol % of PTABS, 3.0 equiv. of K_3PO_4 , 1.5 mL of water, stirring at 30 °C temperature for 22 h. Isolated yield.



h. The addition of the Cu(II)/PTABS catalyst system therefore proves to be beneficial for promoting this transformation, and accordingly we proceeded toward performing the recyclability studies. Excellent recyclability was also exhibited by the Cu(II)/PTABS system with no loss in activity observed even after recycling the catalyst solution 12 times. ICP-AES analysis of some of the products isolated (using the column-free protocol) showed no presence of any metallic copper species, suggesting the higher stability of the in situ-formed complex and subsequent affinity to the water phase.

The catalytic efficiency of Cu(II)/PTABS was further tested by performing the catalyst loading experiments (Scheme 8). At 1.0 mol % catalyst concentration, quantitative product formation was observed for the coupling of 2-chlorobenzoxazole with morpholine. These experiments however were carried out using new Schlenk tubes, and stirrer bars gave the relevance of trace metals in catalyzing synthetic transformations. A 10-fold reduction in the catalyst concentration (0.1 mol % of Cu(II) + 0.2 mol % PTABS) also provided a very good yield (92% and TON = 920). Further reduction to 0.01 mol % Cu(II) concentration also proved to be effective (97% & TON = 9700), while a similar observation was made at 0.001 mol % concentration (95%, TON 95000). Excellent reactivity was further exploited to reduce the catalyst concentration to 0.0001

Scheme 8. Catalyst Loading Experiments for the Cu(II)/PTABS Catalytic System**Catalyst loadings**

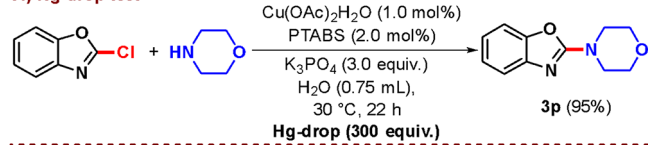
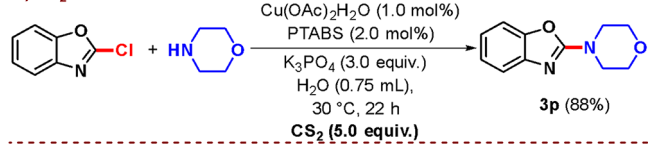
No.	$\text{Cu}(\text{OAc})_2$ (mol%)	PTABS (mol%)	%Yield	TON
1.	1.0	2.0	99	99
2.	0.1	0.2	92	920
3.	0.01	0.02	97	9700
4.	0.001	0.002	95	95000
5.	0.0001	0.0002	98	980000

^aReaction conditions: 1.0 mmol of 2-chlorobenzoxazole, 1.2 mmol of morpholine, x mol % of catalyst, x mol % of ligand, 3.0 equiv K_3PO_4 , 0.75 mL of water, stirring at 30 °C temperature for 22 h. Isolated yield.

mol %, which still provided excellent results (TON = 980,000). These are unprecedented results for the coupling of chloroheteroarenes with amine nucleophiles.

■ TEST FOR HOMOGENEITY OF THE CATALYST SYSTEM

Cu(II)/PTABS has proven to be a highly efficient catalytic system for the amination of chloroheteroarenes under the developed conditions, and the initial indications from the various catalytic reactions suggest the presence of a homotopic catalyst that is promoting the transformations under the developed conditions.³⁶ To ascertain such a possibility, we conducted a series of catalyst poisoning experiments. First, we investigated the effect of the addition of Hg drop³⁶ to the catalytic reaction between 2-chlorobenzoxazole and morpholine (A, Scheme 9).

Scheme 9. Catalyst Poisoning Experiments**Catalyst poisoning experiments****A) Hg-drop test****B) CS_2 -addition test**

^aReaction conditions: 1.0 mmol of 2-chlorobenzoxazole, 1.2 mmol of morpholine, 1.0 mol % $\text{Cu}(\text{OAc})_2 \cdot \text{H}_2\text{O}$, 2.0 mol % PTABS, 3.0 equiv of K_3PO_4 , 0.75 mL of water, stirring at 30 °C temperature for 22 h. Isolated yield. (A) Hg drop (300 equiv). (B) CS_2 (5.0 equiv).

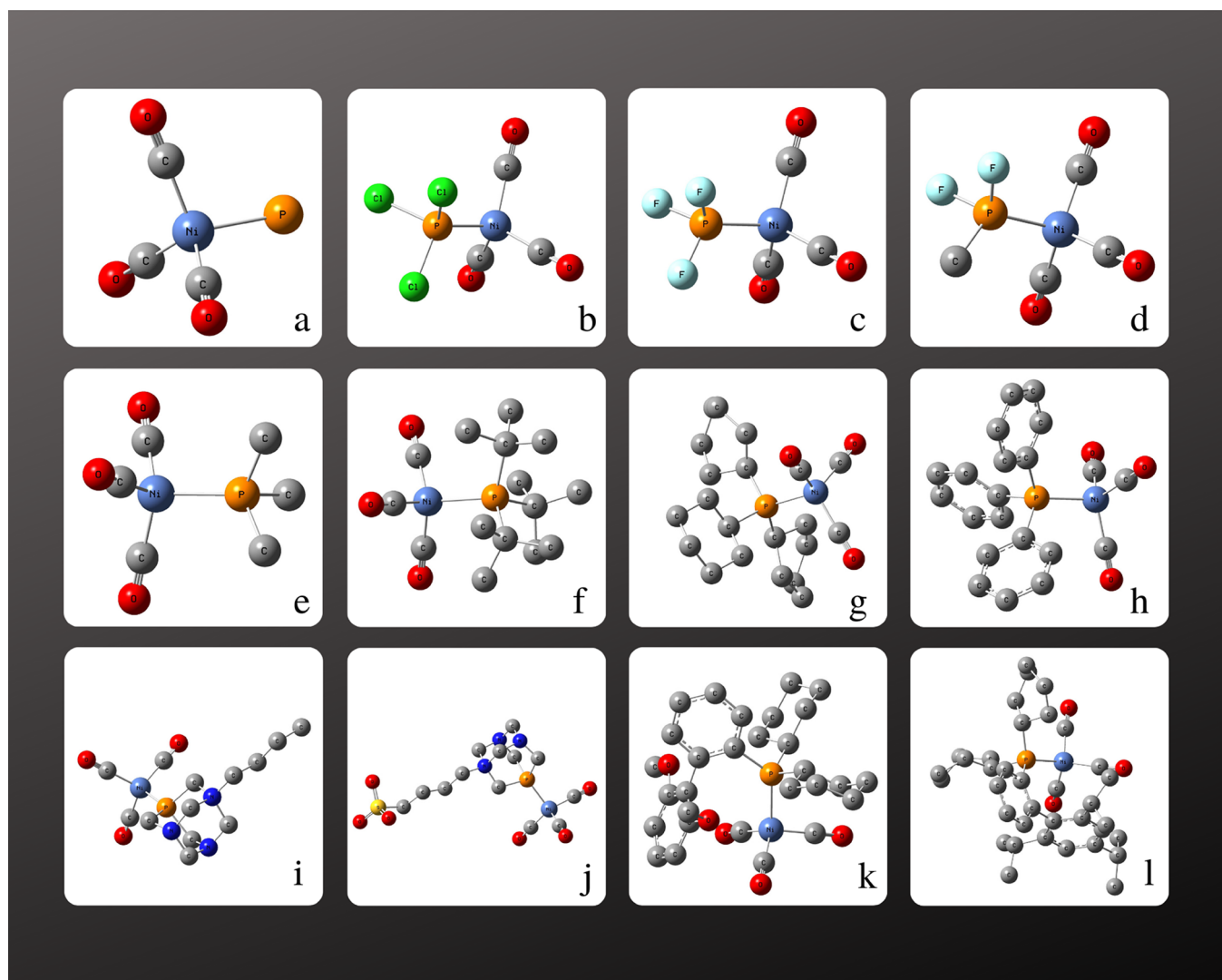


Figure 2. Structures of the most stable nickel complexes without hydrogen atoms. (a) $\text{Ni}(\text{CO})_3(\text{PH}_3)$, (b) $\text{Ni}(\text{CO})_3(\text{PCl}_3)$, (c) $\text{Ni}(\text{CO})_3(\text{PF}_3)$, (d) $\text{Ni}(\text{CO})_3(\text{PMeF}_2)$, (e) $\text{Ni}(\text{CO})_3(\text{PMe}_3)$, (f) $\text{Ni}(\text{CO})_3(\text{tBu}_3)$, (g) $\text{Ni}(\text{CO})_3(\text{PCy}_3)$, (h) $\text{Ni}(\text{CO})_3(\text{PPh}_3)$, (i) $\text{Ni}(\text{CO})_3(\text{PTABX})$, (j) $\text{Ni}(\text{CO})_3(\text{PTABS})$, (k) $\text{Ni}(\text{CO})_3(\text{SPhos})$, and (l) $\text{Ni}(\text{CO})_3(\text{XPhos})$.

With the reactivity unaffected by the addition of the Hg drop, a result strongly suggesting the presence of Cu(II)/PTABS as a homotopic catalyst, addition of excess carbon disulfide (CS_2)^{36b,c} as a catalyst poison was carried out. Although a slight dip in the product formation was observed (88%, B, Scheme 9), the result still points strongly toward the presence of a homogeneous system.

The homogeneity of the Cu(II)/PTABS in water could be explained based on the higher solubility of the PTABS ligand, which on strong coordination with the Cu(II) species helps solubilize the in situ-formed catalyst. However, to explain the dramatic improvement in catalytic activity exerted by PTABS in combination with Cu(II), it is important to investigate the electronic and steric properties of the ligand, which could be predicted using density functional theory (DFT).

THEORETICAL STUDIES ON ELECTRONIC AND STERIC PROPERTIES OF PTABS

The unusual reactivity of the PTABS ligand and the complex it forms could be understood by studying the bonds of metal–PTABS using the Dewar–Chatt–Duncanson model.³⁷ Tolman

properties predicted that using the substitution of a CO ligand in $\text{Ni}(\text{CO})_4$ with a PR_3 could be employed as the most acceptable model for this purpose as the Ni metal core can provide the molecular orbital base to PTABS for obtaining such useful information. Nickel has been the metal of choice (especially $\text{Ni}(\text{CO})_4$) for calculating Tolman properties as the theoretical data for other phosphine ligands for comparison is more readily available for Ni rather than for Cu. It was therefore decided to go with Ni for parametric understanding. Accordingly, to analyze the electronic properties of the PTABS ligand and compare it to the whole ligand space, an assortment of phosphine ligands was chosen for reference.³⁸ The aim was to understand the possible back bonding interaction of PTABS and gauge the predicted π -accepting capacity³⁹ of the ligand. Phosphine back bonding depends not only on the phosphine substituents (PR_3) but also on other ligands present on the metal atom. To eliminate any interferences from the metal side, the other three ligands bonded to Ni metal were held constant as CO ligand⁴⁰ (Figure 2).

Electronic Properties of PTABS. In short, Ni has four unfilled hybridized sp^3 orbitals, which accept lone pairs from four ligands, one of them being PTABS and the remaining three are CO. These sp^3 orbitals are made up of 4s and 4p atomic

orbitals that are quite large compared to the 3p lone pair of phosphorus.

Due to the size difference, the overlap between these two orbitals is not sufficient, and the energy difference is also too large to provide any energy reduction to Ni. The energetics alone make it hard to justify why the Ni-PTABS bond will form naturally. The fact that such a complex could exist can be attributed to the energy reduction by forming metal-ligand three-center four-electron ω bonds⁴¹ and through π -back bonding interaction between the metal and ligand.

Using second-order perturbation theory, all filled bonding orbital interactions and all empty antibonding orbitals of all complexes were estimated (Figure 3). As back bonding⁴² is an

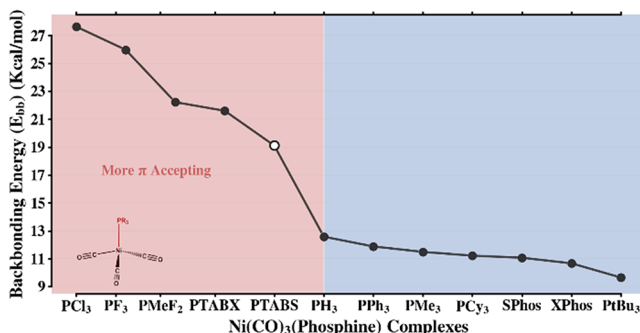


Figure 3. Backbonding energy of Ni complexes.

interaction between Ni d lone pairs and P-R σ^* antibonding orbitals, all interactions between Ni five d orbitals and three σ^* antibonding orbitals were recorded. The sum of all these interactions gives us an estimate of the complex's back bonding energy⁴³ (E_{bb}).

The C–H bond is considered as a reference to compare bond polarities in many molecules. An atom X pulling more electron density from the carbon center of a C–X bond compared to what H atoms would be capable of attracting from the carbon center of a C–H bond is commonly considered to be electronegative. The carbon atom therefore acquires an electropositive character in such a case. The same principle could be applied to substrates attached to phosphines. Using PH₃ as a reference, we can divide the phosphines into two groups, which are more π -accepting than PH₃ and others that are less π -accepting, i.e., more σ -donating than PH₃. Between π -accepting and σ -donating groups, the sharp drop in back bonding energy clearly defines the two groups according to their nature. Being derived from a weakly σ -donating PTA ligand, PTABS could also be predicted to follow the general tendency to be σ -donating in nature. However, PTABS subverts this expectation by portraying strong back bonding that can only be compared with the π -acceptor halogen phosphines (PX₃).

Due to the three-center four-electron Ni bonds, every ligand has a combined stake in the ligand electron structure that lies opposite to it, as one electron is shared across all three atomic centers. When one phosphine is attached to Ni, the electron density donated to the P-R σ^* antibonding orbital is partly compensated for by CO ligands. The loss of electron density leads to an increase in CO stretching frequency (Figure 4). The CO bond order decreases in a similar trend with an increase in CO bond length. Compared to PH₃, we see a steady decline in CO stretching frequency as phosphines' nature slowly changes from π -accepting to σ -donating. PTABS is more accepting than

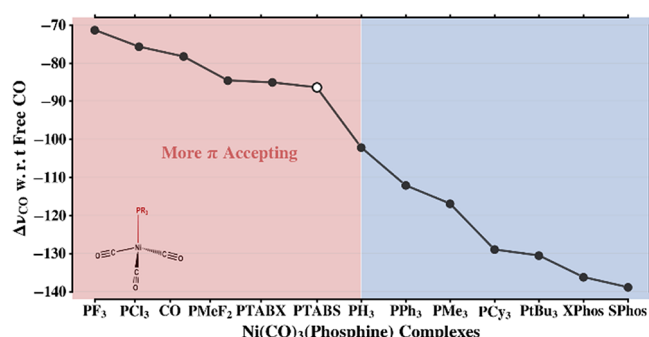


Figure 4. CO stretching frequency of Ni(CO)₃(Phosphine) complex.

PH₃, a stark contrast from the biphenyl-based phosphines, XPhos and SPhos.

When a ligand that has stronger backbonding than CO is added to the metal complex, the electron density at the metal center decreases, which is reflected by an increase in back bonding. Thus, a ligand, upon whose addition increases C–O stretching frequency and increases the Ni–P bond length at the cost of pulling the three carbonyls towards itself (decrease in Ni–C bond length), is a π -acidic or π -accepting ligand (Figure 5). With these observations, a general trend⁴⁴ of electronic effects of phosphines is established, with a better understanding of the π -accepting nature of PTABS ligands.

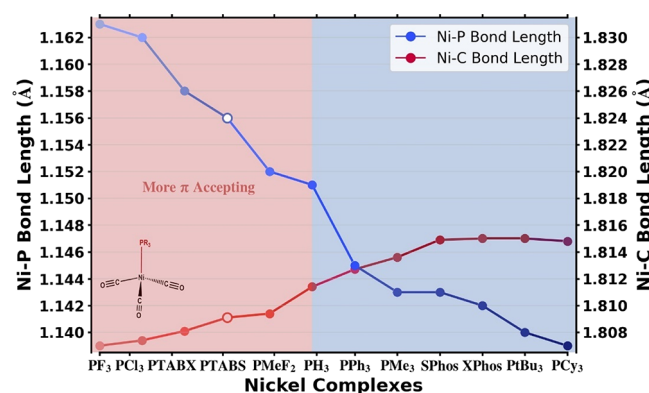


Figure 5. Variation in Ni-P and Ni-C bond lengths.

When a ligand that has a stronger back bonding than CO is added, it has been already predicted that the CO stretching frequency will decrease leading to an increased back bonding. Three-center four-electron bonds thus are found to share the electrons, and Ni will accordingly divert the d orbital electrons of Ni and some electron density of nearby atoms to the P-R σ^* molecular orbital. The extent of this transfer depends on the LUMO's energy, which in turn depends on the electronegativity of the atom directly attached to Ni. It is not surprising that the highly electronegative halogens such as F, Cl, and their derivatives would be capable of pulling a major part of the electron density from P to lower its LUMO to such an extent that Ni can transfer a large amount of d electron density and in turn lower its energy. However, it is surprising that PTABS, wherein P is attached to a C, can display a similar phenomenon and can be grouped with the highly π -accepting halogens on every metric tested.

Steric Properties of the PTABS Ligand. The atom next to P is not the only important parameter in back bonding. The energy, shape, and orientation of the P-R σ^* antibonding orbital

also play a vital role.⁴⁵ Most of the energy and shape of the antibonding orbital depends on atoms directly attached to P or close to it, i.e., the chemical environment that P is in (Figure 6).

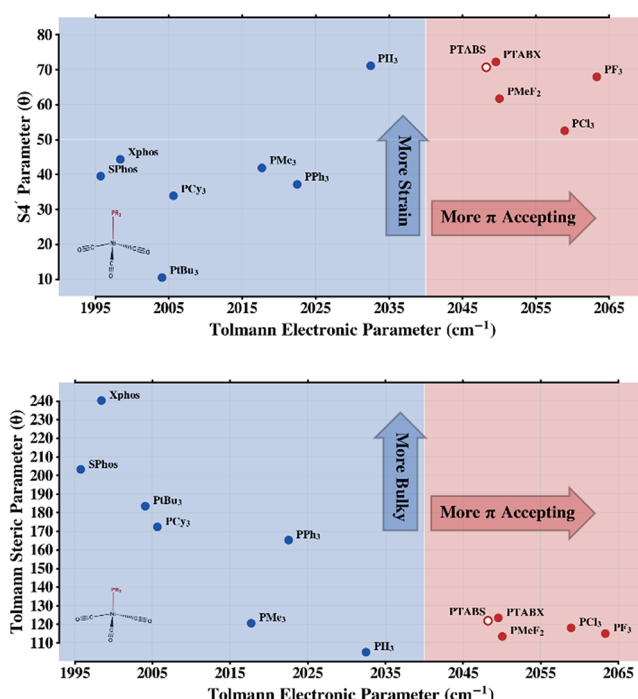


Figure 6. Ligand space of phosphines.

However, the overall bulk of the ligand or a caged structure can force the angle of orbital overlap away from ideal geometry, forcing the orbitals to overlap in a different way than it would for a less bulky ligand. These steric effects can have a drastic impact on back bonding, especially in the case of caged ligands such as PTABS.

PTABS has around ten times as many atoms as PF₃, but in terms of steric bulk exerted on the metal center, PTABS is very close to PF₃. The low steric bulk is due to the ligand's unique long shape (figure in SI) and its curious electronic properties.⁴⁶ When steric bulk increases, the angle between two P substituents (R₁-P-R₂) swells up, while the bulk pushes down the Ni-P-R angle. The S4' parameter ($\Sigma R_1\text{-P-R}_2 - \Sigma \text{Ni-P-R}$) provides an

insight into the strain exerted by the bulk on the Ni-P bond. Plotted against Tolman's electronic parameter,⁴⁷ we get a visualization of phosphine ligand space.

Many ligands that are less π -donating than PH₃ have been explored, while PF₃, PCl₃, and its derivatives remained as lonesome examples beyond the PH₃ region of the phosphine map. There have been many attempts at exploring this unexplored region of the phosphine ligand space. Considering the high atom count, PTABS surprisingly fits into the low straining, the highly π -accepting region of the phosphine ligand space. Whether such a subtle balance in the steric and electronic properties could be the reason for the success of PTABS in the given catalytic cycle with Cu(II) species is debatable but a possibility worth exploring. We plan to return to this aspect in great detail in the near future.

NMR PARAMETERS FOR DEFINING THE π -ACCEPTING ABILITY OF PTABS

One of the methods effectively used in the literature to ascertain the σ -donating or π -accepting ability of the phosphines is to convert them into their corresponding phosphine selenides by the reaction with Se powder or in some cases with KSeCN in a suitable solvent.⁴⁸ NMR parameters of these phosphine selenides have been used by many research groups for determining the electronic alignment of the phosphorus atom in different phosphines. The $^{1}\text{J}_{\text{P}-\text{Se}}$ coupling constant obtained from the ^{31}P NMR analysis of the formed phosphine selenides signifies the electronic properties based on the presence of electron-attracting or electron-releasing groups on the phosphorus atom. A shift to the higher J value ($^{1}\text{J}_{\text{P}-\text{Se}}$ coupling constant) signifies the presence of an electron-poor phosphine (π -accepting phosphorus). One such explanation given for this drift by McFarlane and Rycroft⁴⁹ was due to the less electron sharing taking place between the phosphorus and selenium atoms leading to an increase in the σ -character and a subsequent decrease in the π -character of the resultant P=Se bond.

From the previous theoretical study, PTABS was predicted to be having a π -accepting ability, and to verify this we, first reacted PTABS with Se powder to obtain the $^{1}\text{J}_{\text{P}-\text{Se}}$ coupling constant from the ^{31}P NMR of the reaction (performed in D₂O). A relatively high $^{1}\text{J}_{\text{P}-\text{Se}}$ value of 800 Hz was observed for PTABS=Se and when compared to the literature values of both σ -donating (e.g., SPhos, XPhos, PtBu₃, PCy₃, etc.) and π -accepting

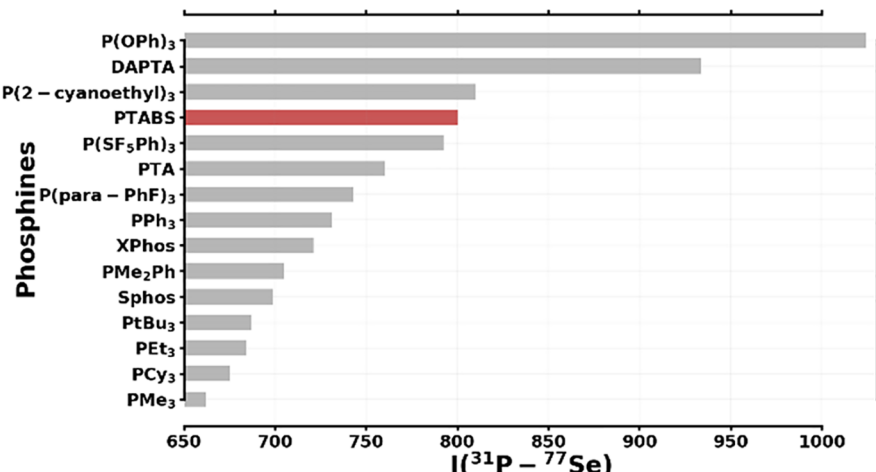


Figure 7. Comparison graph for $^{1}\text{J}_{\text{P}-\text{Se}}$ values of σ -donating and π -accepting phosphines.

phosphines (e.g., P(OPh)₃, DAPTA, etc.). Figure 7 provides the J_{P-Se} values of all the ligands and PTABS when compared fits well in the ligand space having π -accepting properties. This result confirms the predictions obtained from the theoretical studies and would eventually be responsible for providing improved catalytic activity.

SUBSTRATE STRUCTURE VS CATALYTIC ACTIVITY

The developed Cu(II)/PTABS catalytic system was developed for the functionalization of chloroheteroarenes; however, the substrate reactivity and the position of the chloro group were found to play an important role in defining the catalytic activity of the developed system.

Position of the Chloro Leaving Group. Another interesting observation from the catalytic processes is the position of the chloro leaving group on the heteroarene ring and its effect on the outcome of catalysis. Based on the results obtained previously, Figure 8 summarizes and clearly depicts the

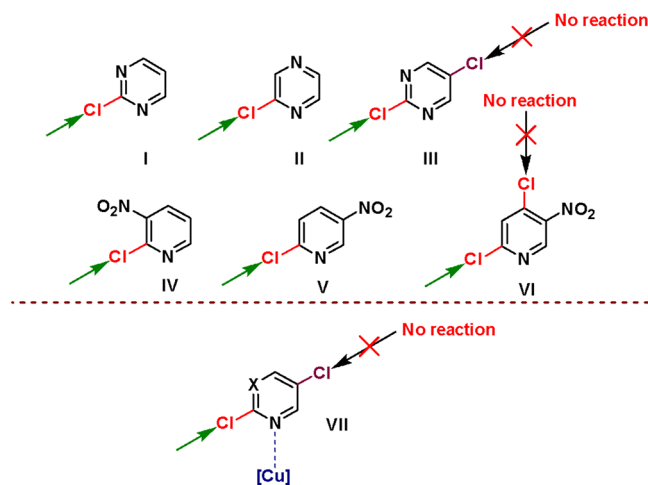


Figure 8. Effect of chloro leaving group position on catalytic activity.

positions that are beneficial for obtaining a successful outcome in the catalytic amination reaction (Figure 8). The commonly electrophilic positions (2, 4, and 6 for structures I and II) would be preferred than the nucleophilic position (5 in this case of structure III) for functionalization with different nucleophiles. Similar observations could also be made for pyridine (2nd position in structures IV and V); however, the 4th position (structure VI) that is also electrophilic fails to undergo any catalytic functionalization.

It is therefore concluded that, besides the usual reactivity of certain positions on the heteroaromatic molecules, the influence of the heteroatom present in the vicinity of the C–Cl bond could be playing a vital role in defining the reactivity possibly by offering weak coordinative assistance to the Cu(II)/PTABS system leading to the preferential functionalization (VII).

INVESTIGATION OF THE COPPER SPECIES IN THE CATALYTIC SOLUTION

The discussion till now was centered around the nature (electronic factor) of the PTABS ligand as well as the influence of the heteroatom on the catalytic activity (position of the C–Cl bond). We, next, decided to explore the nature of the copper

species (Cu^I or Cu^{II}) present in the catalytic solution. From the initial studies, it is clear that the catalytic system follows a homogeneous pathway possibly involving a PTABS coordinated copper species. Preliminary observation of the colors of the catalyst solutions, i.e., Cu(OAc)₂ in H₂O (pale blue), Cu(OAc)₂ + PTABS in H₂O (deepened blue), and the catalytic reaction mixture in H₂O (reaction of 2-chloropyrazine with morpholine under the developed set of conditions; bluish-green), suggests the possibility of a Cu(II) species rather than Cu(I) (Figure 9).

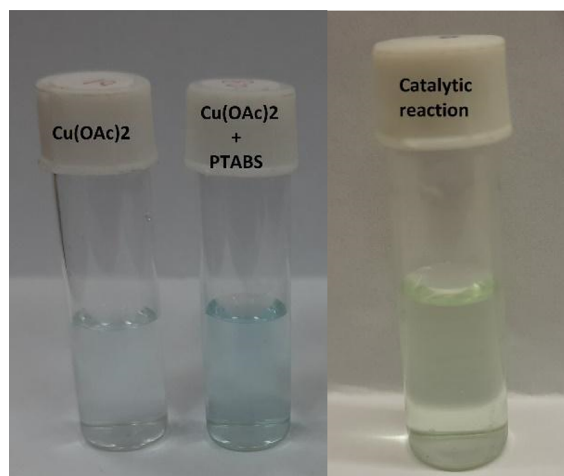


Figure 9. Solutions of Cu(OAc)₂ in H₂O and Cu(OAc)₂ + 2PTABS in H₂O and catalytic reaction in H₂O.

These solutions were further subjected to UV–VIS spectral analysis to understand the effect of the ligand addition to Cu(OAc)₂ containing an unpaired electron.⁵⁰ UV–VIS analysis of Cu(OAc)₂ in H₂O provided maxima at $\lambda = 289$ nm (absorbance intensity = 0.1872) and the addition of 2.0 equiv of PTABS ligand brought about an increase in the intensity of the absorbance signal at $\lambda = 287$ nm (absorbance intensity = 0.28). This could be attributed to the possible d–d transition taking place in Cu(II) species due to the presence of an unpaired electron (Figure 10). A similar enhancement in intensity was also observed in the case of the catalytic reaction ($\lambda = 294$ nm; absorbance intensity = 0.7827), although at this stage, it is

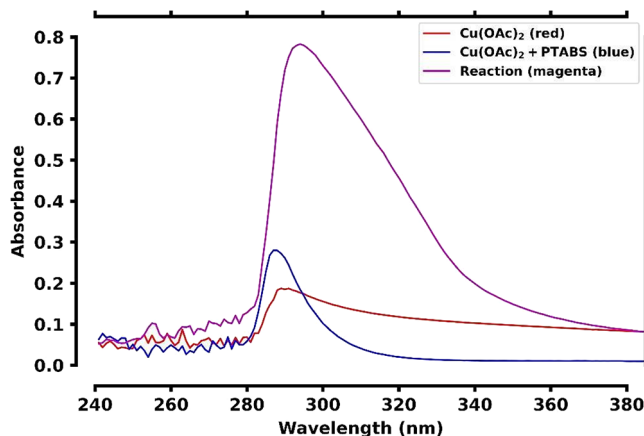


Figure 10. UV–VIS spectral analysis of (a) Cu(OAc)₂ in H₂O (red) and (b) Cu(OAc)₂ + 2PTABS in H₂O (blue) and catalytic reaction in H₂O (magenta).

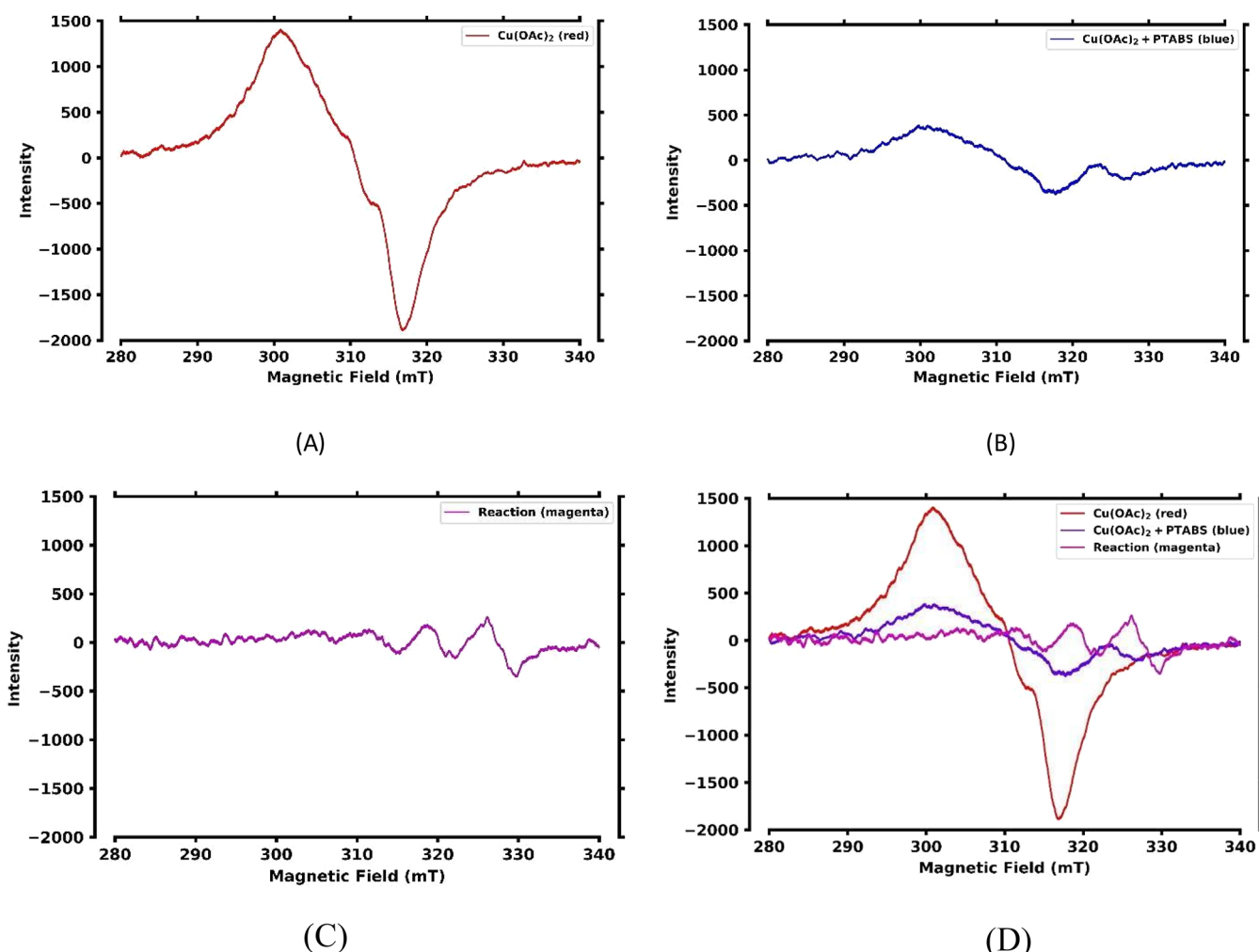


Figure 11. ESR spectra for (A) $\text{Cu}(\text{OAc})_2$ in H_2O , (B) $\text{Cu}(\text{OAc})_2 + 2\text{PTABS}$ in H_2O , (C) catalytic reaction in H_2O , and (D) all the spectra together.

difficult to predict the exact nature of the Cu(II) species present in the reaction mixture.

Electron spin resonance spectroscopy (ESR) is one of the most commonly used spectral techniques for confirming the presence of Cu(II) ions possessing an unpaired electron as well as determining the change in the oxidation state of the copper species in the reaction mixture.⁵¹ The ESR signal of $\text{Cu}(\text{OAc})_2$, which is commonly existing as a copper(II) acetate dimer $[\text{Cu}_2(\text{OAc})_4(\text{H}_2\text{O})_2]$, was done at room temperature in H_2O , providing a characteristic signal (A, Figure 11). The addition of 2.0 equiv of PTABS ligand brought about a slight reduction in the intensity of the ESR signal (B, Figure 11), while the catalytic reaction when subjected to ESR analysis in H_2O led to the appearance of a four-line signal characteristic of a mononuclear isotropic super hyperfine splitting, suggesting possible coordination of a nitrogen-containing substrate (either 2-chloropyrazine or 2-morpholinopyrazine) with copper in a Cu(II) oxidation state (C, Figure 11). All the above observations, although preliminary, strongly point toward the presence of copper in the +2 oxidation state coordinated with the PTABS ligand.

■ PLAUSIBLE MECHANISM

The possibility of the Cu(II)/PTABS system to promote the given transformation via the classical Ullmann-type coupling (Goldberg reaction)⁵² that proceeds through the oxidative

addition of copper species with the heteroaryl chloride looks highly unlikely. Unlike Pd, wherein low-temperature or ambient-temperature protocols¹¹ are commonplace, Cu, especially in the case of the Ullmann-type C–N coupling,¹³ has not proceeded at such low temperature, suggesting the difficulty of Cu to oxidatively add into the C–X bond. Earlier studies have also revealed the Cu(II) oxidation state possibly getting retained throughout the transformation, making the oxidative addition at such low temperature practically difficult. Preliminary electrospray ionization mass spectrometric analysis of the reaction mixture failed to provide any evidence of such oxidative addition species. It could, therefore, be concluded that Cu(II)/PTABS does not follow the classical Ullmann-type coupling mechanism (Goldberg reaction).

Another possibility is an aromatic nucleophilic substitution mechanism ($S_{\text{N}}\text{Ar}$), wherein copper species could resist undergoing oxidative addition/reductive elimination pathway and moreover act as a promoter could not be ruled out. It is to be noted here that a metal-free S_NAr amination protocol of chloroheteroarenes has been reported by Moody and co-workers⁵³ that proceeds via the direct attack of the amine functionality on the C–X bond of the substrate. However, such a process takes place at a relatively high temperature (100 °C) as there is no added catalyst or promoter to perform the reaction at ambient temperature, which is what has been achieved using the Cu(II)/PTABS system.

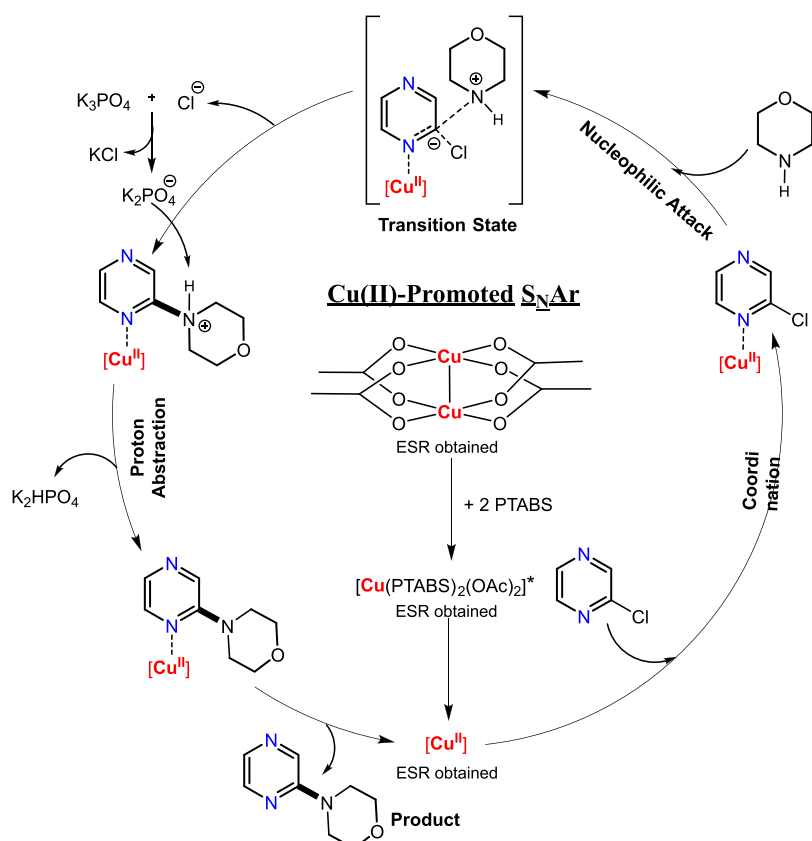


Figure 12. Plausible mechanism for Cu(II)/PTABS-promoted SNAr of chloroheteroarenes.

In view of all the above details, we consider Cu(II)/PTABS to act as a promoter by activating the chloroheteroarenes via weak coordination to the heteroatom and the subtle electronic effects on Cu(II) is regulated by the presence of a π -acidic PTABS ligand to make it more effective in comparison to other ligands. The position of the C–Cl bonds as well as its reactivity certainly assists the process and influences the outcome of the given transformation. Activation of the chloroheteroarene by Cu(II)/PTABS would then promote the attack of the nucleophilic amine (1° or 2°). Here, the weak coordination of the heteroarene via the heteroatom to the electron-deficient Cu(II) species (partial loss of electron density to the coordinating π -acidic PTABS ligand via back donation) could provide the necessary stabilization for the S_NAr to proceed at ambient temperature. Accordingly, we have provided herewith the plausible mechanism, highlighting all the points described above (Figure 12). However, it is also to be noted that any discussion on the type of ligand coordinated (OAc, PTABS) to the central copper atom, possible transition states involved, or the geometry around the metal center is out of the scope of the current report, and a complete investigation into the mechanism as well as the characterization of the active catalytic species is ongoing and will be reported separately.

CONCLUSIONS

(Hetero)arylamines are useful synthetic substrates having an abundant presence in naturally occurring molecules, active pharmaceutical ingredients, and agrochemicals. Catalytic processes derived from palladium have significantly improved the efficiency of the amination reaction with aryl as well as heteroaryl halides even at ambient temperature. However, the

escalating cost of the palladium metal, low earth abundance, and restrictions over the recycling of the metal catalyst have been some of the major hurdles toward their commercial exploitation. The employment of an earth-abundant metal catalyst such as Cu, Ni, and Fe would be an attractive alternative to the costly palladium precursors, and therefore, keeping this in mind, we report herein a copper-based efficient catalytic system, Cu/PTABS, for the amination of chloroheteroarenes.

The copper-based catalytic system showed significant improvement in the catalytic efficiency by promoting the amination of chloroheteroarenes with primary as well as secondary amines at ambient temperature in H_2O as the sole reaction solvent. The water-soluble nature of the PTABS ligand assists the solubilization of the $Cu(OAc)_2$ precursor and the resultant Cu(II)/PTABS catalytic system, which therefore performs significantly well in aqueous conditions with the isolation of the desired product carried out under column-free conditions. High-purity products (>95% HPLC purity) were obtained in most cases and the catalytic reaction was further extended toward the late-stage functionalization of active pharmaceutical ingredients such as floxacins (antibiotic) & anticancer drugs such as ciprofloxacin, norfloxacin, certinib, etc.

Excellent reactivity of the developed catalytic system also provided the ideal opportunity to reduce the catalyst concentration to 0.0001 mol %, therefore helping to achieve a significantly high turn over number of 980,000. Recyclability of the developed catalyst system was also tested, suggesting no significant reduction in the yield after 12 recycles, while a scaleup reaction of 25 mmol also provided a quantitative yield of the desired product. Furthermore, the homogeneity of the catalyst system was investigated using various catalyst poison experiments.

Density functional theoretical calculations conducted on the nature of the PTABS ligand suggested the dramatic reduction in the lone-pair donation capacity of the phosphorus atom, thus making PTABS an excellent π -acceptor ligand. Subtle electronic effects of the ligand combined with the basic character of the heteroaromatics as well as the possible position of the chloro leaving group could have a combined effect on the exceedingly high catalytic reactivity of the Cu(II)/PTABS system. Finally, preliminary analysis of the catalytic system using UV–VIS as well as electron spin resonance spectroscopy suggests the presence of copper in the +2 oxidation state, while further investigations into the exact nature of the catalyst, possible structure, and geometry of the active catalyst are ongoing and will be reported shortly.

EXPERIMENTAL SECTION

General Information. All the reactions were performed under atmospheric conditions using oven-dried standard Schlenk glassware. Demineralized water was used for the reaction. ^1H NMR (300 MHz) and $^{13}\text{C}\{\text{H}\}$ NMR (75 MHz) spectra were recorded on a Bruker Avance Neo with an Ascend 300 spectrometer, and ^1H NMR (400 MHz) and $^{13}\text{C}\{\text{H}\}$ NMR (100 MHz) spectra were recorded on a Varian 400 MHz NMR spectrometer. Chemical shifts δ are given in ppm, and the solvent residual peaks (CDCl_3 : ^1H , δ = 7.27; ^{13}C , δ = 77.0, CH_2Cl_2 : ^1H , δ = 5.27; ^{13}C , δ = 54.0 and $\text{DMSO}-d_6$: ^1H , δ = 2.50; ^{13}C , δ = 40) were used as internal standards. Peak multiplicities are specified as follows: s, singlet; d, doublet; t, triplet; q, quartet; quint, quintet; heptd, septet; m, multiplet; br, broad. Reaction monitoring and APCI-MS (m/z) spectra were recorded on a high-performance liquid chromatograph (Agilent 1260) equipped with an Agilent 6120 LCMS detector with ChemStation software. HR-LCMS spectra were recorded on Agilent Technologies, USA, 1290 Infinity UHPLC System. For those reaction involving heating, a temperature-regulated magnetic stirrer in an oil bath was used as the heat source.

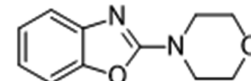
Theoretical Methods. Minimum energy structures, frequency, and molecular orbital calculations of all ligands and their corresponding Ni complexes were performed applying the Gaussian16 suite of software⁵⁴ for molecular electronic structure calculations. Electronic structures were visualized using Gaussview 6.⁵⁵ The ω B97XD functional and cc-pVQZ basis set was used for all atoms, including Ni, as this dispersion-corrected DFT functional correlated basis functions are known to provide good results for such systems. Second-order perturbation energies were calculated by the NBO program⁵⁶ using the MO and geometries previously calculated applying DFT. As many small interactions below 0.5 kcal/mol can add up to significant energy, the threshold for printing energies in the NBO program was lowered from default 0.5 kcal/mol to 0.05 kcal/mol to capture the small interactions between molecular orbitals in second-order perturbation energy. The cone angle was calculated using the Mathematica⁵⁷ script provided by Bilbrey⁵⁸ et al. Bond order calculations were performed applying the Multiwfn⁵⁹ program for electronic wavefunction analysis.

Experimental Procedures. *General Procedure for the Synthesis of 3a–ac, 6a–f, 7a–h, and 8a–d.* A 30 mL oven-dried Schlenk tube was given with 1 mol % $\text{Cu}(\text{OAc})_2\text{H}_2\text{O}$ and 2 mol % PTABS (ligand). The resultant mixture was dissolved in 0.75 mL of water and stirred for 60 min. Then, 1 mmol of chloroheterocyclic derivative was added under atmospheric conditions, the reaction mixture was stirred for 10 min, and 1.2 equiv of the corresponding secondary amine and 3.0 equiv of potassium phosphate tribasic were added followed by stirring at room temperature for 22 h. After consumption of the starting material (monitored by HPLC analysis), dichloromethane was added for extraction of the product. Separate layer, and organic layer was taken for recovery of the solvent. The solvent was removed by using a rotavapor under atmospheric conditions, and the desired product was obtained by degassing of the residue under vacuum.

General Procedure for the Synthesis of 5a–j and 7i. A 30 mL oven-dried Schlenk tube was given with 1 mol % $\text{Cu}(\text{OAc})_2\text{H}_2\text{O}$ and 2 mol % PTABS (ligand). The resultant mixture was dissolved in 0.75 mL of

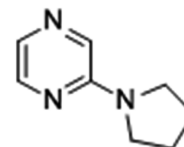
water and stirred for 60 min. Then, 1 mmol of chloroheterocyclic derivative was added under atmospheric conditions, the reaction mixture was stirred for 10 min, and 1.2 equiv of the corresponding secondary amine and 3.0 equiv of potassium phosphate tribasic were added followed by stirring at room temperature for 22 h. After consumption of the starting material (monitored by HPLC analysis), water was evaporated. Then, the residue was dissolved in 5–10 mL of methanol and filtered using a Buckner funnel. Methanol was evaporated using a rotavapor and then to the residue was added 3–5 mL of dichloromethane and the desired product was obtained by simple filtration using a Buckner funnel.

Scaleup Synthesis of 2-Morpholinobenzo[d]oxazole on a 25 mmol Scale.



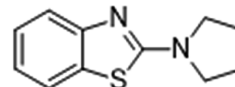
To a four-neck 100 mL round-bottom flask was charged copper acetate monohydrate (0.05 g, 0.25 mmol), and PTABS (phosphatriazene butane sulfonate) (0.15 g, 0.05 mmol) and water (18.75 mL) were added. The flask was stirred for 60 min at room temperature. 2-Chlorobenzoxazole (3.84 g, 25.00 mmol) was added to the reaction flask, the solution was stirred for 10 min at room temperature, and morpholine (2.61 g, 30.00 mmol) followed by potassium phosphate tribasic (15.92 g, 75.00 mmol) was added. The reaction mixture was stirred for 22 h at room temperature. After this time, the reaction mixture was extracted with dichloromethane (2 × 375 mL). The combined organics were distilled at 50 °C using a rotavapor under atmospheric conditions. After complete recovery of dichloromethane (total recovered dichloromethane: 740 mL, 98.67% recovery), the resultant mixture was degassed under vacuum to give the title compound as a light brown solid, 99% yield (5.04 g, HPLC purity: 99.15%).

Amination of Chloroheteroarenes with Secondary Amines. 2-(Pyrrolidin-1-yl)pyrazine (3a).

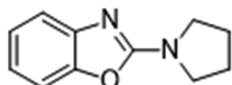


General Procedure was followed using 2-chloropyrazine (114.5 mg, 1 mmol) and pyrrolidine (0.099 mL, 1.2 mmol, 1.2 equiv), yielding the desired 2-(pyrrolidin-1-yl)pyrazine (125.1 mg, 0.84 mmol, 84%, HPLC purity: 99.82%) as a white solid. ^1H NMR (300 MHz, CDCl_3) δ 8.00 (dd, J = 2.7, 1.5 Hz, 1H), 7.85 (d, J = 1.5 Hz, 1H), 7.74 (d, J = 2.8 Hz, 1H), 3.56–3.38 (m, 4H), 2.09–1.94 (m, 4H). $^{13}\text{C}\{\text{H}\}$ NMR (75 MHz, CDCl_3) δ 153.0, 142.1, 131.2, 130.8, 46.3, 25.4. (+ve) APCI-MS m/z = 149.10 calcd. for $\text{C}_8\text{H}_{11}\text{N}_3$ [M], found: 149.85 [M + H]. The compound exhibited identical ^1H and $^{13}\text{C}\{\text{H}\}$ NMR data to previous reports.¹²

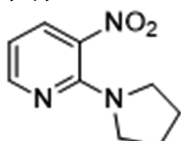
2-(Pyrrolidin-1-yl)benzo[d]thiazole (3b).



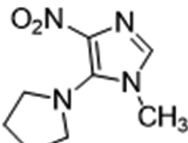
General Procedure was followed using 2-chloro benzothiazole (169.6 mg, 1 mmol) and pyrrolidine (0.099 mL, 1.2 mmol, 1.2 equiv), yielding the desired 2-(pyrrolidin-1-yl)benzo[d]thiazole (201.1 mg, 0.98 mmol, 98%, HPLC purity: 98.53%) as a yellow solid. ^1H NMR (300 MHz, CDCl_3) δ 7.63–7.53 (m, 2H), 7.28 (d, J = 8.3 Hz, 1H), 7.09–6.98 (m, 1H), 3.58 (td, J = 5.5, 2.9 Hz, 4H), 2.16–1.99 (m, 4H). $^{13}\text{C}\{\text{H}\}$ NMR (75 MHz, CDCl_3) δ 165.4, 153.4, 130.8, 125.9, 120.7, 120.7, 118.7, 49.5, 25.7. (+ve) APCI-MS m/z = 204.07 calcd. for $\text{C}_{11}\text{H}_{12}\text{N}_2\text{S}$ [M], found: 205.00 [M + H]. The compound exhibited identical ^1H and $^{13}\text{C}\{\text{H}\}$ NMR data to previous reports.^{11c}

2-(Pyrrolidin-1-yl) benzo[d]oxazole (3c).

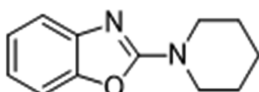
General Procedure was followed using 2-chlorobenzoxazole (153.6 mg, 1 mmol) and pyrrolidine (0.099 mL, 1.2 mmol, 1.2 equiv), yielding the desired 2-(pyrrolidin-1-yl) benzo[d] oxazole (176.1 mg, 0.935 mmol, 94%, HPLC purity: 99.90%) as a yellow solid. ^1H NMR (300 MHz, CDCl_3) δ 7.35 (d, $J = 7.8$ Hz, 1H), 7.24 (d, $J = 7.6$ Hz, 1H), 7.14 (td, $J = 7.7$, 1.2 Hz, 1H), 6.98 (td, $J = 7.7$, 1.3 Hz, 1H), 3.74–3.56 (m, 4H), 2.12–1.95 (m, 4H). $^{13}\text{C}\{\text{H}\}$ NMR (75 MHz, CDCl_3) δ 161.0, 149.1, 143.7, 123.8, 120.0, 116.0108.6, 47.4, 25.6. (+ve) APCI-MS m/z = 188.09 calcd. for $\text{C}_{11}\text{H}_{12}\text{N}_2\text{O}$ [M], found: 189.00 [M + H]. The compound exhibited identical ^1H and $^{13}\text{C}\{\text{H}\}$ NMR data to previous reports.¹²

3-Nitro-2(pyrrolidin-1-yl)pyridine (3d).

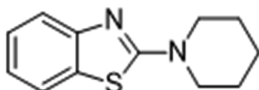
General Procedure was followed using 2-chloro-3-nitropyridine (158.5 mg, 1 mmol) and pyrrolidine (0.099 mL, 1.2 mmol, 1.2 equiv), yielding the desired 3-nitro-2(pyrrolidin-1-yl)pyridine (187.5 mg, 0.97 mmol, 97%, HPLC purity: 98.70%) as a yellow liquid. ^1H NMR (300 MHz, CDCl_3) δ 8.32 (dd, $J = 4.5$, 1.7 Hz, 1H), 8.07 (dd, $J = 8.0$, 1.7 Hz, 1H), 6.67–6.60 (m, 1H), 3.45–3.30 (m, 4H), 2.06–1.89 (m, 4H). $^{13}\text{C}\{\text{H}\}$ NMR (75 MHz, CDCl_3) δ 151.9, 150.4, 134.9, 131.8, 111.0, 49.5, 25.5. (+ve) APCI-MS m/z = 193.09 calcd. for $\text{C}_9\text{H}_{11}\text{N}_3\text{O}_2$ [M], found: 194.00 [M + H]. The compound exhibited identical ^1H and $^{13}\text{C}\{\text{H}\}$ NMR data to previous reports.⁶⁰

1-Methyl-4-nitro-5-(pyrrolidin-1-yl)-1*H*-imidazole (3e).

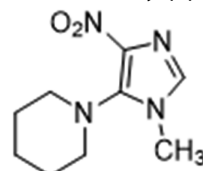
General Procedure was followed using 5-chloro-1-methyl-4-nitro imidazole (161.55 mg, 1 mmol) and pyrrolidine (0.099 mL, 1.2 mmol, 1.2 equiv), yielding the desired 1-methyl-4-nitro-5-(pyrrolidin-1-yl)-1*H*-imidazole (144.7 mg, 0.74 mmol, 74%, HPLC purity: 96.41%) as a yellow solid. ^1H NMR (300 MHz, CDCl_3) δ 7.21 (s, 1H), 3.55 (s, 3H), 3.30 (t, $J = 5.4$ Hz, 4H), 2.11–1.96 (m, 4H). $^{13}\text{C}\{\text{H}\}$ NMR (75 MHz, CDCl_3) δ 139.6, 137.8, 131.9, 51.1, 31.6, 26.2. (+ve) APCI-MS m/z = 196.10 calcd. for $\text{C}_8\text{H}_{12}\text{N}_4\text{O}_2$ [M], found: 197.00 [M + H]. The compound exhibited identical ^1H and $^{13}\text{C}\{\text{H}\}$ NMR data to previous reports.⁶¹

2-(Piperidin-1-yl)benzo[d]oxazole (3f).

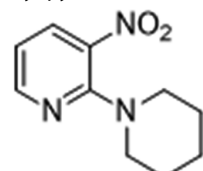
General Procedure was followed by using 2-chlorobenzoxazole (153.6 mg, 1 mmol) and piperidine (0.12 mL, 1.2 mmol, 1.2 equiv), yielding the desired 2-(piperidin-1-yl) benzo[d]oxazole (197.1 mg, 0.97 mmol, 97%, HPLC purity: 97.31%) as a brown solid. ^1H NMR (300 MHz, CDCl_3) δ 7.34 (d, $J = 7.8$ Hz, 1H), 7.23 (d, $J = 7.9$ Hz, 1H), 7.14 (td, $J = 7.7$, 1.2 Hz, 1H), 6.99 (td, $J = 7.7$, 1.3 Hz, 1H), 3.66 (s, 4H), 1.68 (s, 6H). $^{13}\text{C}\{\text{H}\}$ NMR (75 MHz, CDCl_3) δ 162.5, 148.8, 143.5, 123.9, 120.3, 116.0, 108.6, 46.7, 25.3, 24.1. (+ve) APCI-MS m/z = 202.11 calcd. for $\text{C}_{12}\text{H}_{14}\text{N}_2\text{O}$ [M], found: 203.00 [M + H]. The compound exhibited identical ^1H and $^{13}\text{C}\{\text{H}\}$ NMR data to previous reports.⁶²

2-(Piperidin-1-yl)benzo[d]thiazole (3g).

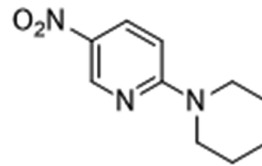
General Procedure was followed using 2-chlorobenzothiazole (169.6 mg, 1 mmol) and piperidine (0.12 mL, 1.2 mmol, 1.2 equiv), yielding the desired 2-(piperidin-1-yl)benzo[d] thiazole (216.0 mg, 0.99 mmol, 99%, HPLC purity: 98.95%) as a yellow solid. ^1H NMR (300 MHz, CDCl_3) δ 7.56 (d, $J = 8.0$ Hz, 2H), 7.33–7.22 (m, 1H), 7.04 (td, $J = 7.6$, 1.2 Hz, 1H), 3.65–3.60 (br s, 4H), 1.79–1.62 (m, 6H). $^{13}\text{C}\{\text{H}\}$ NMR (75 MHz, CDCl_3) δ 168.9, 153.0, 130.7, 125.9, 121.1, 120.6, 118.8, 49.7, 25.4, 24.3. (+ve) APCI-MS m/z = 218.09 calcd. for $\text{C}_{12}\text{H}_{14}\text{N}_2\text{S}$ [M], found: 219.00 [M + H]. The compound exhibited identical ^1H and $^{13}\text{C}\{\text{H}\}$ NMR data to previous reports.^{11c}

1-(1-Methyl-4-nitro-1*H*-imidazol-5-yl)piperidine (3h).

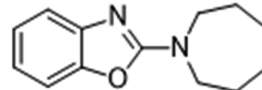
General Procedure was followed using 5-chloro-1-methyl-4-nitro imidazole (161.55 mg, 1 mmol) and piperidine (0.12 mL, 1.2 mmol, 1.2 equiv), yielding the desired 1-(1-methyl-4-nitro-1*H*-imidazol-5-yl)piperidine (179.0 mg, 0.85 mmol, 85%, HPLC purity: 98.01%) as a white solid. ^1H NMR (300 MHz, CDCl_3) δ 7.21 (s, 1H), 3.54 (s, 3H), 3.09 (dd, $J = 6.8$, 3.4 Hz, 4H), 1.76–1.57 (m, 6H). $^{13}\text{C}\{\text{H}\}$ NMR (75 MHz, CDCl_3) δ 140.8, 138.5, 131.6, 50.5, 30.9, 26.3, 23.6. (+ve) APCI-MS m/z = 210.11 calcd. for $\text{C}_9\text{H}_{14}\text{N}_4\text{O}_2$ [M], found: 211.00 [M + H]. The compound exhibited identical ^1H NMR and $^{13}\text{C}\{\text{H}\}$ NMR data to previous reports.⁶¹

3-Nitro-2-(piperidin-1-yl)pyridine (3i).

General Procedure was followed using 2-chloro-3-nitropyridine (158.5 mg, 1 mmol) and piperidine (0.12 mL, 1.2 mmol, 1.2 equiv), yielding the desired 3-nitro-2-(piperidin-1-yl)pyridine (202.0 mg, 0.97 mmol, 97%, HPLC purity: 99.14%) as a colorless liquid. ^1H NMR (300 MHz, CDCl_3) δ 8.30 (d, $J = 4.5$ Hz, 1H), 8.09 (d, $J = 8.1$ Hz, 1H), 6.71–6.63 (m, 1H), 3.39 (dq, $J = 4.1$, 2.5 Hz, 4H), 1.73–1.57 (m, 6H). $^{13}\text{C}\{\text{H}\}$ NMR (75 MHz, CDCl_3) δ 153.3, 151.8, 135.7, 132.6, 112.6, 49.2, 25.7, 24.3. (+ve) APCI-MS m/z = 207.10 calcd. for $\text{C}_{10}\text{H}_{13}\text{N}_3\text{O}_2$ [M], found: 208.00 [M + H]. The compound exhibited identical ^1H and $^{13}\text{C}\{\text{H}\}$ NMR data to previous reports.⁶⁰

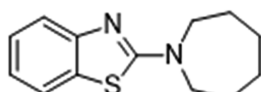
5-Nitro-2-(piperidin-1-yl)pyridine (3j).

General Procedure was followed using 2-chloro-5-nitropyridine (158.5 mg, 1 mmol) and piperidine (0.12 mL, 1.2 mmol, 1.2 equiv), yielding the desired 5-nitro-2-(piperidin-1-yl)pyridine (158.9 mg, 0.77 mmol, 77%, HPLC purity: 93.64%) as a yellow solid. ^1H NMR (300 MHz, CDCl_3) δ 9.02 (d, $J = 2.8$ Hz, 1H), 8.15 (dd, $J = 9.6$, 2.8 Hz, 1H), 6.54 (d, $J = 9.6$ Hz, 1H), 3.79–3.69 (m, 4H), 1.80–1.57 (m, 6H). $^{13}\text{C}\{\text{H}\}$ NMR (75 MHz, CDCl_3) δ 160.3, 146.9, 134.4, 133.0, 104.5, 46.3, 25.8, 24.6. (+ve) APCI-MS m/z = 207.10 calcd. for $\text{C}_{10}\text{H}_{13}\text{N}_3\text{O}_2$ [M], found: 208.00 [M + H]. The compound exhibited identical ^1H and $^{13}\text{C}\{\text{H}\}$ NMR data to previous reports.^{11c}

2-(Azepan-1-yl)benzo[d]oxazole (3k).

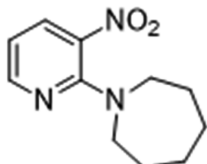
General Procedure was followed using 2-chlorobenzoxazole (153.6 mg, 1 mmol) and azepan (0.14 mL, 1.2 mmol, 1.2 equiv), yielding the desired 2-(azepan-1-yl)benzo[*d*]oxazole (214.0 mg, 0.99 mmol, 99%, HPLC purity: 98.71%) as an off-white solid. ¹H NMR (300 MHz, CDCl₃) δ 7.35 (d, *J* = 7.8 Hz, 1H), 7.25 (d, *J* = 7.9 Hz, 1H), 7.15 (td, *J* = 7.7, 1.2 Hz, 1H), 6.98 (td, *J* = 7.7, 1.3 Hz, 1H), 3.77–3.67 (m, 4H), 1.93–1.79 (m, 4H), 1.70–1.55 (m, 4H). ¹³C{¹H} NMR (75 MHz, CDCl₃) δ 162.7, 148.9, 143.8, 123.8, 119.9, 115.8, 108.5, 48.1, 28.3, 27.5. (+ve) APCI-MS *m/z* = 216.18 calcd. for C₁₃H₁₆N₂O [M], found: 217.00 [M + H]. The compound exhibited identical ¹H and ¹³C{¹H} NMR data to previous reports.^{11c}

2-(Azepan-1-yl)benzo[*d*]thiazole (3l).



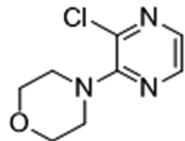
General Procedure was followed using 2-chloro benzothiazole (169.6 mg, 1 mmol) and azepan (0.14 mL, 1.2 mmol, 1.2 equiv), yielding the desired 2-(azepan-1-yl)benzo[*d*]thiazole (230.0 mg, 0.99 mmol, 99%, HPLC purity: 99.64%) as a pale yellow oil. ¹H NMR (300 MHz, CDCl₃) δ 7.56 (m, 2H), 7.27 (d, *J* = 8.1 Hz, 1H), 7.08–6.97 (m, 1H), 3.73–3.63 (m, 4H), 1.94–1.79 (m, 4H), 1.69–1.54 (m, 4H). ¹³C{¹H} NMR (75 MHz, CDCl₃) δ 168.1, 153.4, 130.6, 125.9, 120.6, 120.5, 118.5, 50.8, 27.9, 27.6. (+ve) APCI-MS *m/z* = 232.10 calcd. for C₁₃H₁₆N₂S [M], found: 233.00 [M + H]. The compound exhibited identical ¹H and ¹³C{¹H} NMR data to previous reports.^{11c}

1-(3-Nitropyridin-2-yl)azepane (3m).



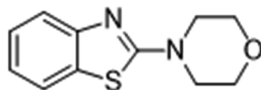
General Procedure was followed using 2-chloro-3-nitropyridine (158.5 mg, 1 mmol) and azepan (0.14 mL, 1.2 mmol, 1.2 equiv), yielding the desired 1-(3-nitropyridin-2-yl)azepane (220.1 mg, 0.99 mmol, 99%, HPLC purity: 99.49%) as a yellow liquid. M.p. 35 °C. ¹H NMR (300 MHz, CDCl₃) δ 8.29 (dd, *J* = 4.4, 1.8 Hz, 1H), 8.06 (dd, *J* = 8.0, 1.7 Hz, 1H), 6.62 (dd, *J* = 8.0, 4.4 Hz, 1H), 3.46–3.36 (m, 4H), 1.92–1.78 (m, 4H), 1.61–1.45 (m, 4H). ¹³C{¹H} NMR (75 MHz, CDCl₃) δ 152.8, 151.1, 135.5, 131.4, 111.3, 49.9, 28.3, 28.0. (+ve) APCI-MS *m/z* = 221.12 calcd. for C₁₁H₁₅N₃O₂ [M], found: 222.00 [M + H]. HRMS (ESI) *m/z*: (M + H)⁺ calcd. for C₁₁H₁₆N₃O₂: 222.1243; found: 222.1236.

4-(3-Chloropyrazin-2-yl)morpholine (3n).



General Procedure was followed using 2,3-dichloropyrazine (149.0 mg, 1 mmol) and morpholine (0.21 mL, 2.4 mmol, 2.4 equiv), yielding the desired 4-(3-chloropyrazin-2-yl)morpholine (192.5 mg, 0.77 mmol, 77%, HPLC purity: 99.09%) as a light yellow liquid. ¹H NMR (300 MHz, CDCl₃) δ 8.09 (d, *J* = 2.5 Hz, 1H), 7.87 (d, *J* = 2.5 Hz, 1H), 3.87–3.77 (m, 4H), 3.47–3.37 (m, 4H). ¹³C{¹H} NMR (75 MHz, CDCl₃) δ 154.8, 140.2, 140.1, 135.6, 66.7, 49.0. (+ve) APCI-MS *m/z* = 199.05 calcd. for C₈H₁₀ClN₃O [M], found: 200.00 [M + H]. The compound exhibited identical ¹H NMR and ¹³C{¹H} NMR data to previous reports.^{11c}

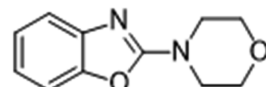
4-(Benzo[*d*]thiazol-2-yl)morpholine (3o).



General Procedure was followed using 2-chloro benzothiazole (169.6 mg, 1 mmol) and morpholine (0.10 mL, 1.2 mmol, 1.2 equiv), yielding the desired 4-(benzo[*d*]thiazol-2-yl)morpholine (209.7 mg, 0.95

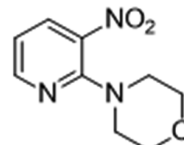
mmol, 95%, HPLC purity: 93.74%) as a white solid. ¹H NMR (300 MHz, CDCl₃) δ 7.60 (d, *J* = 12.7 Hz, 2H), 7.31 (d, *J* = 8.3 Hz, 1H), 7.23–7.04 (m, 1H), 3.88–3.79 (m, 4H), 3.73–3.58 (m, 4H). ¹³C{¹H} NMR (75 MHz, CDCl₃) δ 169.1, 152.6, 130.6, 126.2, 121.8, 120.8, 119.4, 66.3, 48.6. (+ve) APCI-MS *m/z* = 220.07 calcd. for C₁₁H₁₂N₂OS [M], found: 221.00 [M + H]. The compound exhibited identical ¹H and ¹³C{¹H} NMR data to previous reports.^{11c}

2-Morpholinobenzo[*d*]oxazole (3p).



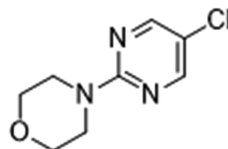
General Procedure was followed using 2-chlorobenzoxazole (153.6 mg, 1 mmol) and morpholine (0.10 mL, 1.2 mmol, 1.2 equiv), yielding the desired 2-(morpholin-4-yl)benzo[*d*] oxazole (199.7 mg, 0.98 mmol, 98%, HPLC purity: 99.15%) as a light brown solid. ¹H NMR (300 MHz, CDCl₃) δ 7.36 (d, *J* = 7.8 Hz, 1H), 7.32–7.20 (m, 1H), 7.16 (td, *J* = 7.7, 1.2 Hz, 1H), 7.02 (td, *J* = 7.7, 1.3 Hz, 1H), 3.84–3.72 (m, 4H), 3.74–3.62 (m, 4H). ¹³C{¹H} NMR (75 MHz, CDCl₃) δ 162.2, 148.8, 142.9, 124.2, 121.0, 116.6, 108.9, 66.3, 45.8. (+ve) APCI-MS *m/z* = 204.09 calcd. for C₁₁H₁₂N₂O₂ [M], found: 205 [M + H]. The compound exhibited identical ¹H and ¹³C{¹H} NMR data to previous reports.⁶²

4-(3-Nitropyridin-2-yl)morpholine (3q).



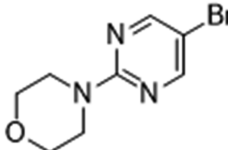
General Procedure was followed using 2-chloro-3-nitropyridine (158.5 mg, 1 mmol) and morpholine (0.10 mL, 1.2 mmol, 1.2 equiv), yielding the desired 4-(3-nitropyridin-2-yl)morpholine (183.5 mg, 0.88 mmol, 88%, HPLC purity: 96.82%) as a yellow solid. ¹H NMR (300 MHz, CDCl₃) δ 8.34 (dd, *J* = 4.5, 1.8 Hz, 1H), 8.13 (dd, *J* = 8.0, 1.7 Hz, 1H), 6.78 (dd, *J* = 8.0, 4.5 Hz, 1H), 3.84–3.75 (m, 4H), 3.50–3.41 (m, 4H). ¹³C{¹H} NMR (75 MHz, CDCl₃) δ 152.8, 151.9, 135.7, 133.3, 113.9, 66.7, 48.5. (+ve) APCI-MS *m/z* = 209.08 calcd. for C₉H₁₁N₃O₃ [M], found: 210.00 [M + H]. The compound exhibited identical ¹H and ¹³C{¹H} NMR data to previous reports.⁶³

4-(5-Chloropyrimidin-2-yl)morpholine (3r).



General Procedure was followed using 2,5-dichloropyrimidine (149.0 mg, 1 mmol) and morpholine (0.10 mL, 1.2 mmol, 1.2 equiv), yielding the desired 4-(5-chloropyrimidin-2-yl)morpholine (173.2 mg, 0.87 mmol, 87%, HPLC purity: 99.25%) as a light yellow solid. ¹H NMR (300 MHz, CDCl₃) δ 8.23 (s, 2H), 3.79–3.72 (m, 8H). ¹³C{¹H} NMR (75 MHz, CDCl₃) δ 160.0, 155.9, 118.7, 66.7, 44.5. (+ve) APCI-MS *m/z* = 199.05 calcd. for C₈H₁₀ClN₃O [M], found: 200.00 [M + H]. The compound exhibited identical ¹H and ¹³C{¹H} NMR data to previous reports.⁶⁴

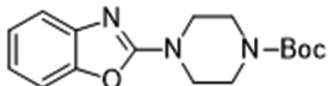
4-(5-Bromopyrimidin-2-yl)morpholine (3s).



General Procedure was followed using 5-bromo-2-chloropyrimidine (193.4 mg, 1 mmol) and morpholine (0.10 mL, 1.2 mmol, 1.2 equiv), yielding the desired 4-(5-bromopyrimidin-2-yl)morpholine (202.1 mg, 0.83 mmol, 83%, HPLC purity: 99.52%) as a light yellow solid. ¹H NMR (300 MHz, CDCl₃) δ 8.30 (s, 2H), 3.83–3.62 (m, 8H). ¹³C{¹H} NMR (75 MHz, CDCl₃) δ 160.1, 158.0, 106.3, 66.8, 44.4. (+ve) APCI-

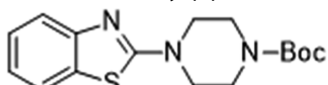
MS m/z = 243.00 calcd. For $C_8H_{10}BrN_3O$ [M], found: 244.00 [M + H]. The compound exhibited identical 1H and $^{13}C\{^1H\}$ NMR data to previous reports.⁶⁵

tert-Butyl-4-(benzo[d]oxazol-2-yl)piperazine-1-carboxylate (**3t**).



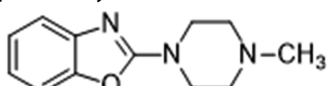
General Procedure was followed using 2-chlorobenzoxazole (153.6 mg, 1 mmol) and *tert*-butyl piperazine-1-carboxylate (223.5 mg, 1.2 mmol, 1.2 equiv), yielding the desired *tert*-butyl 4-(benzo[d]oxazol-2-yl)piperazine-1-carboxylate (295.0 mg, 0.97 mmol, 97%, HPLC purity: 96.23%) as a brown solid. 1H NMR (300 MHz, $CDCl_3$) δ 7.36 (dd, J = 7.8, 1.3 Hz, 1H), 7.26 (dd, J = 7.9, 1.2 Hz, 1H), 7.17 (td, J = 7.7, 1.2 Hz, 1H), 7.04 (td, J = 7.7, 1.3 Hz, 1H), 3.67 (dd, J = 6.5, 3.5 Hz, 4H), 3.56 (dd, J = 6.4, 3.5 Hz, 4H), 1.49 (s, 9H). $^{13}C\{^1H\}$ NMR (75 MHz, $CDCl_3$) δ 162.0, 154.6, 148.8, 142.9, 124.1, 121.0, 116.5, 108.9, 80.4, 45.5, 28.4. (+ve) APCI-MS m/z = 303.16 calcd. For $C_{16}H_{21}N_3O_3$ [M], found: 304.00 [M + H]. The compound exhibited identical 1H and $^{13}C\{^1H\}$ NMR data to previous reports.⁶⁶

tert-Butyl-4-(benzo[d]thiazol-2-yl)piperazine-1-carboxylate (**3u**).



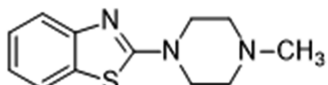
General Procedure was followed using 2-chloro benzothiazole (169.6 mg, 1 mmol) and *tert*-butyl-piperazine-1-carboxylate (223.5 mg, 1.2 mmol, 1.2 equiv), yielding the desired *tert*-butyl-4-(benzo[d]thiazol-2-yl)piperazine-1-carboxylate (312.0 mg, 0.98 mmol, 98%, HPLC purity: 99.85%) as a brown solid. 1H NMR (300 MHz, $CDCl_3$) δ 7.59 (dd, J = 14.2, 0.6 Hz, 2H), 7.31 (t, J = 7.4 Hz, 1H), 7.09 (t, J = 7.4 Hz, 1H), 3.67–3.53 (m, 8H), 1.49 (s, 9H). $^{13}C\{^1H\}$ NMR (75 MHz, $CDCl_3$) δ 168.6, 154.5, 152.6, 130.7, 126.1, 121.7, 120.8, 119.3, 80.4, 48.2, 43.0, 28.4. (+ve) APCI-MS m/z = 319.14 calcd. For $C_{16}H_{21}N_3O_2S$ [M], found: 320.20 [M + H]. The compound exhibited identical 1H and $^{13}C\{^1H\}$ NMR data to previous reports.⁶⁷

2-(4-Methylpiperazin-1-yl)benzo[d]oxazole (**3v**).



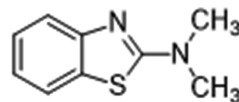
General Procedure was followed using 2-chlorobenzoxazole (153.6 mg, 1 mmol) and *N*-methyl piperazine (0.13 mL, 1.2 mmol, 1.2 equiv), yielding the desired 2-(4-methylpiperazin-1-yl)benzo[d]oxazole (212.0 mg, 0.98 mmol, 98%, HPLC purity: 98.20%) as a white solid. 1H NMR (300 MHz, $CDCl_3$) δ 7.31 (dd, J = 7.8, 1.3 Hz, 1H), 7.20 (dd, J = 7.9, 1.2 Hz, 1H), 7.11 (td, J = 7.7, 1.2 Hz, 1H), 6.97 (td, J = 7.7, 1.3 Hz, 1H), 3.78–3.48 (m, 4H), 2.59–2.37 (m, 4H), 2.29 (s, 3H). $^{13}C\{^1H\}$ NMR (75 MHz, $CDCl_3$) δ 162.2, 148.7, 143.1, 124.0, 120.7, 116.3, 108.7, 54.2, 46.2, 45.5. (+ve) APCI-MS m/z = 217.12 calcd. For $C_{12}H_{15}N_3O$ [M], found: 218.00 [M + H]. The compound exhibited identical 1H and $^{13}C\{^1H\}$ NMR data to previous reports.⁶⁸

2-(4-Methylpiperazin-1-yl)benzo[d]thiazole (**3w**).



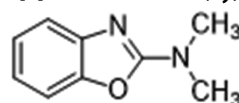
General Procedure was followed using 2-chlorobenzothiazole (169.6 mg, 1 mmol) and *N*-methyl piperazine (0.13 mL, 1.2 mmol, 1.2 equiv), yielding the desired 2-(4-methylpiperazin-1-yl)benzo[d]thiazole (205.4 mg, 0.88 mmol, 88%, HPLC purity: 99.42%) as an off-white solid. 1H NMR (300 MHz, $CDCl_3$) δ 7.64–7.50 (m, 2H), 7.35–7.23 (m, 1H), 7.07 (td, J = 7.6, 1.2 Hz, 1H), 3.70–3.61 (m, 4H), 2.53 (dd, J = 5.9, 4.4 Hz, 4H), 2.35 (s, 3H). $^{13}C\{^1H\}$ NMR (75 MHz, $CDCl_3$) δ 168.7, 152.7, 130.8, 126.0, 121.4, 120.7, 119.1, 54.3, 48.3, 46.2. (+ve) APCI-MS m/z = 233.10 calcd. For $C_{12}H_{15}N_3S$ [M], found: 234.00 [M + H]. The compound exhibited identical 1H and $^{13}C\{^1H\}$ NMR data to previous reports.⁶⁸

N,N-Dimethylbenzo[d]thiazol-2-amine (**3x**).



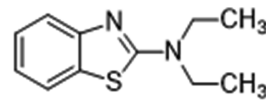
General Procedure was followed using 2-chlorobenzothiazole (169.6 mg, 1 mmol) and dimethylamine 40% (0.15 mL, 1.2 mmol, 1.2 equiv), yielding the desired *N,N*-dimethylbenzo[d]thiazol-2-amine (136.5 mg, 0.77 mmol, 77%, HPLC purity: 98.78%) as a white solid. 1H NMR (300 MHz, $CDCl_3$) δ 7.64–7.52 (m, 2H), 7.34–7.23 (m, 1H), 7.05 (td, J = 7.6, 1.2 Hz, 1H), 3.20 (s, 6H). $^{13}C\{^1H\}$ NMR (75 MHz, $CDCl_3$) δ 168.7, 153.3, 131.1, 125.9, 120.9, 120.6, 118.7, 40.1. (+ve) APCI-MS m/z = 178.06 calcd. for $C_9H_{10}N_2S$ [M], found: 179.00 [M + H]. The compound exhibited identical 1H and $^{13}C\{^1H\}$ NMR data to previous reports.⁶⁹

N,N-Dimethylbenzo[d]oxazol-2-amine (**3y**).



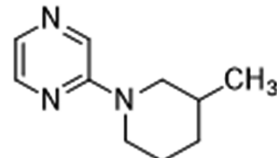
General Procedure was followed using 2-chlorobenzoxazole (153.6 mg, 1 mmol) and dimethylamine 40% (0.15 mL, 1.2 mmol, 1.2 equiv), yielding the desired *N,N*-dimethylbenzo-[d]oxazol-2-amine (144.4 mg, 0.89 mmol, 89%, HPLC purity: 98.05%) as a brown solid. 1H NMR (300 MHz, $CDCl_3$) δ 7.35 (dd, J = 7.8, 0.6 Hz, 1H), 7.24 (dd, J = 7.9, 0.6 Hz, 1H), 7.14 (td, J = 7.7, 1.2 Hz, 1H), 6.99 (td, J = 7.7, 1.3 Hz, 1H), 3.19 (s, 6H). $^{13}C\{^1H\}$ NMR (75 MHz, $CDCl_3$) δ 163.0, 149.0, 143.6, 123.8, 120.1, 115.9, 108.5, 37.6. (+ve) APCI-MS m/z = 162.08 calcd. for $C_9H_{10}N_2O$ [M], found: 163.00 [M + H]. The compound exhibited identical 1H and $^{13}C\{^1H\}$ NMR data to previous reports.⁷⁰

N,N-Diethylbenzo[d]thiazol-2-amine (**3z**).

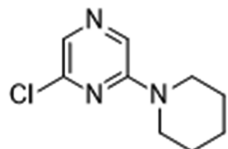


General Procedure was followed using 2-chlorobenzothiazole (169.6 mg, 1 mmol) and diethylamine (0.12 mL, 1.2 mmol, 1.2 equiv), yielding the desired *N,N*-diethylbenzo[d]thiazol-2-amine (101.3 mg, 0.49 mmol, 49%, HPLC purity: 95.39%) as a colorless oil. 1H NMR (300 MHz, $CDCl_3$) δ 7.65–7.49 (m, 2H), 7.35–7.23 (m, 1H), 7.05 (td, J = 7.6, 1.2 Hz, 1H), 3.59 (q, J = 7.1 Hz, 4H), 1.30 (t, J = 7.1 Hz, 6H). $^{13}C\{^1H\}$ NMR (75 MHz, $CDCl_3$) δ 167.4, 153.4, 130.7, 125.9, 120.8, 120.6, 118.6, 45.5, 12.9. (+ve) APCI-MS m/z = 206.09 calcd. for $C_{11}H_{14}N_2S$ [M], found: 207.00 [M + H]. The compound exhibited identical 1H and $^{13}C\{^1H\}$ NMR data to previous reports.⁷¹

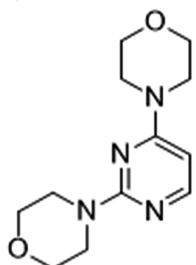
2-(3-Methylpiperidin-1-yl)pyrazine (**3aa**).



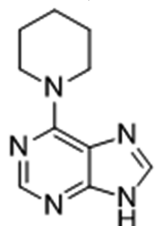
General Procedure was followed using 2-chloropyrazine (114.5 mg, 1 mmol) and 3-methylpiperidine (0.14 mL, 1.2 mmol, 1.2 equiv), yielding the desired 2-(3-methylpiperidin-1-yl)pyrazine (69.0 mg, 0.39 mmol, 39%, HPLC purity: 99.47%) as a yellow liquid. 1H NMR (300 MHz, $CDCl_3$) δ 8.05 (s, 3H), 4.34–3.95 (m, 2H), 2.85–2.77 (m, 1H), 2.47 (d, J = 10.6 Hz, 1H), 1.89–1.46 (m, 4H), 1.16–1.10 (m, 1H), 0.91 (s, 3H). $^{13}C\{^1H\}$ NMR (75 MHz, $CDCl_3$) δ 150.1, 142.7, 131.7, 131.1, 52.3, 45.1, 33.2, 31.1, 24.9, 19.3. (+ve) APCI-MS m/z = 177.13 calcd. for $C_{10}H_{15}N_3$ [M], found: 178.00 [M + H]. The compound exhibited identical 1H and $^{13}C\{^1H\}$ NMR data to previous reports.^{11c}

2-Chloro-6-(piperidin-1-yl)pyrazine (3ab).

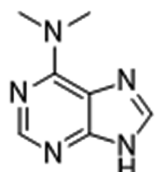
General Procedure was followed using 2,6-dichloropyrazine (149.0 mg, 1 mmol) and piperidine (0.24 mL, 2.4 mmol, 2.4 equiv), yielding the desired 2-chloro-6-(piperidin-1-yl)pyrazine (135.8 mg, 0.69 mmol, 69%, HPLC purity: 94.54%) as a yellow oil. ^1H NMR (300 MHz, CDCl_3) δ 7.94 (s, 1H), 7.71 (s, 1H), 3.62–3.44 (m, 4H), 1.74–1.56 (m, 6H). $^{13}\text{C}\{\text{H}\}$ NMR (75 MHz, CDCl_3) δ 154.3, 146.7, 129.7, 128.0, 45.6, 25.4, 24.5. (+ve) APCI-MS m/z = 197.07 calcd. for $\text{C}_9\text{H}_{12}\text{ClN}_3$ [M], found: 198.00 [M + H]. Data obtained is same as the published report.⁷²

4,4'-(Pyrimidine-2,4-diyl)dimorpholine (3ac).

General Procedure was followed using 2,4-dichloropyrimidine (148.98 mg, 1 mmol) and morpholine (0.21 mL, 2.4 mmol, 2.4 equiv), yielding the desired 4,4'-(pyrimidine-2,4-diyl)dimorpholine (180.0 mg, 0.72 mmol, 72%, HPLC purity: 99.85%) as an off-white solid. ^1H NMR (300 MHz, CDCl_3) δ 7.97 (d, J = 6.0 Hz, 1H), 5.87 (d, J = 6.0 Hz, 1H), 3.94–3.63 (m, 12H), 3.56 (t, J = 4.8 Hz, 4H). $^{13}\text{C}\{\text{H}\}$ NMR (75 MHz, CDCl_3) δ 162.6, 161.3, 156.5, 93.2, 66.9, 66.6, 44.3, 44.1. (+ve) APCI-MS m/z = 250.14 calcd. for $\text{C}_{12}\text{H}_{18}\text{N}_4\text{O}_2$ [M], found: 251.00 [M + H]. The compound exhibited identical ^1H and $^{13}\text{C}\{\text{H}\}$ NMR data to previous reports.^{11c}

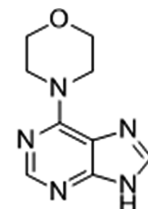
Catalytic Amination of Purine and Purine Riboside with Secondary Amines. 6-(Piperidin-1-yl)-9H-purine (5a).

General Procedure was followed using 6-chloro-9H-purine (154.56 mg, 1 mmol) and piperidine (0.12 mL, 1.2 mmol, 1.2 equiv), yielding the desired 6-(piperidin-1-yl)-9H-purine (187.7 mg, 0.85 mmol, 85%, HPLC purity: 91.84%) as a white solid. ^1H NMR (400 MHz, DMSO- d_6) δ 12.92 (br s, 1H), 8.17 (s, 1H), 8.08 (s, 1H), 4.20 (br s, 4H), 1.72–1.68 (m, 2H), 1.61–1.55 (m, 4H). $^{13}\text{C}\{\text{H}\}$ NMR (101 MHz, DMSO- d_6) δ 153.1, 151.8, 151.4, 137.8, 118.6, 45.6, 25.7, 24.3. (+ve) APCI-MS m/z = 203.12 calcd. for $\text{C}_{10}\text{H}_{13}\text{N}_5$ [M], found: 204.00 [M + H]. The compound exhibited identical ^1H and $^{13}\text{C}\{\text{H}\}$ NMR data to previous reports.^{11c}

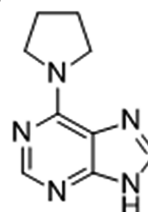
***N,N*-Dimethyl-9H-purin-6-amine (5b).**

General Procedure was followed using 6-chloro-9H-purine (154.56 mg, 1 mmol) and dimethyl amine 40% (0.15 mL, 1.2 mmol, 1.2 equiv), yielding the desired *N,N*-dimethyl-9H-purin-6-amine (127.0 mg, 0.78

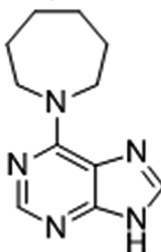
mmol, 78%, HPLC purity: 92.46%) as a white solid. ^1H NMR (400 MHz, DMSO) δ 8.13 (s, 1H), 7.98 (d, J = 13.9 Hz, 1H), 3.44 (s, 6H). $^{13}\text{C}\{\text{H}\}$ NMR (101 MHz, DMSO) δ 154.1, 152.9, 151.1, 139.9, 119.4, 37.9. (+ve) APCI-MS m/z = 163.09 calcd. for $\text{C}_7\text{H}_9\text{N}_5$ [M], found: 164.00 [M + H]. The compound exhibited identical ^1H and $^{13}\text{C}\{\text{H}\}$ NMR data to previous reports.⁷³

4-(9H-Purin-6-yl)morpholine (5c).

General Procedure was followed using 6-chloro-9H-purine (154.56 mg, 1 mmol) and morpholine (0.10 mL, 1.2 mmol, 1.2 equiv), yielding the desired 4-(9H-purin-6-yl)morpholine (107.3 mg, 0.52 mmol, 52%, HPLC purity: 99.46%) as a white solid. ^1H NMR (400 MHz, DMSO) δ 13.04 (br s, 1H), 8.23 (s, 1H), 8.14 (s, 1H), 4.21 (br s, 4H), 3.72 (t, J = 4.8 Hz, 4H). $^{13}\text{C}\{\text{H}\}$ NMR (101 MHz, DMSO) δ 153.2, 151.8, 151.5, 138.3, 118.9, 66.2, 45.2. (+ve) APCI-MS m/z = 205.10 calcd. for $\text{C}_9\text{H}_{11}\text{N}_5\text{O}$ [M], found: 206.00 [M + H]. The compound exhibited identical ^1H and $^{13}\text{C}\{\text{H}\}$ NMR data to previous reports.^{11c}

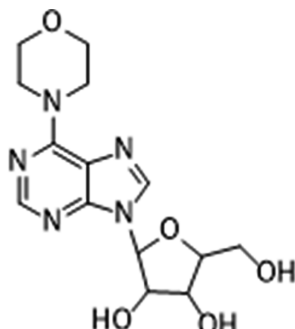
6-(Pyrrolidin-1-yl)-9H-purine (5d).

General Procedure was followed using 6-chloro-9H-purine (154.56 mg, 1 mmol) and pyrrolidine (0.099 mL, 1.2 mmol, 1.2 equiv), yielding the desired 6-(pyrrolidin-1-yl)-9H-purine (160.0 mg, 0.85 mmol, 85%, HPLC purity: 99.67%) as a white solid. ^1H NMR (400 MHz, DMSO) δ 12.85 (br s, 1H), 8.17 (s, 1H), 8.06 (s, 1H), 4.03 (br s, 2H), 3.65 (br s, 2H), 1.95 (br s, 4H). $^{13}\text{C}\{\text{H}\}$ NMR (101 MHz, DMSO) δ 152.4, 152.2, 150.9, 138.3, 118.9, 45.1, 25.6. (+ve) APCI-MS m/z = 189.10 calcd. for $\text{C}_9\text{H}_{11}\text{N}_5$ [M], found: 190.00 [M + H]. The compound exhibited identical ^1H and $^{13}\text{C}\{\text{H}\}$ NMR data to previous reports.^{11c}

6-(Hexahydro-1H-azepin-1-yl)-9H-purine (5e).

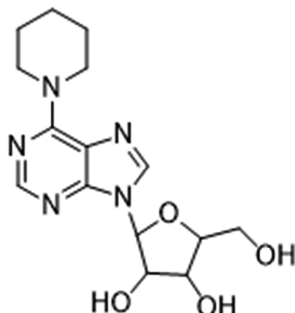
General Procedure was followed using 6-chloro-9H-purine (154.56 mg, 1 mmol) and azepane (0.14 mL, 1.2 mmol, 1.2 equiv), yielding the desired 6-(hexahydro-1H-azepin-1-yl)-9H-purine (174.8 mg, 0.80 mmol, 80%, HPLC purity: 99.15%) as a white solid. ^1H NMR (400 MHz, DMSO) δ 12.88 (br s, 1H), 8.17 (s, 1H), 8.07 (s, 1H), 4.34 (br s, 2H), 3.85 (br s, 2H), 1.78 (quint, J = 5.3 Hz, 4H), 1.49 (heptd, J = 4.7 Hz, 4H). $^{13}\text{C}\{\text{H}\}$ NMR (101 MHz, DMSO) δ 153.5, 151.9, 151.2, 138.0, 118.4, 47.7, 28.7, 26.3. (+ve) APCI-MS m/z = 217.13 calcd. for $\text{C}_{11}\text{H}_{15}\text{N}_5$ [M], found: 218.00 [M + H]. The compound exhibited identical ^1H and $^{13}\text{C}\{\text{H}\}$ NMR data to previous reports.^{11c}

*2-(Hydroxymethyl)-5-(6-morpholino-9*H*-purin-9-yl)-tetrahydrofuran-3,4-diol (5f).*



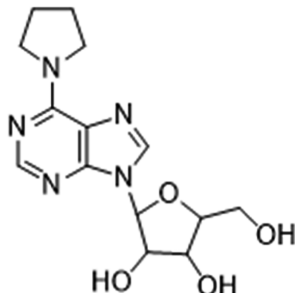
General Procedure was followed using 6-chloropurine riboside (286.67 mg, 1 mmol) and morpholine (0.10 mL, 1.2 mmol, 1.2 equiv), yielding the desired 2-(hydroxymethyl)-5-(6-morpholino-9*H*-purin-9-yl)-tetrahydrofuran-3,4-diol (302.5 mg, 0.90 mmol, 90%, HPLC purity: 99.25%) as a white solid. ¹H NMR (400 MHz, DMSO) δ 8.43 (s, 1H), 8.27 (s, 1H), 5.93 (d, *J* = 5.8 Hz, 1H), 5.48 (d, *J* = 5.4 Hz, 1H), 5.36–5.29 (m, 1H), 5.21 (d, *J* = 4.3 Hz, 1H), 4.58 (d, *J* = 0.0 Hz, 1H), 4.22 (br s, 4H), 4.15 (d, *J* = 3.8 Hz, 1H), 3.97 (d, *J* = 3.6 Hz, 1H), 3.72 (t, *J* = 4.7 Hz, 4H), 3.73–3.63 (m, 1H), 3.61–3.51 (m, 1H). ¹³C{¹H} NMR (101 MHz, DMSO) δ 153.3, 151.8, 150.3, 139.0, 119.7, 87.8, 85.8, 73.6, 70.5, 66.2, 61.5, 45.3. (+ve) APCI-MS *m/z* = 337.14 calcd. for C₁₄H₁₉N₅O₅ [M], found: 338.00 [M + H]. The compound exhibited identical ¹H and ¹³C{¹H} NMR data to previous reports.⁷⁴

*2-(Hydroxymethyl)-5-(6-(piperidin-1-yl)-9*H*-purin-9-yl)-tetrahydrofuran-3,4-diol (5g).*



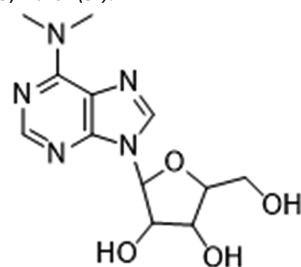
General Procedure was followed using 6-chloropurine riboside (286.67 mg, 1 mmol) and piperidine (0.12 mL, 1.2 mmol, 1.2 equiv), yielding the desired 2-(hydroxymethyl)-5-(6-(piperidin-1-yl)-9*H*-purin-9-yl)-tetrahydrofuran-3,4-diol (257.2 mg, 0.77 mmol, 77%, HPLC purity: 98.92%) as a white solid. ¹H NMR (400 MHz, DMSO) δ 8.38 (s, 1H), 8.21 (s, 1H), 5.91 (d, *J* = 6.0 Hz, 1H), 5.46 (d, *J* = 5.6 Hz, 1H), 5.37 (t, *J* = 5.4 Hz, 1H), 5.20 (s, 1H), 4.58 (d, *J* = 5.2 Hz, 1H), 4.23–4.18 (m, 4H), 4.14 (s, 1H), 3.96 (d, *J* = 3.6 Hz, 1H), 3.72–3.63 (m, 1H), 3.60–3.50 (m, 1H), 1.75–1.65 (m, 2H), 1.63–1.50 (m, 4H). ¹³C{¹H} NMR (101 MHz, DMSO) δ 153.2, 151.8, 150.2, 138.5, 119.5, 87.8, 85.8, 73.5, 70.6, 61.6, 45.7, 25.7, 24.3. (+ve) APCI-MS *m/z* = 335.16 calcd. for C₁₅H₂₁N₅O₄ [M], found: 336.00 [M + H]. The compound exhibited identical ¹H and ¹³C{¹H} NMR data to previous reports.^{11c}

*2-(Hydroxymethyl)-5-(6-(yridineib-1-yl)-9*H*-purin-9-yl)-tetrahydrofuran-3,4-diol (5h).*



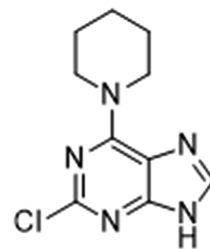
General Procedure was followed using 6-chloropurine riboside (286.67 mg, 1 mmol) and pyrrolidine (0.099 mL, 1.2 mmol, 1.2 equiv), yielding the desired 2-(hydroxymethyl)-5-(6-(yridineib-1-yl)-9*H*-purin-9-yl)-tetrahydrofuran-3,4-diol (285.0 mg, 0.89 mmol, 89%, HPLC purity: 99.49%) as a white solid. ¹H NMR (400 MHz, DMSO) δ 8.35 (s, 1H), 8.21 (s, 1H), 5.91 (d, *J* = 5.9 Hz, 1H), 5.48–5.41 (m, 2H), 5.23–5.18 (m, 1H), 4.64–4.55 (m, 1H), 4.16 (s, 1H), 4.06 (s, 2H), 4.01–3.95 (m, 1H), 3.78–3.47 (m, 4H), 2.17–1.63 (m, 4H). ¹³C{¹H} NMR (101 MHz, DMSO) δ 152.6, 152.1, 149.5, 139.1, 120.0, 87.9, 85.8, 73.5, 70.6, 61.7, 48.5, 47.1, 25.8, 23.8. (+ve) APCI-MS *m/z* = 321.14 calcd. for C₁₄H₁₉N₅O₄ [M], found: 322.00 [M + H]. The compound exhibited identical ¹H and ¹³C{¹H} NMR data to previous reports.⁷⁴

*2-(6-(Dimethylamino)-9*H*-purin-9-yl)-5-(hydroxymethyl)-tetrahydrofuran-3,4-diol (5i).*



General Procedure was followed using 6-chloropurine riboside (286.67 mg, 1 mmol) and dimethyl amine 40% (0.15 mL, 1.2 mmol, 1.2 equiv), yielding the desired 2-(6-(dimethylamino)-9*H*-purin-9-yl)-5-(hydroxymethyl)tetrahydrofuran-3,4-diol (285.0 mg, 0.97 mmol, 97%, HPLC purity: 98.10%) as a white solid. ¹H NMR (400 MHz, DMSO) δ 8.30 (s, 1H), 8.17 (s, 1H), 5.58 (d, *J* = 4.5 Hz, 1H), 4.30 (s, 2H), 3.82 (s, 1H), 3.71 (s, 2H), 3.60 (d, *J* = 11.4 Hz, 2H), 3.46 (s, 6H), 3.11 (s, 1H). ¹³C{¹H} NMR (101 MHz, DMSO) δ 154.2, 151.5, 150.0, 138.2, 119.6, 90.8, 87.2, 76.9, 71.0, 62.2, 37.9. (+ve) APCI-MS *m/z* = 295.13 calcd. for C₁₂H₁₇N₅O₄ [M], found: 296.00 [M + H]. The compound exhibited identical ¹H and ¹³C{¹H} NMR data to previous reports.⁷³

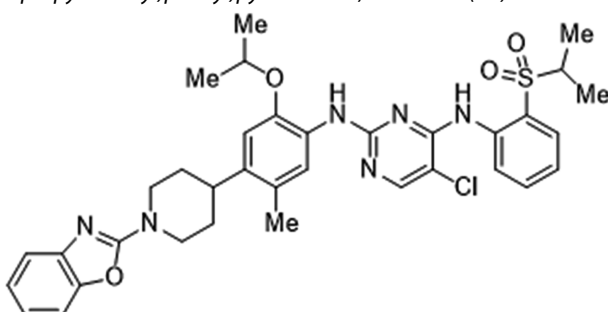
*2-Chloro-6-(piperidin-1-yl)-9*H*-purine (5j).*



General Procedure was followed using 2,6-dichloro purine (189.0 mg, 1 mmol) and piperidine (0.24 mL, 2.4 mmol, 2.4 equiv), yielding the desired 2-chloro-6-(piperidin-1-yl)-9*H*-purine (222.1 mg, 0.93 mmol, 93%, HPLC purity: 95.19%) as a white solid. ¹H NMR (400 MHz, DMSO) δ 13.01 (s, 1H), 8.10 (s, 1H), 4.16 (s, 4H), 1.73–1.63 (m, 2H), 1.63–1.54 (m, 4H). ¹³C{¹H} NMR (101 MHz, DMSO) δ 153.2, 152.5, 138.5, 117.5, 50.7, 25.6, 24.1. (+ve) APCI-MS *m/z* = 237.08 calcd. For C₁₀H₁₂ClN₅ [M], found: 238.00 [M + H].⁷⁴

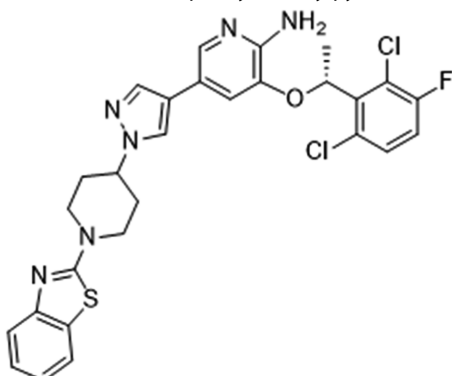
Late-Stage Modification of Active Pharmaceutical ingredients (APIs) using Cu(II)/PTABS System. N²-(4-(1-(Benzo[d]oxazol-2-yl)-

piperidin-4-yl)-2-isopropoxy-5-methylphenyl)-5-chloro-N⁴-(2-(isopropylsulfonyl)phenyl)pyrimidine-2,4-diamine (6a).



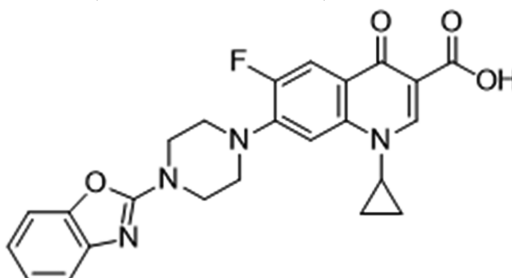
General Procedure was followed using 2-chlorobenzoxazole (77.0 mg, 0.5 mmol) and ceritinib (279.85 mg, 0.5 mmol, 1.0 equiv), yielding the desired *N*²-(4-(1-(benzo[d]oxazol-2-yl)piperidin-4-yl)-2-isopropoxy-5-methylphenyl)-5-chloro-N⁴-(2-(isopropylsulfonyl)phenyl)pyrimidine-2,4-diamine (320.0 mg, 0.95 mmol, 95%, HPLC purity: 97.38%) as a white solid. M.p. >250 °C. ¹H NMR (300 MHz, CDCl₃) δ 9.51 (s, 1H), 8.58 (d, *J* = 8.3 Hz, 1H), 8.16 (s, 1H), 8.05 (s, 1H), 7.94 (dd, *J* = 8.0, 1.6 Hz, 1H), 7.69–7.58 (m, 1H), 7.55 (s, 1H), 7.37 (d, *J* = 7.7 Hz, 1H), 7.26–7.12 (m, 1H), 7.03 (td, *J* = 7.7, 1.3 Hz, 1H), 6.71 (s, 1H), 6.24 (s, 2H), 4.59–4.49 (m, 2H), 4.47 (s, 1H), 3.33–3.21 (m, 2H), 3.17 (d, *J* = 2.8 Hz, 1H), 3.02–2.88 (m, 1H), 2.21 (s, 3H), 1.90 (d, *J* = 12.9 Hz, 2H), 1.77 (tt, *J* = 12.9, 6.4 Hz, 2H), 1.33 (t, *J* = 6.4 Hz, 12H). ¹³C{¹H} NMR (75 MHz, CDCl₃) δ 162.3, 157.5, 155.4, 148.9, 144.8, 143.4, 138.6, 136.7, 134.7, 131.3, 128.0, 127.0, 125.0, 124.0, 123.7, 123.2, 120.8, 120.6, 116.2, 110.9, 108.8, 105.9, 71.7, 55.6, 46.8, 38.0, 32.3, 22.3, 19.1, 15.4. (+ve) APCI-MS *m/z* = 674.24 calcd. for C₃₅H₃₉FN₆O₄S [M], found: 675.20 [M + H]. HRMS (ESI) *m/z*: (M + H)⁺ calcd. for C₃₅H₄₀FN₆O₄S: 675.2520; found: 675.2541.

(R)-5-(1-(1-(Benzo[d]thiazol-2-yl)piperidin-4-yl)-1*H*-pyrazol-4-yl)-3-(1-(2,6-dichloro-3-fluorophenyl)ethoxy)pyridin-2-amine (6b).



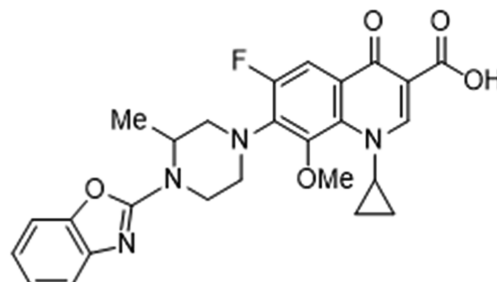
General Procedure was followed using 2-chlorobenzothiazole (84.82 mg, 0.5 mmol) and crizotinib (225.17 mg, 0.5 mmol, 1.0 equiv), yielding the desired (R)-5-(1-(1-(benzo[d]thiazol-2-yl)piperidin-4-yl)-1*H*-pyrazol-4-yl)-3-(1-(2,6-dichloro-3-fluorophenyl)ethoxy)pyridin-2-amine (138.2 mg, 0.47 mmol, 47%, HPLC purity: 86.65%) as an off-white solid. M.p. >250 °C. ¹H NMR (300 MHz, CDCl₃) δ 7.74 (d, *J* = 1.7 Hz, 1H), 7.66–7.53 (m, 3H), 7.53–7.45 (m, 1H), 7.37–7.25 (m, 2H), 7.15–6.98 (m, 2H), 6.86 (d, *J* = 1.8 Hz, 1H), 6.06 (q, *J* = 6.7 Hz, 1H), 4.88 (s, 2H), 4.46–4.35 (m, 1H), 4.31 (d, *J* = 13.7 Hz, 2H), 3.33 (dd, *J* = 11.7, 3.0 Hz, 2H), 2.28 (s, 2H), 2.23–2.06 (m, 2H), 1.85 (d, *J* = 6.7 Hz, 3H). ¹³C{¹H} NMR (75 MHz, CDCl₃) δ 168.4, 152.8, 149.1, 148.4, 139.9, 136.9, 136.0, 135.2, 131.0, 130.0, 129.0, 126.1, 122.8, 121.7, 120.8, 120.2, 119.2, 118.9, 116.9, 116.6, 115.0, 72.5, 58.9, 47.6, 31.8, 18.9. (+ve) APCI-MS *m/z* = 582.12 calcd. for C₂₈H₂₅Cl₂FN₆OS [M], found: 583.20 [M + H]. HRMS (ESI) *m/z*: (M + H)⁺ calcd. for C₂₈H₂₆Cl₂FN₆OS: 583.1250; found: 583.1263.

7-(4-(Benzo[d]oxazol-2-yl)piperazin-1-yl)-1-cyclopropyl-6-fluoro-4-oxo-1,4-dihydroquinoline-3-carboxylic Acid (6c).



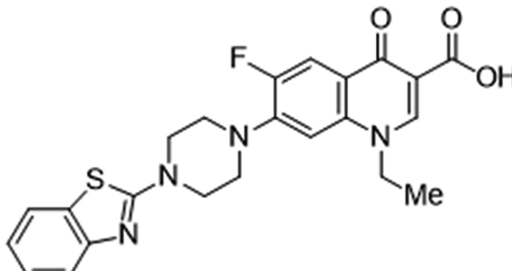
General Procedure was followed using 2-chlorobenzoxazole (77.0 mg, 0.5 mmol) and ciprofloxacin (166.20 mg, 0.5 mmol, 1.0 equiv), yielding the desired *7*-(4-(benzo[d]oxazol-2-yl)piperazin-1-yl)-1-cyclopropyl-6-fluoro-4-oxo-1,4-dihydroquinoline-3-carboxylic acid (189.5 mg, 0.84 mmol, 84%, HPLC purity: 98.57%) as a white solid. M.p. >250 °C. ¹H NMR (300 MHz, CDCl₃) δ 14.89 (s, 1H), 8.76 (s, 1H), 8.05 (s, 1H), 7.39 (d, *J* = 7.9 Hz, 2H), 7.30 (d, *J* = 7.9 Hz, 1H), 7.20 (t, *J* = 7.7 Hz, 1H), 7.07 (t, *J* = 7.7 Hz, 1H), 3.96 (s, 4H), 3.64 (s, 1H), 3.46 (s, 4H), 1.40 (s, 2H), 1.25 (s, 2H). ¹³C{¹H} NMR (75 MHz, CDCl₃) δ 178.5, 166.6, 161.9, 149.0, 142.9, 128.2, 124.4, 121.3, 116.7, 109.1, 70.7, 49.5, 45.6, 29.8, 8.4. (+ve) APCI-MS *m/z* = 448.15 calcd. For C₂₄H₂₁FN₄O₄ [M], found: 449.20 [M + H]. HRMS (ESI) *m/z*: (M + H)⁺ calcd. for C₂₄H₂₂FN₄O₄: 449.1625; found: 449.1637.

7-(4-(Benzo[d]oxazol-2-yl)-3-methylpiperazin-1-yl)-1-cyclopropyl-6-fluoro-8-methoxy-4-oxo-1,4-dihydroquinoline-3-carboxylic Acid (6d).



General Procedure was followed using 2-chlorobenzoxazole (77.0 mg, 0.5 mmol) and gatifloxacin (188.23 mg, 0.5 mmol, 1.0 equiv), yielding the desired *7*-(4-(benzo[d]oxazol-2-yl)-3-methylpiperazin-1-yl)-1-cyclopropyl-6-fluoro-8-methoxy-4-oxo-1,4-dihydroquinoline-3-carboxylic acid (223.8 mg, 0.91 mmol, 91%, HPLC purity: 95.21%) as an off-white solid. M.p. >250 °C. ¹H NMR (300 MHz, CDCl₃) δ 8.61 (s, 1H), 7.61 (s, 1H), 7.35 (d, *J* = 7.7 Hz, 1H), 7.23 (s, 1H), 7.18–7.09 (m, 1H), 7.00 (td, *J* = 7.7, 1.3 Hz, 1H), 4.49 (s, 1H), 4.07 (d, *J* = 12.1 Hz, 1H), 3.75 (s, 2H), 3.58 (s, 5H), 3.32 (s, 1H), 3.19 (s, 1H), 1.44 (d, *J* = 6.5 Hz, 3H), 0.94–0.70 (m, 4H). ¹³C{¹H} NMR (75 MHz, CDCl₃) δ 174.9, 161.9, 156.6, 153.3, 150.2, 148.8, 145.7, 143.1, 137.4, 133.4, 125.9, 124.1, 120.8, 117.3, 116.4, 108.9, 108.3, 63.1, 55.4, 50.8, 49.6, 41.5, 38.6, 29.8, 15.0, 9.4. (+ve) APCI-MS *m/z* = 492.18 calcd. For C₂₆H₂₅FN₄O₅ [M], found: 493.20 [M + H]. HRMS (ESI) *m/z*: (M + H)⁺ calcd. for C₂₆H₂₆FN₄O₅: 493.1887; found: 493.1886.

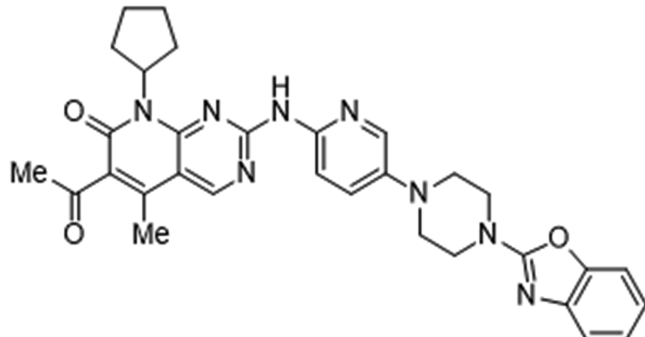
7-(4-(Benzo[d]thiazol-2-yl)piperazin-1-yl)-1-ethyl-6-fluoro-4-oxo-1,4-dihydroquinoline-3-carboxylic acid (6e).



General Procedure was followed using 2-chlorobenzothiazole (84.82 mg, 0.5 mmol) and norfloxacin (159.67 mg, 0.5 mmol, 1.0 equiv),

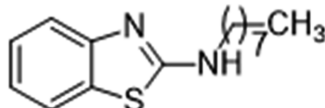
yielding the desired 7-(4-(benzo[d]thiazol-2-yl)piperazin-1-yl)-1-ethyl-6-fluoro-4-oxo-1,4-dihydroquinoline-3-carboxylic acid (63.0 mg, 0.28 mmol, 28%, HPLC purity: 94.85%) as a light brown solid. M.p. >250 °C. ^1H NMR (300 MHz, CDCl_3) δ 14.85 (s, 1H), 8.60 (s, 1H), 8.01 (d, J = 12.7 Hz, 1H), 7.54 (dd, J = 13.8, 7.9 Hz, 2H), 7.26 (t, J = 7.7 Hz, 1H), 7.05 (t, J = 7.6 Hz, 1H), 6.82 (d, J = 6.8 Hz, 1H), 4.26 (q, J = 7.3 Hz, 2H), 3.83 (t, J = 5.0 Hz, 4H), 3.39 (t, J = 5.0 Hz, 4H), 1.20 (d, J = 9.3 Hz, 3H). $^{13}\text{C}\{\text{H}\}$ NMR (75 MHz, CDCl_3) δ 177.1, 168.5, 167.2, 159.1, 152.6, 147.4, 145.9, 137.2, 131.0, 126.4, 122.1, 121.0, 119.6, 113.1, 108.7, 104.4, 49.9, 49.5, 49.5, 48.3, 29.8, 14.7. (+ve) APCI-MS m/z = 452.13 calcd. for $\text{C}_{23}\text{H}_{21}\text{FN}_4\text{O}_3\text{S}$ [M], found: 453.00 [M + H]. HRMS (ESI) m/z : (M + H) $^+$ calcd. for $\text{C}_{23}\text{H}_{22}\text{FN}_4\text{O}_3\text{S}$: 453.1397; found: 453.1407.

6-Acetyl-2-((5-(4-(benzo[d]oxazol-2-yl)piperazin-1-yl)pyridine-2-yl)amino)-8-cyclopentyl-5-methylpyrido[2,3-d]pyrimidin-7(8H)-one (6f).



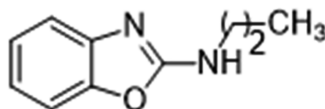
General Procedure was followed using 2-chlorobenzoxazole (77.0 mg, 0.5 mmol) and yridineib (224.40 mg, 0.5 mmol, 1.0 equiv), yielding the desired 6-acetyl-2-((5-(4-(benzo[d]oxazol-2-yl)piperazin-1-yl)pyridine-2-yl)amino)-8-cyclopentyl-5-methylpyrido[2,3-d] pyrimidin-7(8H)-one (241.5 mg, 0.85 mmol, 85%, HPLC purity: 85.35%) as a yellow solid. M.p. >250 °C. ^1H NMR (300 MHz, CDCl_3) δ 8.86 (s, 1H), 8.58 (s, 1H), 8.22 (d, J = 9.1 Hz, 1H), 8.12 (s, 1H), 7.39 (d, J = 8.2 Hz, 2H), 7.19 (t, J = 7.8 Hz, 1H), 7.05 (t, J = 7.8 Hz, 1H), 5.94–5.82 (m, 1H), 3.90 (t, J = 5.1 Hz, 4H), 3.47–3.39 (m, 1H), 3.30 (t, J = 5.0 Hz, 4H), 2.55 (s, 3H), 2.38 (s, 4H), 2.07 (s, 3H), 1.89 (s, 3H), 1.28–1.16 (m, 1H). $^{13}\text{C}\{\text{H}\}$ NMR (75 MHz, CDCl_3) δ 189.9, 161.5, 157.4, 155.7, 149.0, 145.9, 141.9, 137.7, 131.0, 127.1, 124.3, 121.2, 116.7, 109.0, 54.2, 49.6, 45.7, 31.7, 28.2, 25.9, 14.1. (+ve) APCI-MS m/z = 564.26 calcd. For $\text{C}_{31}\text{H}_{32}\text{N}_8\text{O}_3$ [M], found: 565.25 [M + H]. HRMS (ESI) m/z : (M + H) $^+$ calcd. for $\text{C}_{31}\text{H}_{32}\text{N}_8\text{O}_3$: 565.25; found: 565.25 [M + H].

Primary Alkyl Amines as Coupling Partners for the Cu(II)/PTABs-Catalyzed Amination. N-Octylbenzo[d]thiazol-2-amine (7a).



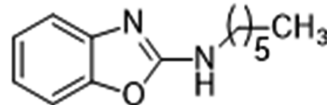
General Procedure was followed using 2-chloro benzothiazole (169.6 mg, 1 mmol) and *n*-octyl amine (0.20 mL, 1.2 mmol, 1.2 equiv), yielding the desired N-octylbenzo[d]thiazol-2-amine (237.0 mg, 0.90 mmol, 90%, HPLC purity: 98.37%) as a pale yellow oil. ^1H NMR (300 MHz, CDCl_3) δ 7.59 (dd, J = 7.8, 1.2 Hz, 1H), 7.52 (d, J = 8.0 Hz, 1H), 7.30 (dd, J = 7.4, 1.3 Hz, 1H), 7.07 (t, J = 7.6 Hz, 1H), 5.62 (br s, 1H), 3.40 (t, J = 7.1 Hz, 2H), 1.68 (quint, J = 7.2 Hz, 2H), 1.48–1.36 (m, 2H), 1.35–1.22 (m, 8H), 0.93–0.83 (m, 3H). $^{13}\text{C}\{\text{H}\}$ NMR (75 MHz, CDCl_3) δ 168.2, 152.6, 130.4, 126.0, 121.4, 120.9, 118.7, 45.9, 31.9, 29.7, 29.3, 29.3, 27.0, 22.7, 14.2. (+ve) APCI-MS m/z = 262.15 calcd. For $\text{C}_{15}\text{H}_{22}\text{N}_2\text{S}$ [M], found: 263.10 [M + H]. The compound exhibited identical ^1H and $^{13}\text{C}\{\text{H}\}$ NMR data to previous reports.⁷⁵

N-Propylbenzo[d]oxazol-2-amine (7b).



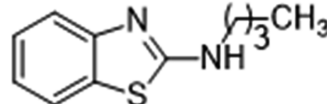
General Procedure was followed using 2-chlorobenzoxazole (153.6 mg, 1 mmol) and *n*-propylamine (0.10 mL, 1.2 mmol, 1.2 equiv), yielding the desired N-propylbenzo[d]oxazol-2-amine (138.3 mg, 0.78 mmol, 78%, HPLC purity: 98.39%) as a white solid. ^1H NMR (300 MHz, CDCl_3) δ 7.35 (d, J = 7.8 Hz, 1H), 7.24 (d, J = 7.9 Hz, 1H), 7.15 (td, J = 7.6, 1.2 Hz, 1H), 7.01 (td, J = 7.7, 1.1 Hz, 1H), 5.59 (s, 1H), 3.45 (t, J = 7.2 Hz, 2H), 1.71 (h, J = 7.3 Hz, 2H), 1.01 (t, J = 7.4 Hz, 3H). $^{13}\text{C}\{\text{H}\}$ NMR (75 MHz, CDCl_3) δ 162.7, 148.5, 143.1, 123.9, 120.5, 115.9, 108.7, 44.8, 23.1, 11.3. (+ve) APCI-MS m/z = 176.09 calcd. for $\text{C}_{10}\text{H}_{12}\text{N}_2\text{O}$ [M], found: 177.00 [M + H]. The compound exhibited identical ^1H and $^{13}\text{C}\{\text{H}\}$ NMR data to previous reports.⁷⁶

N-Hexylbenzo[d]oxazol-2-amine (7c).



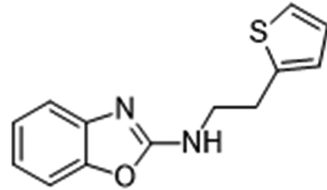
General Procedure was followed using 2-chlorobenzoxazole (153.6 mg, 1 mmol) and *n*-hexyl amine (0.16 mL, 1.2 mmol, 1.2 equiv), yielding the desired N-hexylbenzo[d]oxazol-2-amine (208.0 mg, 0.95 mmol, 95%, HPLC purity: 95.01%) as a brown solid. ^1H NMR (300 MHz, CDCl_3) δ 7.36 (d, J = 7.7 Hz, 1H), 7.24 (d, J = 7.6 Hz, 1H), 7.15 (t, J = 7.7 Hz, 1H), 7.01 (t, J = 7.7 Hz, 1H), 5.36 (s, 1H), 3.53–3.42 (m, 2H), 1.67 (quint, J = 7.1 Hz, 2H), 1.47–1.36 (m, 2H), 1.35–1.11 (m, 4H), 0.94–0.83 (m, 3H). $^{13}\text{C}\{\text{H}\}$ NMR (75 MHz, CDCl_3) δ 162.6, 148.6, 143.2, 123.9, 120.5, 116.0, 108.7, 43.1, 31.5, 29.8, 26.5, 22.6, 14.0. (+ve) APCI-MS m/z = 218.14 calcd. For $\text{C}_{13}\text{H}_{18}\text{N}_2\text{O}$ [M], found: 219.20 [M + H]. The compound exhibited identical ^1H and $^{13}\text{C}\{\text{H}\}$ NMR data to previous reports.⁷⁶

N-Butylbenzo[d]thiazol-2-amine (7d).

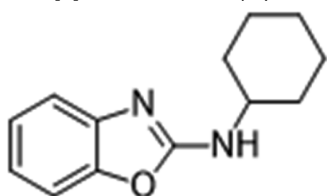


General Procedure was followed using 2-chloro benzothiazole (169.6 mg, 1 mmol) and *n*-butyl amine (0.12 mL, 1.2 mmol, 1.2 equiv), yielding the desired N-butylbenzo[d]thiazol-2-amine (190.9 mg, 0.93 mmol, 93%, HPLC purity: 95.21%) as a pale yellow solid. ^1H NMR (300 MHz, CDCl_3) δ 7.64–7.55 (m, 1H), 7.52 (d, J = 8.0 Hz, 1H), 7.30 (dd, J = 7.4, 1.3 Hz, 1H), 7.07 (t, J = 7.6 Hz, 1H), 5.73 (s, 1H), 3.41 (t, J = 7.1 Hz, 2H), 1.75–1.60 (m, 2H), 1.53–1.32 (m, 2H), 0.96 (t, J = 7.3 Hz, 3H). $^{13}\text{C}\{\text{H}\}$ NMR (75 MHz, CDCl_3) δ 168.5, 152.6, 125.9, 125.8, 121.2, 120.9, 118.4, 45.6, 31.6, 20.1, 13.8. (+ve) APCI-MS m/z = 206.09 calcd. for $\text{C}_{11}\text{H}_{14}\text{N}_2\text{S}$ [M], found: 207.00 [M + H]. The compound exhibited identical ^1H and $^{13}\text{C}\{\text{H}\}$ NMR data to previous reports.⁷⁷

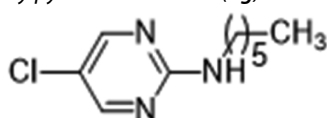
N-(2-Thiophen-2-yl)ethylbenzo[d]oxazol-2-amine (7e).



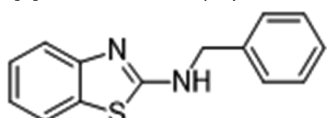
General Procedure was followed using 2-chlorobenzoxazole (153.6 mg, 1 mmol) and 2-thiopheneethethylamine (0.14 mL, 1.2 mmol, 1.2 equiv), yielding the desired N-(2-(thiophen-2-yl)ethyl)benzo[d]oxazol-2-amine (209.0 mg, 0.86 mmol, 86%, HPLC purity: 89.85%) as a dark yellow solid. M.p. 111 °C. ^1H NMR (300 MHz, CDCl_3) δ 7.38 (dd, J = 7.8, 1.3 Hz, 1H), 7.25 (d, J = 7.4 Hz, 1H), 7.20 (dd, J = 2.7, 1.2 Hz, 1H), 7.16 (dd, J = 7.5, 1.2 Hz, 1H), 7.04 (td, J = 7.8, 1.1 Hz, 1H), 6.96 (dd, J = 5.1, 3.4 Hz, 1H), 6.88 (dq, J = 3.3, 1.0 Hz, 1H), 5.25 (s, 1H), 3.77 (t, J = 6.6 Hz, 2H), 3.22 (td, J = 6.6, 0.9 Hz, 2H). $^{13}\text{C}\{\text{H}\}$ NMR (75 MHz, CDCl_3) δ 162.0, 148.7, 143.0, 140.8, 127.2, 125.7, 124.2, 124.0, 120.9, 116.3, 108.9, 44.3, 30.1. (+ve) APCI-MS m/z = 244.07 calcd. For $\text{C}_{13}\text{H}_{14}\text{N}_2\text{OS}$ [M], found: 245.00 [M + H]. HRMS (ESI) m/z : (M + H) $^+$ calcd. for $\text{C}_{13}\text{H}_{14}\text{N}_2\text{OS}$: 245.0670; found: 245.0726.

N-Cyclohexylbenzo[d]oxazol-2-amine (7f).

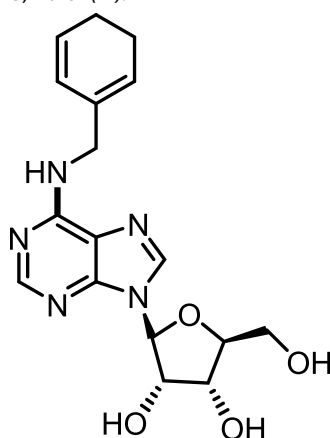
General Procedure was followed using 2-chlorobenzoxazole (153.6 mg, 1 mmol) and cyclohexyl amine (0.14 mL, 1.2 mmol, 1.2 equiv), yielding the desired *N*-cyclohexylbenzo[d]oxazol-2-amine (210.0 mg, 0.97 mmol, 97%, HPLC purity: 97.49%) as a yellow solid. ^1H NMR (300 MHz, CDCl_3) δ 7.36 (d, $J = 7.8$ Hz, 1H), 7.23 (d, $J = 7.9$ Hz, 1H), 7.15 (td, $J = 7.7, 1.2$ Hz, 1H), 7.01 (td, $J = 7.7, 1.1$ Hz, 1H), 5.15 (d, $J = 7.2$ Hz, 1H), 3.75 (dq, $J = 13.4, 5.2$ Hz, 1H), 2.20–2.06 (m, 2H), 1.79 (t, $J = 4.2$ Hz, 2H), 1.77–1.54 (m, 2H), 1.52–1.35 (m, 2H), 1.33–1.14 (m, 2H). $^{13}\text{C}\{\text{H}\}$ NMR (75 MHz, CDCl_3) δ 161.8, 148.4, 143.2, 123.9, 120.5, 116.0, 108.7, 52.1, 33.6, 25.6, 24.9. (+ve) APCI-MS m/z = 216.13 calcd. for $\text{C}_{13}\text{H}_{16}\text{N}_2\text{O}$ [M], found: 217.00 [M + H]. The compound exhibited identical ^1H and $^{13}\text{C}\{\text{H}\}$ NMR data to previous reports.⁷⁷

5-Chloro-N-hexylpyrimidin-2-amine (7g).

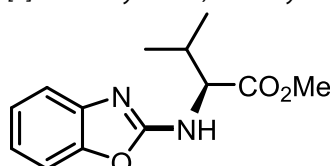
General Procedure was followed using 2,5-dichloropyrimidine (149.0 mg, 1 mmol) and *n*-hexyl amine (0.16 mL, 1.2 mmol, 1.2 equiv), yielding the desired 5-chloro-N-hexylpyrimidin-2-amine (207.0 mg, 0.97 mmol, 97%, HPLC purity: 99.38%) as a yellow solid. M.p. 70 °C. ^1H NMR (300 MHz, CDCl_3) δ 8.19 (s, 2H), 5.20 (s, 1H), 3.36 (td, $J = 7.1, 5.8$ Hz, 2H), 1.67–1.51 (m, 2H), 1.45–1.35 (m, 2H), 1.35–1.20 (m, 4H), 0.97–0.82 (m, 3H). $^{13}\text{C}\{\text{H}\}$ NMR (75 MHz, CDCl_3) δ 160.8, 156.3, 118.5, 41.9, 31.6, 29.5, 26.7, 22.7, 14.1. (+ve) APCI-MS m/z = 213.10 calcd. for $\text{C}_{10}\text{H}_{16}\text{ClN}_3$ [M], found: 214.00 [M + H]. HRMS (ESI) m/z : (M + H)⁺ calcd. for $\text{C}_{10}\text{H}_{17}\text{ClN}_3$: 214.1111; found: 214.1120.

N-Benzylbenzo[d]thiazol-2-amine (7h).

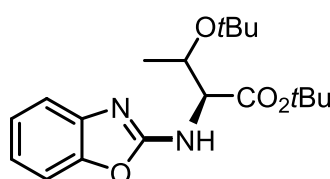
General Procedure was followed using 2-chlorobenzothiazole (169.6 mg, 1 mmol) and benzyl amine (0.13 mL, 1.2 mmol, 1.2 equiv), yielding the desired *N*-benzylbenzo[d]thiazol-2-amine (172.6 mg, 0.72 mmol, 72%, HPLC purity: 92.45%) as a pale yellow oil. ^1H NMR (300 MHz, CDCl_3) δ 7.58 (d, $J = 7.9$ Hz, 1H), 7.50–7.26 (m, 6H), 7.31–7.22 (m, 1H), 7.08 (td, $J = 7.6, 1.2$ Hz, 1H), 6.43 (br s, 1H), 4.64 (s, 2H). $^{13}\text{C}\{\text{H}\}$ NMR (75 MHz, CDCl_3) δ 167.9, 152.4, 137.6, 130.5, 128.9, 128.0, 127.8, 126.1, 121.7, 121.0, 119.0, 49.6. (+ve) APCI-MS m/z = 240.07 calcd. for $\text{C}_{14}\text{H}_{12}\text{N}_2\text{S}$ [M], found: 241.00 [M + H]. The compound exhibited identical ^1H and $^{13}\text{C}\{\text{H}\}$ NMR data to previous reports.⁷⁸

2-(6-(Benzylamino)-9H-β-purin-9-yl)-5-(hydroxymethyl)-tetrahydrofuran-3,4-diol (7i).

General Procedure was followed using 6-chloropurine riboside (286.67 mg, 1 mmol) and benzyl amine (0.13 mL, 1.2 mmol, 1.2 equiv), yielding the desired 2-(6-(benzylamino)-9H-purin-9-yl)-5-(hydroxymethyl)-tetrahydrofuran-3,4-diol (330.0 mg, 0.92 mmol, 92%, HPLC purity: 91.55%) as a white solid. ^1H NMR (400 MHz, DMSO) δ 8.38 (s, 1H), 8.20 (br s, 1H), 7.33 (d, $J = 7.5$ Hz, 2H), 7.29 (t, $J = 7.5$ Hz, 2H), 7.24–7.16 (m, 1H), 5.89 (d, $J = 6.1$ Hz, 1H), 5.40 (s, 1H), 5.23 (s, 2H), 4.71 (br s, 2H), 4.62 (t, $J = 5.6$ Hz, 1H), 4.18–4.11 (m, 1H), 3.96 (q, $J = 3.4$ Hz, 1H), 3.79 (s, 1H), 3.67 (dd, $J = 12.6, 3.5$ Hz, 1H), 3.55 (d, $J = 12.3$ Hz, 1H). $^{13}\text{C}\{\text{H}\}$ NMR (101 MHz, DMSO) δ 154.5, 152.4, 148.4, 140.0, 134.6, 128.3, 127.1, 126.7, 119.8, 88.0, 85.9, 73.5, 70.7, 61.7, 42.9. (+ve) APCI-MS m/z = 357.14 calcd. for $\text{C}_{17}\text{H}_{19}\text{N}_5\text{O}_4$ [M], found: 358.20 [M + H]. The compound exhibited identical ^1H and $^{13}\text{C}\{\text{H}\}$ NMR data to previous reports.⁷⁹

Amino Acid Functionalization Using the Cu(II)/PTABS System. (S)-Methyl-2-(benzo[d]oxazol-2-ylamino)-3-methylbutanoate (8a).

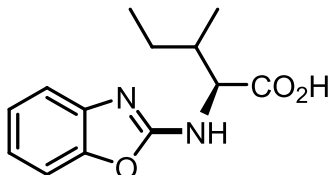
General Procedure was followed using 2-chlorobenzoxazole (153.6 mg, 1 mmol) and L-valine methyl ester hydrochloride (201.16 mg, 1.2 mmol, 1.2 equiv), yielding the desired (S)-methyl 2-(benzo[d]oxazol-2-ylamino)-3-methylbutanoate (213.2 mg, 0.86 mmol, 86%, HPLC purity: 90.88%) as a white solid. M.p. >170 °C (decomposed). ^1H NMR (300 MHz, CDCl_3) δ 7.37 (dd, $J = 7.8, 1.3$ Hz, 1H), 7.27–7.09 (m, 2H), 7.01 (td, $J = 7.7, 1.3$ Hz, 1H), 6.35 (s, 1H), 4.54 (d, $J = 5.2$ Hz, 1H), 3.76 (s, 3H), 2.31 (heptd, $J = 6.9, 5.2$ Hz, 1H), 1.02 (dd, $J = 10.1, 6.9$ Hz, 6H). $^{13}\text{C}\{\text{H}\}$ NMR (75 MHz, CDCl_3) δ 172.7, 161.9, 148.6, 142.7, 124.0, 121.1, 116.6, 108.9, 61.2, 52.4, 31.4, 19.0, 17.9. (+ve) APCI-MS m/z = 248.12 calcd. for $\text{C}_{13}\text{H}_{16}\text{N}_2\text{O}_3$ [M], found: 249.00 [M + H]. HRMS (ESI) m/z : (M + H)⁺ calcd. for $\text{C}_{13}\text{H}_{17}\text{N}_2\text{O}_3$: 249.1239; found: 249.1241.

(2S,3R)-tert-Butyl 2-(benzo[d]oxazol-2-ylamino)-3-(tert-butoxy)butanoate (8b).

General Procedure was followed using 2-chlorobenzoxazole (153.6 mg, 1 mmol) and o-*tert*-butyl-L-threonine *tert*-butyl ester (0.30 mL, 1.2 mmol, 1.2 equiv), yielding the desired (2S,3R)-*tert*-butyl 2-(benzo[d]oxazol-2-ylamino)-3-(*tert*-butoxy)butanoate (302.75 mg, 0.87 mmol, 87%, HPLC purity: 86.50%) as a brown solid. M.p. >170 °C (decomposed). ^1H NMR (300 MHz, CH_2Cl_2) δ 7.33 (d, $J = 7.8$ Hz,

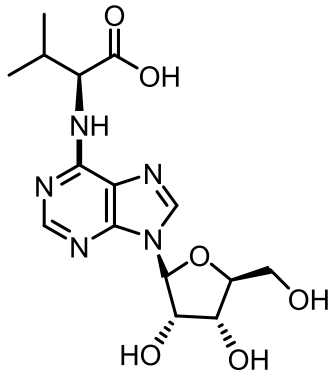
1H), 7.30–7.19 (m, 1H), 7.14 (tt, J = 7.6, 1.1 Hz, 1H), 7.01 (td, J = 7.7, 1.2 Hz, 1H), 5.68 (d, J = 9.8 Hz, 1H), 4.30 (dd, J = 5.3, 1.8 Hz, 1H), 4.27 (d, J = 6.2 Hz, 1H), 1.47–1.41 (m, 9H), 1.29 (dd, J = 6.4, 0.9 Hz, 3H), 1.18 (d, J = 0.9 Hz, 9H). $^{13}\text{C}\{\text{H}\}$ NMR (75 MHz, CH_2Cl_2) δ 170.1, 162.4, 148.8, 143.0, 123.9, 121.0, 116.6, 108.9, 82.3, 74.1, 67.2, 62.4, 28.8, 28.1, 21.4. (+ve) APCI-MS m/z = 348.20 calcd. for $\text{C}_{19}\text{H}_{28}\text{N}_2\text{O}_4$ [M], found: 349.20 [M + H]. HRMS (ESI) m/z : (M + H) $^+$ calcd. for $\text{C}_{19}\text{H}_{29}\text{N}_2\text{O}_4$: 349.2127; found: 349.2123.

2-(Benzod[d]oxazol-2-ylamino)-3-methylpentanoic acid (8c).



General Procedure was followed using 2-chlorobenzoxazole (153.6 mg, 1 mmol) and L-isoleucine methyl ester hydrochloride salt (217.99 mg, 1.2 mmol, 1.2 equiv), yielding the desired 2-(benzo[d]oxazol-2-ylamino)-3-methylpentanoic acid (238.20 mg, 0.96 mmol, 96%, HPLC purity: 90.60%) as an off-white solid. M.p. >150 °C (decomposed). ^1H NMR (300 MHz, DMSO) δ 7.27 (d, J = 7.8 Hz, 1H), 7.19 (d, J = 7.7 Hz, 1H), 7.12–7.01 (m, 1H), 6.98–6.86 (m, 1H), 3.83 (d, J = 3.9 Hz, 1H), 1.90 (s, 1H), 1.64–1.46 (m, 1H), 1.32–1.11 (m, 1H), 0.89 (s, 1H), 0.88–0.86 (m, 3H), 0.81 (s, 3H). $^{13}\text{C}\{\text{H}\}$ NMR (75 MHz, DMSO) δ 173.0, 162.4, 148.0, 143.7, 123.5, 119.8, 115.2, 108.3, 62.8, 37.6, 25.1, 16.0, 12.1. (–ve) APCI-MS m/z = 248.12 calcd. For $\text{C}_{13}\text{H}_{16}\text{N}_2\text{O}_3$ [M], found: 247.20 [M-H]. HRMS (ESI) m/z : (M + H) $^+$ calcd. for $\text{C}_{13}\text{H}_{17}\text{N}_2\text{O}_3$: 249.1239; found: 249.1243.

2-((9-(3,4-Dihydroxy-5-(hydroxymethyl)tetrahydrofuran-2-yl)-9H-purin-6-yl)amino)-3-methylbutanoic Acid (8d).



General Procedure was followed using 6-chloropurine riboside (286.67 mg, 1 mmol) and L-valine methyl ester hydrochloride salt (201.16 mg, 1.2 mmol, 1.2 equiv), yielding the desired 2-((9-(3,4-dihydroxy-5-(hydroxymethyl)tetrahydrofuran-2-yl)-9H-purin-6-yl)amino)-3-methylbutanoic acid (74.0 mg, 0.20 mmol, 20%, HPLC purity: 87.01%) as an off-white solid. M.p. >150 °C (decomposed). ^1H NMR (300 MHz, DMSO) δ 8.33 (s, 1H), 8.15 (s, 1H), 5.86 (d, J = 6.0 Hz, 1H), 5.59 (s, 1H), 4.58 (t, J = 5.5 Hz, 1H), 4.20 (s, 1H), 4.19–4.07 (m, 1H), 3.96 (q, J = 3.4 Hz, 1H), 3.66 (dd, J = 12.4, 3.6 Hz, 2H), 3.56–3.48 (m, 1H), 3.16 (s, 1H), 2.22 (s, 1H), 1.71 (s, 1H), 0.93 (d, J = 6.7 Hz, 3H), 0.85 (d, J = 6.7 Hz, 3H). $^{13}\text{C}\{\text{H}\}$ NMR (75 MHz, DMSO) δ 173.8, 154.3, 152.6, 148.1, 139.9, 120.0, 88.3, 86.1, 73.8, 70.7, 61.8, 48.7, 31.1, 19.4, 18.8. (+ve) APCI-MS m/z = 367.15 calcd. for $\text{C}_{15}\text{H}_{21}\text{N}_5\text{O}_6$ [M], found: 368.20 [M + H]. HRMS (ESI) m/z : (M + H) $^+$ calcd. for $\text{C}_{15}\text{H}_{22}\text{N}_5\text{O}_6$: 368.1570; found: 368.1577.

ASSOCIATED CONTENT

Supporting Information

The Supporting Information is available free of charge at <https://pubs.acs.org/doi/10.1021/acs.joc.1c00845>.

^1H and ^{13}C NMR spectra of all compounds ([PDF](#))

AUTHOR INFORMATION

Corresponding Author

Anant R. Kapdi – Department of Chemistry, Institute of Chemical Technology, Mumbai 400019, India; orcid.org/0000-0001-9710-8146; Email: ar.kapdi@ictmumbai.edu.in

Authors

Udaysinh Parmar – Aether Industries Limited, Surat 394230, Gujarat, India

Dipesh Somvanshi – Department of Chemistry, Institute of Chemical Technology, Mumbai 400019, India

Santosh Kori – Department of Chemistry, Institute of Chemical Technology, Mumbai 400019, India; Department of Industrial and Engineering Chemistry, Institute of Chemical Technology-Indian Oil Odisha Campus, IIT Kharagpur extension Centre, Bhubaneswar 751013, Odisha, India

Aman A. Desai – Aether Industries Limited, Surat 394230, Gujarat, India

Rambabu Dandela – Department of Industrial and Engineering Chemistry, Institute of Chemical Technology-Indian Oil Odisha Campus, IIT Kharagpur extension Centre, Bhubaneswar 751013, Odisha, India

Dilip K. Maity – Chemical Sciences, Homi Bhabha National Institute, Mumbai 400094, India; Chemical Sciences, Bhabha Atomic Research Centre, Mumbai 400085, India; orcid.org/0000-0003-4284-3578

Complete contact information is available at:

<https://pubs.acs.org/10.1021/acs.joc.1c00845>

Notes

The authors declare no competing financial interest.

ACKNOWLEDGMENTS

A.R.K. would like to thank the Institute of Chemical Technology and Institute of Chemical Technology-Indian Oil Odisha Campus for Ph.D. fellowship to S.K. The authors also would like to thank ICT for providing an industrial Ph.D. possibility to U.P.

REFERENCES

- (a) Ruiz-Castillo, P.; Buchwald, S. L. Applications of Palladium-Catalyzed C–N Cross-Coupling Reactions. *Chem. Rev.* **2016**, *116*, 12564–12649. (b) Schlummer, B.; Scholz, U. Palladium-Catalyzed C–N and C–O coupling-A practical guide from an industrial vantage point. *Adv. Synth. Catal.* **2004**, *346*, 1599–1626. (c) Dorel, R.; Grugel, C. P.; Haydl, A. M. The Buchwald–Hartwig amination after 25 years. *Angew. Chem., Int. Ed.* **2019**, *58*, 17118–17129. (d) Yin, J.; Buchwald, S. L. Pd-Catalyzed Intermolecular Amidation of Aryl Halides: The Discovery that Xantphos Can Be Trans-Chelating in a Palladium Complex. *J. Am. Chem. Soc.* **2002**, *124*, 6043–6048. (e) Torraca, K. E.; Huang, X.; Parrish, C. A.; Buchwald, S. L. An Efficient Intermolecular Palladium-Catalyzed Synthesis of Aryl Ethers. *J. Am. Chem. Soc.* **2001**, *123*, 10770–10771.
- (2) Affouard, C.; Crockett, R. D.; Diker, K.; Farrell, R. P.; Gorins, G.; Huckins, J. R.; Caille, S. Multi-kilo delivery of AMG 925 featuring a Buchwald–Hartwig amination and processing with insoluble synthetic intermediates. *Org. Process Res. Dev.* **2015**, *19*, 476–485.
- (3) Feng, J.; Zhang, Z.; Wallace, M. B.; Stafford, J. A.; Kaldor, S. W.; Kassel, D. B.; Navre, M.; Shi, L.; Skene, R. J.; Asakawa, T.; Takeuchi, K.; Xu, R.; Webb, D. R.; Gwaltney, S. L. Discovery of Alogliptin: A potent, selective, bioavailable, and efficacious inhibitor of dipeptidyl peptidase IV. *J. Med. Chem.* **2007**, *50*, 2297.
- (4) (a) Sirohi, B.; Rastogi, S.; Dawood, S. Buparlisib in breast cancer. *Future Oncol.* **2015**, *11*, 1463. (b) Speranza, M.-C.; Nowicki, M. O.; Behera, P.; Cho, C.-F.; Chiocca, E. A.; Lawler, S. E. BKM-120

- (Buparlisib): A phosphatidyl-inositol-3 kinase inhibitor with anti-invasive properties in glioblastoma. *Sci. Rep.* **2016**, *6*, 20189.
- (5) Abraham, R. T.; Acquarone, M.; Andersen, A.; Asensi, A.; Belle, R.; Berger, F.; Bergonioux, C.; Brunn, G.; Buquet-Fagot, C.; Fagot, D.; Glab, N.; Goudeau, H.; Guerrier, P.; Houghton, P.; Hendriks, H.; Kloareg, B.; Lippal, M.; Marie, D.; Maro, B.; Meijer, L.; Mester, J.; Mulner-Lorillon, O.; Poulet, S. A.; Schrienerberg, B.; Schutte, B.; Vaulot, D.; Verlhac, M. H. Cellular effects of olomoucine, an inhibitor of cyclin-dependent kinases. *Biol. Cell* **1995**, *83*, 105–120.
- (6) Takatsuki, K.-I.; Ohgushi, S.; Kohmoto, S.; Kishikawa, K.; Yamamoto, M. A simple and efficient synthesis of puromycin, 2,2'-anhydro-pyrimidine nucleosides, cytidines and 2,3'-anhydroadenosine from 3',5'-O-sulfinylylo-nucleosides. *Nucleosides, Nucleotides and Nucleic Acids* **2006**, *25*, 719–734.
- (7) Oumata, N.; Ferandin, Y.; Meijer, L.; Galons, H. Practical synthesis of Roscovitine and CR8. *Org. Process Res. Dev.* **2009**, *13*, 641–644.
- (8) Fleckenstein, C. A.; Plenio, H. Sterically demanding trialkylphosphines for palladium-catalyzed cross coupling reactions—alternatives to PbBu_3 . *Chem. Soc. Rev.* **2010**, *39*, 694.
- (9) (a) Organ, M. G.; Abdel-Hadi, M.; Avola, S.; Dubovik, I.; Hadei, N.; Kantchev, E. A. B.; O'Brien, C. J.; Sayah, M.; Valente, C. Pd-catalyzed aryl amination mediated by well-defined, N-heterocyclic carbene (NHC)-Pd precatalysts, PEPPSI. *Chem. – Eur. J.* **2008**, *14*, 2443. (b) Lombardi, C.; Day, J.; Chandrasoma, N.; Mitchell, D.; Rodriguez, M. J.; Farmer, J. L.; Organ, M. G. Selective cross-coupling of (hetero)aryl halides with ammonia to produce primary arylamines using Pd-NHC complexes. *Organometallics* **2017**, *36*, 251.
- (10) Roiban, G.-D.; Mehler, G.; Reetz, M. T. Palladium-catalyzed amination of aryl- and heteroaryl halides using tert-butyl tetraisopropylphosphorodiimidite as an easily accessible and air-stable ligand. *Eur. J. Org. Chem.* **2014**, *2014*, 2070.
- (11) (a) Shet, H.; Parmar, U.; Bhilare, S.; Kapdi, A. R. A comprehensive review of caged phosphines: synthesis, catalytic applications, and future perspectives. *Org. Chem. Front.* **2021**, *8*, 1599–1656. (b) Bandaru, S. S. M.; Bhilare, S.; Cardozo, J.; Chrysochos, N.; Schulzke, C.; Sanghvi, Y. S.; Gunturu, K. C.; Kapdi, A. R. Pd/PTABS: Low-Temperature Thioetherification of Chloro(hetero)arenes. *J. Org. Chem.* **2019**, *84*, 8921–8940. (for more information on etherification protocol with chloroheteroarenes see: Thioetherification of Chloroheteroarenes: A Binuclear Catalyst Promotes Wide Scope and High Functional-Group Tolerance. Platon, M.; Wijaya, N.; Rampazzi, V.; Cui, L.; Roussel, Y.; Saeys, M.; Hiero, J.-C. *Chem. Eur. J.* **2014**, *20*, 12584–12594.) (c) Bhujabal, Y. B.; Vadagaonkar, K. S.; Ghopal, A.; Sanghvi, Y. S.; Dandale, R.; Kapdi, A. R. HFIP Promoted Low-Temperature SNAr of Chloroheteroarenes Using Thiols and Amines. *J. Org. Chem.* **2019**, *84*, 15343–15354. (d) Bhilare, S.; Bandaru, S. S. M.; Shah, J.; Chrysochos, N.; Schulzke, C.; Sanghvi, Y. S.; Kapdi, A. R. Pd/PTABS: Low Temperature Etherification of Chloroheteroarenes. *J. Org. Chem.* **2018**, *83*, 13088–13102. (for more information on etherification protocol with chloroheteroarenes see: Platon, M.; Cui, L.; Mom, S.; Richard, P.; Saeys, M.; Hiero, J.-C. Etherification of Functionalized Phenols with Chloroheteroarenes at Low Palladium Loading: Theoretical Assessment of the Role of Triphosphane Ligands in C–O Reductive Elimination. *Adv. Synth. Catal.* **2011**, *353*, 3403–3414) (e) Bhilare, S.; Bandaru, S. S. M.; Kapdi, A. R.; Sanghvi, Y. S.; Schulzke, C. Pd/PTABS: An Efficient Water-Soluble Catalytic System for the Amination of 6-Chloropurine Ribonucleoside and Synthesis of Alogliptin. *Curr. Protoc. Nucleic Acid Chem.* **2018**, *74*, 58.
- (12) Murthy Bandaru, S. S.; Bhilare, S.; Chrysochos, N.; Gayakhe, V.; Trentin, I.; Schulzke, C.; Kapdi, A. R. Pd/PTABS: Catalyst for Room Temperature Amination of Heteroarenes. *Org. Lett.* **2018**, *20*, 473–476.
- (13) (a) Monnier, F.; Taillefer, M. Catalytic C–C, C–N, C–O Ullmann-Type Coupling Reactions. *Angew. Chem., Int. Ed.* **2009**, *48*, 6954–6971. (b) Evano, G.; Blanchard, N.; Toumi, M. Copper-Mediated Coupling Reactions and Their Applications in Natural Products and Designed Biomolecules Synthesis. *Chem. Rev.* **2008**, *108*, 3054–3131. (c) Ma, D.; Cai, Q. Copper/Amino Acid Catalyzed Cross-Couplings of Aryl and Vinyl Halides with Nucleophiles. *Acc. Chem. Res.* **2008**, *41*, 1450–1460.
- (d) Bhunia, S.; Pawar, G. G.; Kumar, S. V.; Jiang, Y.; Ma, D. Selected Copper-based Reactions for C–N, C–O, C–S and C–C bond formation. *Angew. Chem., Int. Ed.* **2017**, *56*, 16136. (e) Neetha, M.; Saranya, S.; Harry, N. A.; Anilkumar, G. Recent Advances and Perspectives in the Copper-Catalysed Amination of Aryl and Heteroaryl Halides. *Chem. Select* **2020**, *5*, 736–753. (f) Goldberg, I. Ueber Phenyllirungen bei Gegenwart von Kupfer als Katalysator. *Ber. Dtsch. Chem. Ges.* **1906**, *39*, 1691.
- (14) (a) Gao, J.; Bhunia, S.; Wang, K.; Gan, L.; Xia, S.; Ma, D. Discovery of *N*-(Naphthalen-1-yl)-*N'*-alkyl Oxalamide Ligands Enables Cu-Catalyzed Aryl Amination with High Turnovers. *Org. Lett.* **2017**, *19*, 2809–2812. (b) Zhou, W.; Fan, M.; Yin, J.; Jiang, Y.; Ma, D. CuI/Oxalic Diamide Catalyzed Coupling Reaction of (Hetero)Aryl Chlorides and Amines. *J. Am. Chem. Soc.* **2015**, *137*, 11942–11945. (c) Jiao, J.; Zhang, X.-R.; Chang, N.-H.; Wang, J.; Wei, J.-F.; Shi, X.-Y.; Chen, Z.-G. A Facile and Practical Copper Powder-Catalyzed, Organic Solvent- and Ligand-Free Ullmann Amination of Aryl Halides. *J. Org. Chem.* **2011**, *76*, 1180–1183. (d) Chakraborti, G.; Paladhi, S.; Mandal, T.; Dash, J. On Water Promoted Ullmann-Type C–N Bond-Forming Reactions: Application to Carbazole Alkaloids by Selective N-Arylation of Aminophenols. *J. Org. Chem.* **2018**, *83*, 7347–7359. (e) Kwong, F.-Y.; Klapars, A.; Buchwald, S. L. Copper-Catalyzed Coupling of Alkylamines and Aryl Iodides: An Efficient System Even in an Air Atmosphere. *Org. Lett.* **2002**, *4*, 581–584. (f) Sperotto, E.; de Vries, J. G.; van Klink, G. P. M.; van Koten, G. Ligand-free copper (I)-catalyzed N- and O-arylation of aryl halides. *Tetrahedron Lett.* **2007**, *48*, 7366–7370.
- (15) (a) Old, D. W.; Wolfe, J. P.; Buchwald, S. L. A highly active catalyst for palladium-catalyzed cross-coupling: Room-temperature Suzuki couplings and amination of unactivated aryl chlorides. *J. Am. Chem. Soc.* **1998**, *120*, 9722. (b) Wolfe, J. P.; Buchwald, S. L. A highly active catalysts for the room-temperature amination and Suzuki coupling of aryl chlorides. *Angew. Chem., Int. Ed.* **1999**, *38*, 2413.
- (16) Hartwig, J. F.; Kawatsura, M.; Hauck, S. I.; Shaughnessy, K. H.; Alcazar-Roman, L. M. Room-temperature palladium-catalyzed amination of aryl bromides and chlorides and extended scope of aromatic C–N bond formation with a commercial ligand. *J. Org. Chem.* **1999**, *64*, 5575.
- (17) (a) Chirik, P.; Morris, R. Getting down to earth: The renaissance of catalysis with abundant metals. *Acc. Chem. Res.* **2015**, *48*, 2495. (b) Wang, D.; Astruc, D. The recent development of efficient earth-abundant transition metal nanocatalysts. *Chem. Soc. Rev.* **2017**, *46*, 816. (c) Rana, S.; Biswas, J. P.; Paul, S.; Paik, A.; Maiti, D. Organic synthesis with the most abundant transition metal-iron: from rust to multitasking catalysts. *Chem. Soc. Rev.* **2021**, *50*, 243. (d) Cheng, L. J.; Mankad, N. P. C–C and C–X coupling reactions of unactivated alkyl electrophiles using copper catalysis. *Chem. Soc. Rev.* **2020**, *49*, 8036.
- (18) (a) Daigle, D. J.; Decuir, T. J.; Robertson, J. B.; Daresbourg, D. J. 1,3,5-Triaz-7-Phosphatricyclo[3.3.1.13.7]Decane and Derivatives. *Inorg. Synth.* **2007**, *32*, 40. (b) Gonsalvi, L.; Peruzzini, M. 1,3,5-Triaza-7-phosphadamantane (PTA). *Encycl. Reagents Org. Synth.* **2010**, *1*–4. (c) Akbayeva, D. N.; Gonsalvi, L.; Oberhauser, W.; Peruzzini, M.; Vizza, F.; Bruggeller, P.; Romerosa, A.; Sava, G.; Bergamo, A. Synthesis, catalytic properties and biological activity of new water soluble ruthenium cyclopentadienyl PTA complexes [(CSRs)RuCl(PTA)₂] (R = H, Me; PTA = 1,3,5-triaza-7-phosphadamantane). *Chem. Commun.* **2003**, 264. (d) Rampazzi, V.; Massard, A.; Richard, P.; Picquet, M.; Le Gendre, P.; Hiero, J.-C. A Simple Phosphine-Diolefin-Promoted-Copper-Catalyzed N-Arylation of Pyrazoles with (Hetero)aromatic Bromides: The Case of Chloroarenes Revisited. *ChemCatChem* **2012**, *4*, 1828–1835.
- (19) (a) Bergamini, P.; Marvelli, L.; Marchi, A.; Bertolas, V.; Fogagnolo, M.; Formaggio, P.; Sforza, F. New PTA (1,3,5-triaza-7-phosphadamantane) derivatives associating zwitterionic structure and coordinative ability. *Inorg. Chim. Acta* **2013**, *398*, 11. (b) Bhilare, S.; Gayakhe, V.; Ardhapure, A. V.; Sanghvi, Y. S.; Schulzke, C.; Borozdina, Y.; Kapdi, A. R. Novel water-soluble phosphatraizenes: versatile ligands

- for Suzuki-Miyaura, Sonogashira and Heck reactions of nucleosides. *RSC Adv.* **2016**, *6*, 83820.
- (20) Barends, J.; van der Linden, J. B.; van Delft, F. L.; Koomen, G.-J. Palladium-catalyzed amination of 6-chloropurine. Synthesis of N⁶-substituted adenosine analogues. *Nucleosides Nucleotides* **1999**, *18*, 2121.
- (21) Lanver, A.; Schmalz, H.-G. Microwave-assisted amination of a chloropurine derivative in the synthesis of acyclic nucleoside analogues. *Molecules* **2005**, *10*, 508.
- (22) (a) Thomson, P. F.; Lagisetty, P.; Balzarini, J.; De Clercq, E.; Lakshman, M. K. Palladium-catalyzed aryl amination reactions of 6-bromo and 6-chloropurine nucleosides. *Adv. Synth. Catal.* **2010**, *352*, 1728. (b) Champeil, E.; Pradhan, P.; Lakshman, M. K. Palladium-catalyzed synthesis of nucleoside adducts from Bay- and Fjord-region diol epoxides. *J. Org. Chem.* **2007**, *72*, 5035.
- (23) Gayakhe, V.; Ardhapure, A. V.; Kapdi, A. R.; Sanghvi, Y. S.; Serrano, J. L.; Schulzke, C. C-C bond formation: Synthesis of C5 substituted pyrimidine and C8 substituted purine nucleosides using water soluble Pd-imidate complex. *Curr. Protoc. Nucleic Acids Chem.* **2016**, *65*, 1–37.
- (24) Khozin, S.; Blumenthal, G. M.; Zhang, L.; Tang, S.; Brower, M.; Fox, E.; Helms, W.; Leong, R.; Song, P.; Pan, Y.; Liu, Q.; Zhao, P.; Zhao, H.; Lu, D.; Tang, Z.; Hakim, A. A.; Boyd, K.; Keegan, P.; Justice, R.; Pazdur, R. FDA Approval: ceritinib for the treatment of metastatic anaplastic lymphoma kinase-positive non-small cell lung cancer. *Clin. Cancer Res.* **2015**, *21*, 2436.
- (25) de Koning, P. D.; McAndrew, D.; Moore, R.; Moses, I. B.; Boyles, D. C.; Kissick, K.; Stanchina, C. L.; Cuthbertson, T.; Kamatani, A.; Rahman, L.; Rodriguez, R.; Urbina, A.; Sandoval, A.; Rose, P. R. Fit-for-purpose development of the enabling route to Crizotinib (PF-02341066). *Org. Process Res. Dev.* **2011**, *15*, 1018.
- (26) Toogood, P. L.; Harvey, P. J.; Repine, J. T.; Sheehan, D. J.; VenderWel, S. N.; Zhou, H.; Keller, P. R.; McNamara, D. J.; Sherry, D.; Zhu, T.; Brodfuehrer, J.; Choi, C.; Barvian, M. R.; Fry, D. W. Discovery of a potent and selective inhibitor of cyclin-dependent kinase 4/6. *J. Med. Chem.* **2005**, *48*, 2388.
- (27) Heravi, M. M.; Jaddi, Z. S.; Oskooie, H. A.; Khaleghi, S.; Ghassemzadeh, M. Regioselective synthesis of quinolone antibacterials via borate complex of quinolone carboxylic acid. *J. Chem. Res.* **2005**, *578*.
- (28) Villasante, F. J.; Gude, L.; Fernández, S. P.; Alonso, O.; García, E.; Cosme, A. A high-throughput impurity-free synthesis of Gatifloxacin. *Org. Process Res. Dev.* **2008**, *12*, 900.
- (29) Tardiff, B. J.; Stradiotto, M. Buchwald-Hartwig amination of (hetero)aryl chlorides by employing Mor-DalPhos under aqueous and solvent-free conditions. *Eur. J. Org. Chem.* **2012**, *2012*, 3972–3977.
- (30) (a) Shen, Q.; Ogata, T.; Hartwig, J. F. Highly reactive general and long-lived catalysts for palladium-catalyzed amination of heteroaryl and aryl chlorides, bromides and iodides: Scope and structure-activity relationships. *J. Am. Chem. Soc.* **2008**, *130*, 6586. (b) Dennis, J. M.; White, N. A.; Liu, R. Y.; Buchwald, S. L. Breaking the base barrier: An electron-deficient palladium catalyst enables the use of a common soluble base in C-N coupling. *J. Am. Chem. Soc.* **2018**, *140*, 4721.
- (31) Hartwig, J. F.; Shaughnessy, K. H.; Shekhar, S.; Green, R. A. *Organic Reactions* (Hoboken, NJ, United States); ACS Division of Organic Chemistry 2019, *100*, 853–943.
- (32) Patching, S. G.; Baldwin, S. A.; Baldwin, A. D.; Young, J. D.; Gallagher, M. P.; Henderson, P. J. F.; Herbert, R. B. The nucleoside transport proteins, NupC and NuPG, from *Escherichia coli*: specific structural motifs necessary for the binding of ligands. *Org. Biomol. Chem.* **2005**, *3*, 462.
- (33) (a) King, S. M.; Buchwald, S. L. Development of a method for the N-arylation of amino acid esters with aryl triflates. *Org. Lett.* **2016**, *18*, 4128. (b) Young, H. A.; Guthrie, Q. A. E.; Proulx, C. N-arylation of amino acid esters to expand side chain diversity in ketoxime peptide ligations. *J. Org. Chem.* **2020**, *85*, 1748. (c) Sharma, K. K.; Sharma, S.; Kudwal, A.; Jain, R. Room temperature N-arylation of amino acids and peptides using copper(I) and β -diketone. *Org. Biomol. Chem.* **2015**, *13*, 4637.
- (34) Zhang, C.; Vinogradova, E. V.; Spokoyny, A. M.; Buchwald, S. L.; Pentelute, B. L. Arylation chemistry for bioconjugation. *Angew. Chem., Int. Ed.* **2019**, *58*, 4810.
- (35) (a) Bhilare, S.; Kori, S.; Shet, H.; Balaram, G.; Mahendar, K.; Sanghvi, Y. S.; Kapdi, A. R. Scale-up of a Heck alkenylation reaction: Application to the synthesis of an amino-modifier nucleoside ‘Ruth linker’. *Synthesis* **2020**, *S2*, 3595. (b) Kapdi, A.; Ardhapure, A.; Sanghvi, Y. Modulation of the electronic properties of non-innocent (E,E)-dibenzylideneacetone for palladium(0)-mediated Heck alkenylation of 5-iodo-2'-deoxyuridine and scale-up studies. *Synthesis* **2015**, *47*, 1163.
- (36) Limitation of Hg-drop test protocol with regards to homogeneous vs heterogeneous (kinetic studies, filtration tests, selective poisons for catalysts for solid or soluble systems) can be addressed using Rebek-Collman 3-phase tests mentioned in the reference: Lamblin, M.; Nassar-Hardy, L.; Hierso, J.-C.; Fouquet, E.; Felpin, F.-X. Recyclable Heterogeneous Palladium Catalysts in Pure Water: Sustainable Development in Suzuki, Sonogashira, and Tsuji-Trost Reactions. *Adv. Synth. Catal.* **2010**, *352*, 33–79. The following are the references for Hg-drop test: (a) Whitesides, G. M.; Hackett, M.; Brainard, R. L.; Lavallee, J.-P. P. M.; Sowinski, A. F.; Izumi, A. N.; Moore, S. S.; Brown, D. W.; Staudt, E. M. Suppression of unwanted heterogeneous platinum(0)-catalyzed reactions by poisoning with mercury(0) in systems involving competing homogeneous reactions of soluble organoplatinum compounds: thermal decomposition of bis(triethylphosphine)-3,3,4,4-tetramethylplatinacyclopentane. *Organometallics* **1985**, *4*, 1819. (b) Crabtree, R. H. Resolving Heterogeneity Problems and Impurity Artifacts in Operationally Homogeneous Transition Metal Catalysts. *Chem. Rev.* **2012**, *112*, 1536. (c) Khake, S. M.; Soni, V.; Gonnade, R. G.; Punji, B. Design and development of POCN-pincer palladium catalysts for C–H bond arylation of azoles with aryl iodides. *Dalton Trans.* **2014**, *43*, 16084. (d) Prajapati, D.; Schulzke, C.; Kindermann, M. K.; Kapdi, A. R. Selective palladium-catalysed arylation of 2,6-dibromopyridine using N-heterocyclic carbene ligands. *RSC Adv.* **2015**, *5*, 53073.
- (37) Gordon, C. P.; Andersen, R. A.; Coperet, C. Metal-olefin complexes: Revisiting the Dewar-Chatt-Duncanson model and deriving reactivity patterns from carbon-13 NMR chemical shift. *Helvetica* **2019**, *102*, No. e1900151.
- (38) Durand, D. J.; Fey, N. Computational Ligand Descriptors for Catalyst Design. *Chem. Rev.* **2019**, *119*, 6561–6594.
- (39) Jacobsen, H.; Correa, A.; Costabile, C.; Cavallo, L. π -Acidity and π -basicity of N-heterocyclic carbene ligands. A computational assessment. *J. Organomet. Chem.* **2006**, *691*, 4350–4358.
- (40) Flener Lovitt, C.; Frenking, G.; Girolami, G. S. Donor–Acceptor Properties of Bidentate Phosphines. DFT Study of Nickel Carbonyls and Molecular Dihydrogen Complexes. *Organometallics* **2012**, *31*, 4122–4132.
- (41) Reiersolmoen, A.; Battaglia, S.; Øien-Ødegaard, S.; Gupta, A. K.; Fiksahl, A.; Lindh, R.; Erdelyi, M. Symmetry of three-center, four-electron bonds. *Chem. Sci.* **2020**, *11*, 7979–7990.
- (42) Desnoyer, A. N.; He, W.; Behyan, S.; Chiu, W.; Love, J. A.; Kennepohl, P. The Importance of Ligand-Induced Backdonation in the Stabilization of Square Planar d10 Nickel π -Complexes. *Chem. – Eur. J.* **2019**, *25*, 5259–5268.
- (43) Leyssens, T.; Peeters, D.; Orpen, A. G.; Harvey, J. N. How Important Is Metal–Ligand Back-Bonding toward YX₃ Ligands (Y = N, P, C, Si)? An NBO Analysis. *Organometallics* **2007**, *26*, 2637–2645.
- (44) Minenkov, Y.; Occhipinti, G.; Jensen, V. R. Metal–Phosphine Bond Strengths of the Transition Metals: A Challenge for DFT. *J. Phys. Chem. A* **2009**, *113*, 11833–11844.
- (45) Jover, J.; Cirera, J. Computational assessment on the Tolman cone angles for P-ligands. *Dalton Trans.* **2019**, *48*, 15036–15048.
- (46) Mathew, J.; Thomas, T.; Suresh, C. H. Quantitative Assessment of the Stereoelectronic Profile of Phosphine Ligands. *Inorg. Chem.* **2007**, *46*, 10800–10809.
- (47) Kégl, T.; Pálinkás, N.; Kollár, L.; Kégl, T. Computational Characterization of Bidentate P-Donor Ligands: Direct Comparison to Tolmans Electronic Parameters. *Molecules* **2018**, *23*, 3176.

- (48) (a) Roy, D.; Mom, S.; Royer, S.; Lucas, D.; Hierso, J.-C.; Doucet, H. Palladium-catalyzed direct arylation of heteroaromatics with activated aryl chlorides using a sterically relieved ferrocenyl-diphosphane. *ACS Catal.* **2012**, *2*, 1033. (b) Malysheva, S. F.; Belogorlova, N. A.; Vereshchagina, Y. A.; Alimova, A. Z.; Ishmaeva, E. A.; Chachkov, D. V. Synthesis and conformational analysis of phosphine selenides. *Russ. J. Gen. Chem.* **2016**, *86*, 590. (c) Allen, D. W.; Nowell, I. W.; Taylor, B. F. The chemistry of heteroarylphosphorus compounds. Part 16: Unusual substituent effects on selenium-77 nuclear magnetic resonance chemical shifts of heteroaryl- and arylphosphine selenides. X-ray crystal structure of tri(2-furyl)-phosphine selenide. *J. Chem. Soc. Dalton Trans.* **1985**, *12*, 2505.
- (49) McFarlane, W.; Rycroft, D. S. Studies of organophosphorus selenides by heteronuclear magnetic triple resonance. *J. Chem. Soc. Dalton Trans.* **1973**, *20*, 2162.
- (50) Pascher, T. F.; Ončák, M.; van der Linde, C.; Beyer, M. K. UV/VIS spectroscopy of copper formate clusters: Insight into metal-ligand photochemistry. *Chem. – Eur. J.* **2020**, *26*, 8286.
- (51) (a) Sreenath, K.; Yuan, Z.; Macias-Contreras, M.; Ramachandran, V.; Clark, R. J.; Zhu, L. Dual role of acetate in copper(II) acetate catalyzed dehydrogenation of chelating aromatic secondary amines: A kinetic study of copper-catalyzed oxidation reactions. *Eur. J. Org. Chem.* **2016**, *2016*, 3728–3743. (b) Bencini, A.; Bertini, I.; Gatteschi, D.; Scorzafava, A. Single-crystal ESR spectra of copper(II) complexes with geometries intermediate between a square pyramid and a trigonal bipyramidal. *Inorg. Chem.* **1978**, *17*, 3194.
- (52) Sperotto, E.; van Klink, G. P. M.; van Koten, G.; de Vries, J. G. The mechanism of the modified Ullmann reaction. *Dalton Trans.* **2010**, *39*, 10338–10351.
- (53) Walsh, K.; Sneddon, H. F.; Moody, C. J. Amination of Heteroaryl chlorides: Palladium Catalysis or S_NAr in Green Solvents? *ChemSusChem* **2013**, *6*, 1455–1460.
- (54) Frisch, M. J.; Trucks, G. W.; Schlegel, H. B.; Scuseria, G. E.; Robb, M. A.; Cheeseman, J. R.; Scalmani, G.; Barone, V.; Petersson, G. A.; Nakatsuji, H.; Li, X.; Caricato, M.; Marenich, A. V.; Bloino, J.; Janesko, B. G.; Gomperts, R.; Mennucci, B.; Hratchian, H. P.; Ortiz, J. V.; Izmaylov, A. F.; Sonnenberg, J. L.; Williams-Young, D.; Ding, F.; Lipparini, F.; Egidi, F.; Goings, J.; Peng, B.; Petrone, A.; Henderson, T.; Ranasinghe, D.; Zakrzewski, V. G.; Gao, J.; Rega, N.; Zheng, G.; Liang, W.; Hada, M.; Ehara, M.; Toyota, K.; Fukuda, R.; Hasegawa, J.; Ishida, M.; Nakajima, T.; Honda, Y.; Kitao, O.; Nakai, H.; Vreven, T.; Throssell, K.; Montgomery, J. A., Jr.; Peralta, J. E.; Ogliaro, F.; Bearpark, M. J.; Heyd, J. J.; Brothers, E. N.; Kudin, K. N.; Staroverov, V. N.; Keith, T. A.; Kobayashi, R.; Normand, J.; Raghavachari, K.; Rendell, A. P.; Burant, J. C.; Iyengar, S. S.; Tomasi, J.; Cossi, M.; Millam, J. M.; Klene, M.; Adamo, C.; Cammi, R.; Ochterski, J. W.; Martin, R. L.; Morokuma, K.; Farkas, O.; Foresman, J. B.; Fox, D. J. *Gaussian 16*; Revision C.01, Gaussian, Inc.: Wallingford CT, 2016.
- (55) Glendening, E.D.; Reed, A.E.; Carpenter, J.E.; Weinhold, F. *NBO*; Version 3.1. Gaussian Inc.: Pittsburgh, 2003.
- (56) *Mathematica*; Version 12.2, Wolfram Research, Inc.: Champaign, IL (2020).
- (57) Bilbrey, J. A.; Kazez, A. H.; Locklin, J.; Allen, W. D. Exact ligand cone angles. *J. Comput. Chem.* **2013**, *34*, 1189–1197.
- (58) Lu, T.; Chen, F. Multiwfn: A multifunctional wavefunction analyzer. *J. Comput. Chem.* **2012**, *33*, 580–592.
- (59) Hunter, J.; Matplotlib, D. A 2D graphics environment. *Comput. Sci. Eng.* **2007**, *9*, 90–95.
- (60) Nandi, D.; Islam, R. U.; Devi, N.; Siwal, S.; Mallick, K. A palladium nanoparticle-catalyzed aryl–amine coupling reaction: high performance of aryl and pyridyl chlorides as the coupling partner. *New J. Chem.* **2018**, *42*, 812–816.
- (61) Kulkarni, S.; Grimmett, M. R.; Hanton, L. R.; Simpson, J. Nucleophilic Displacements of Imidazoles. I. Oxygen, Nitrogen and Carbon Nucleophiles. *Aust. J. Chem.* **1987**, *40*, 1399–1413.
- (62) Murty, M. S. R.; Ram, K. R.; Rao, R. V.; Yadav, J. S.; Murty, U. S.; Pranay Kumar, K. CsF–Celite catalyzed facile *N*-alkylation of 2(*H*)-benzoxazolones and antimicrobial properties of 2-substituted benzoxazole and 3-substituted-2(*H*)-benzoxazolone derivatives. *Med. Chem. Res.* **2011**, *20*, 626–636.
- (63) Vlaar, C. P.; Castillo-Pichardo, L.; Medina, J. I.; Marrero-Serra, C. M.; Velez, E.; Ramos, Z.; Hernandez, E. Design, synthesis and biological evaluation of new carbazole derivatives as anti-cancer and anti-migratory agents. *Bioorg. Med. Chem.* **2018**, *26*, 884–890.
- (64) Molander, G. A.; Cavalcanti, L. N. Metal-Free Chlorodeboronation of Organotrifluoroborates. *J. Org. Chem.* **2011**, *76*, 7195–7203.
- (65) Matulenko, M. A.; Paight, E. S.; Frey, R. R.; Gomtsyan, A.; DiDomenico, S., Jr.; Jiang, M.; Lee, C.-H.; Stewart, A. O.; Yu, H.; Kohlhass, K. L.; Alexander, K. M.; McGaraughty, S.; Mikusa, J.; Marsh, K. C.; Muchmore, S. W.; Jakob, C. L.; Kowaluk, E. A.; Jarvis, M. F.; Bhagwat, S. S. 4-Amino-5-aryl-6-arylethynylpyrimidines: Structure–activity relationships of non-nucleoside adenosine kinase inhibitors. *Bioorg. Med. Chem.* **2007**, *15*, 1586–1605.
- (66) Cho, S. H.; Kim, J. Y.; Chang, S. Silver-Mediated Direct Amination of Benzoxazoles: Tuning the Amino Group Source from Formamides to Parent Amines. *Angew. Chem., Int. Ed.* **2009**, *48*, 9127–9130.
- (67) Dawei, M.; Lu, X.; Shi, L.; Zhang, H.; Jiang, Y.; Liu, X. Domino Condensation/S-Arylation/Heterocyclization Reactions: Copper-Catalyzed Three-Component Synthesis of 2-N-Substituted Benzothiazoles. *Angew. Chem., Int. Ed.* **2011**, *50*, 1118–1121.
- (68) Dutta, P. K.; Sen, S.; Saha, D.; Dhar, B. Solid Supported Nano Structured Cu-Catalyst for Solvent/Ligand Free C_2 Amination of Azoles. *Eur. J. Org. Chem.* **2018**, 657–665.
- (69) Lee, B. K.; Biscoe, M. R.; Buchwald, S. L. Simple, efficient protocols for the Pd-catalyzed cross-coupling reaction of aryl chlorides and dimethylamine. *Tetrahedron Lett.* **2009**, *50*, 3672–3674.
- (70) Hancock, L. M.; Gilday, L. C.; Kilah, N. L.; Serpell, C. J.; Beer, P. D. A new synthetic route to chloride selective [2]catenanes. *Chem. Commun.* **2011**, *47*, 1725–1727.
- (71) Min, H.; Xiao, G.; Liu, W.; Liang, Y. Copper-catalyzed synthesis of 2-aminobenzothiazoles from 2-iodophenyl isocyanides, potassium sulfide and amines. *Org. Biomol. Chem.* **2016**, *14*, 11088–11091.
- (72) Sengmany, S.; Lebre, J.; Le Gall, E.; Leonel, E. Selective mono-amination of dichlorodiazines. *Tetrahedron* **2015**, *71*, 4859–4867.
- (73) Cechova, L.; Jansa, P.; Sala, M.; Dracinsky, M.; Holy, A.; Janeba, Z. The optimized microwave-assisted decomposition of formamides and its synthetic utility in the amination reactions of purines. *Tetrahedron* **2011**, *67*, 866–871.
- (74) Qu, G. R.; Zhao, L.; Wang, D.-C.; Wu, J.; Guo, H.-M. Microwave-promoted efficient synthesis of C6-cyclo secondary amine substituted purine analogues in neat water. *Green Chem.* **2008**, *10*, 287–289.
- (75) Li, F.; Shan, H.; Chen, L.; Kang, Q.; Zou, P. Direct *N*-alkylation of amino-azoles with alcohols catalyzed by an iridium complex/base system. *Chem. Commun.* **2012**, *48*, 603–605.
- (76) Lok, R.; Leone, R. E.; Williams, A. J. Facile Rearrangements of Alkynylamino Heterocycles with Noble Metal Cations. *J. Org. Chem.* **1996**, *61*, 3289–3297.
- (77) Wang, J.; Hou, J.-T.; Wen, J.; Zhang, J.; Yu, X. Q. Iron-catalyzed direct amination of azoles using formamides or amines as nitrogen sources in air. *Chem. Commun.* **2011**, *47*, 3652–3654.
- (78) Li, F.; Shan, H.; Kang, Q.; Chen, L. Regioselective *N*-alkylation of 2-aminobenzothiazoles with benzylic alcohols. *Chem. Commun.* **2011**, *47*, 5058–5060.
- (79) Wan, Z.-K.; Binnun, E.; Wilson, D. P.; Lee, J. A Highly Facile and Efficient One-Step Synthesis of N^6 -Adenosine and $N^6\text{-}2'$ -Deoxyadenosine Derivatives. *Org. Lett.* **2005**, *7*, 5877–5880.